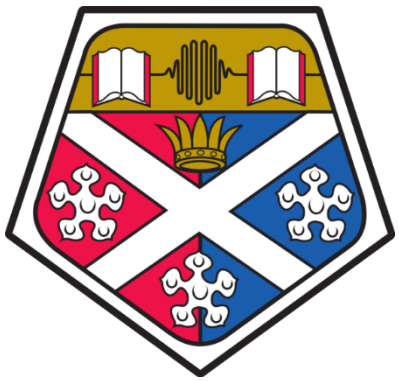

DEPARTMENT OF BIOMEDICAL ENGINEERING
UNIVERSITY OF STRATHCLYDE, GLASGOW, UK

Electrophysiology of Ion Channels in Miniaturised Systems

ALI REZA SALAMATI

A thesis presented in fulfilment of the requirements for the degree of Engineering Doctorate

September 2018

Declaration

The composition of this thesis and work described herein is my own, carried out at the University of Strathclyde. No part of this thesis has been submitted for any other degree or qualification.

Abstract

Cell membranes form a natural protective boundary around cells and their organelles. Ion channels housed within these membranes comprise 1.5% of the human genome and carry out essential cell signalling roles. As such, ion channels are important pharmacological targets and a better understanding of their function would aid drug discovery as well as drug toxicity testing. Although there are methods of studying ion channels, including patch clamping and artificial lipid bilayer system, a number of difficulties limit their experimental efficiency and practicality. In the case of artificial bilayer architectures, reconstitution of membrane proteins into bilayers is challenging. Here we demonstrate the design and development of a scalable droplet interface bilayer system for single ion channel electrophysiology. A combination of this platform and the ion channel reconstitution method addresses the protein integration problem by improving the probability of channel incorporation to 29%. Single channel recordings of gramicidin, alamethicin and alpha hemolysin were acquired for proof of concept work while eukaryotic ion channel BK electrophysiology provides evidence of the success of the project objectives. We anticipate that the suggested reconstitution method in conjunction with the platform developed in this research can be extended to study other pharmacologically relevant human ion channels.

Table of Contents

Table of Figures

Table of Tables

1 Chapter 1: Literature Review

1.1 Thesis Structure

Chapter 1 provides a general background on the structure and role of biological membranes and its main constituents. An overview of types of membrane proteins is presented. Patch clamp electrophysiology is presented as a traditional technique to study ion channels. The advantages of artificial bilayer systems over patch clamping is reviewed and a number of model membrane systems are introduced. A brief overview of ion channel reconstitution methods is given. Finally, the objectives, motivation and novelty of this research project is presented.

Chapter 2 provides a description of the materials and methods used in the experiments of this thesis.

Chapter 3 gives a detailed description of the functional requirements and thinking behind the technology selection, design and development of the droplet interface bilayer platform presented in this thesis. The results from device microscopy and bilayer characterisation tests are presented and optimum bilayer formation conditions are identified.

Chapter 4 validates the suitability of the proposed DIB system in recording peptidic activity. The results of gramicidin, alamethicin and alpha hemolysin single channel electrophysiology are presented. The hypothesis for improved peptide reconstitution time as a result of enhanced ratio of bilayer area to droplet surface area is put to the test.

Chapter 5 focuses on a reliable reconstitution regime for a pharmacologically relevant eukaryotic ion channel. A general background about potassium channel structure and function is given. BK STREX ion channel electrophysiology results are presented. The same theory tested in chapter 5 with regards to area ratios and probability of channel integration is extended to BK STREX experiments.

Chapter 6 is the last chapter and summarises the experimental results observed in this thesis followed by ideas for future developments.

1.2 Cells

Cells are the building blocks of life. Prokaryotic and eukaryotic cells are found enveloped in a plasma membrane just a few nanometres thick. A large variety of cells has resulted in the specialisation of different functions. The diverse functionality and capabilities of these cells are achieved with the complex machinery contained within the cell and the insulating membrane wall (Raven & Johnson, 2002).

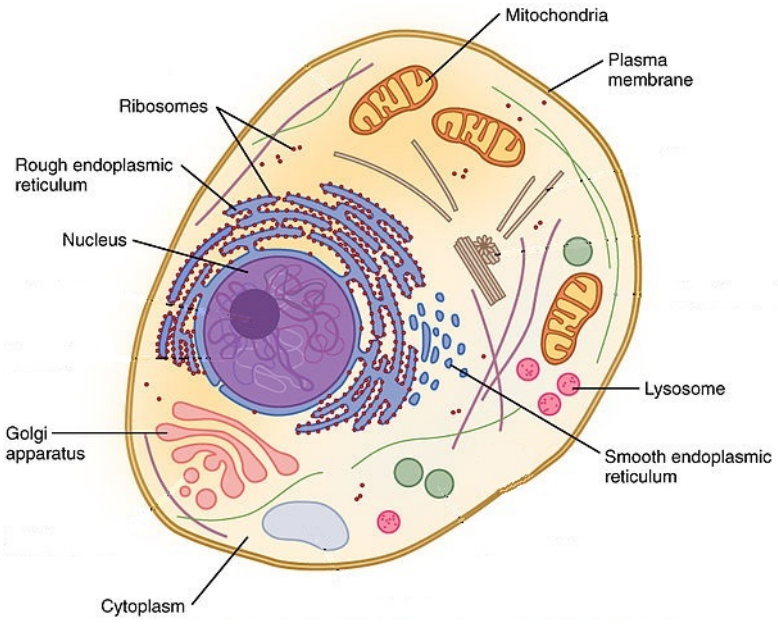

Figure 1.1 Components of a typical eukaryotic cell
Figure taken from www.sciencewithu.weebly.com/cells.html

Some of the complex structures of a typical eukaryotic cell can be seen in Figure 1.1. The content of the cell is maintained in a membrane. The membrane itself is a complex structure and can have several functions. Cell membranes act as the interfaces between the components and chemicals inside of the cell and the exterior world, therefore, the study of their properties and function is an area of great interest.

1.3 Membranes

1.3.1.1 Cell membrane and its components

Cells are formed from a cytoplasm, a fluid matrix with a nucleus and organelles, contained within the cell membrane. Many of the properties of the cell membrane can be attributed to its membrane's structure. The cell membrane is composed of a phospholipid bilayer with embedded proteins, including ion channels, glycoprotein, globular and peripheral protein.

The bilayer is composed of two single layers of phospholipid molecules as can be seen in Figure 1.2. These amphiphilic molecules contain a hydrophilic head and hydrophobic acyl chain tail (Zagnoni, 2012). The tails point towards the inside of the bilayer and the heads are orientated towards the two surfaces of the membrane. Given their hydrophobicity, the tails prefer to pack together and avoid exposure to polar water molecules. Due to these properties and their geometric packing constraints, they can self-assemble into lamellar bilayers when they are in an aqueous solution (Eeman & Deleu, 2010). Typically, the membrane is 3–5 nm thick in animal cells but thicker in bacterial cells. Proteins and other structures such as filaments, microtubules and peptidoglycans can be found attached or embedded into the lipid bilayer.

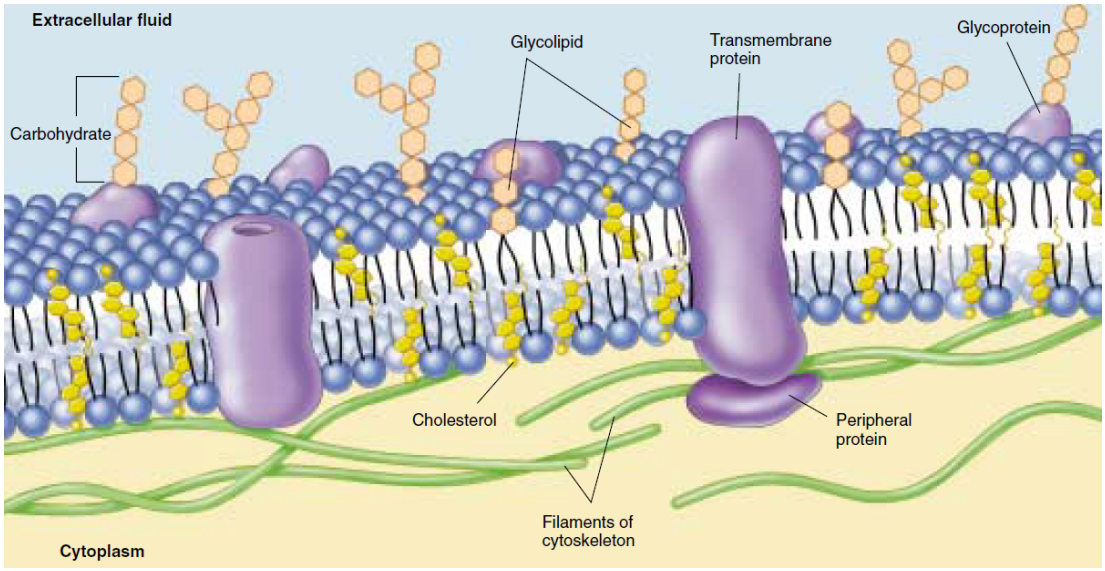

Figure 1.2 The phospholipid bilayer with embedded proteins
Phospholipid molecules composed of head and two tails shown in blue. Figure taken from (Raven & Johnson, 2002)

A cell membrane can contain many different lipid species, this can be up to 100 in some cases. Within the human genome, almost 7500 different genes are the coding for membrane proteins. This is about 30% of the entire human genome (Fagerberg et al., 2010).

Different proteins can project through the membrane of some cells. The nonpolar regions of the proteins can attach to the nonpolar interior of the membrane. Carbohydrate chains can be bound to the extracellular portion of these proteins, as well as to the cell membrane's phospholipid molecules. These chains can serve as unique tags that can be used to identify different cells.

1.3.2 Membrane proteins

1.3.2.1 Membrane proteins types and ion channels

The membranes of cells act as effective barriers between the extracellular and the intracellular environment. It is possible for neutral gases and some water to cross

lipid membrane but transport between the extracellular and the intracellular environment is greatly enabled by proteins that are embedded in or attached to the surface of the membrane. Drugs often target membrane proteins to achieve their desired effect. The significance of membrane proteins as relevant drug targets is shown in Figure 1.3.

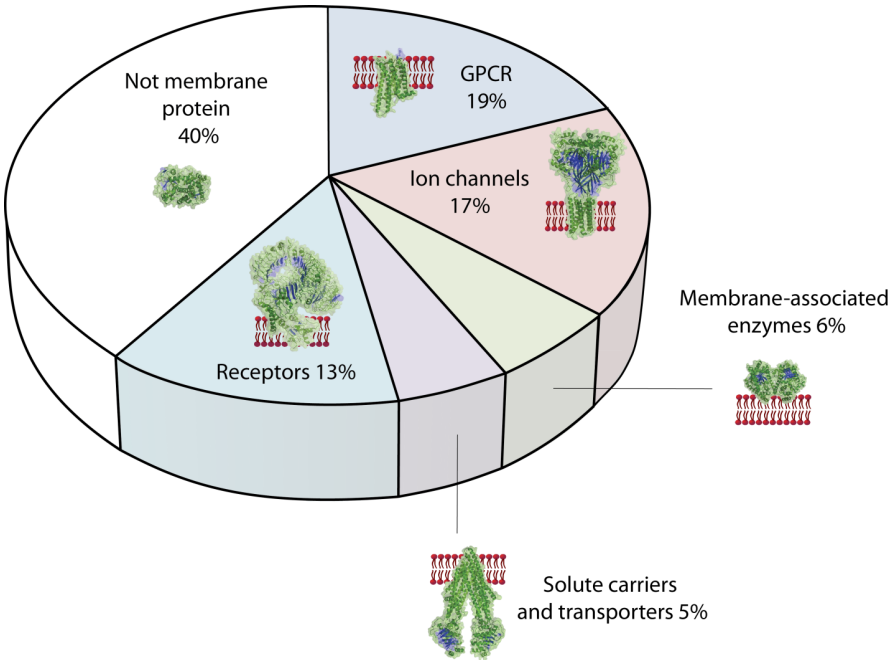

Figure 1.3 Human Membrane Proteins as Drug Targets
17% of drugs target ion channels to achieve their desired effects, 6% target membrane-associated enzymes, 5% target solute carriers and transporters, 13% target receptors, 40% have targets which are not membrane proteins and 19% of drugs target G protein-coupled receptors (GPCRs). Figure taken from (Tiefenauer & Demarche, 2012)

These proteins are vital functional component of the membrane allowing the cell to function correctly. As well as regulating transportation of ions, elements and molecules across the membrane, these proteins allow for energy conversion and signal transduction to occur. Without membrane proteins it would be very difficult for many ions such as potassium, sodium or chloride to pass between the extracellular and the intracellular environment (Nielsen, 2009). Ion channels make up an important group of membrane proteins. These channels are opening-forming

proteins that control the flow of ions across a variety of cell membranes such as nerve, muscle, etc. (Berg et al., 2012) . They are responsible for critical processes such as management of the cardiac rhythm and the excitability of neurons (Terlau & Kirchhoff, 2001).

As shown in Figure 1.3 ion channels comprise almost 20 percent of the membrane protein drug target sites. It is possible to reproduce the natural behaviour of the ion channel and examine the effects of exposure to different drugs (Zhang et al., 2007) by integrating the ion channels into artificial lipid bilayer systems. By placing ion channels in a controlled environment, it is also possible to utilise them as sensitive biosensors and as a drug-screening tool (Durick & Negulescu, 2001; Tanaka & Sackmann, 2005). Since the activation and inactivation of the ion channels integrated into the membrane are too small to view under a traditional microscope, electrical readings are taken to assess the functionality of the ion channels (Atsuta et al., 2004; Terrettaz et al., 2003). Electrical interrogation of functioning ion channels serve to facilitate a greater understanding of the physiology of the cell as well as providing a baseline for detection of abnormal ion channel behaviour in ion channel-related diseases (Abraham et al., 1999; Celesia, 2001).

Ion channel dysfunction leads to a range of disorders, for example mutations of the human Ether-a-go-go (hERG) channel, a voltage gated cardiac myocyte membrane potassium channel, leads to changes in repolarisation of the heart and thus irregular heartbeat in the form of long QT syndrome and torsades de pointes (Finlayson et al., 2004; Masetti et al., 2008; Wible et al., 2005) resulting in potentially fatal cardiac arrhythmias. Hence a better understanding of their function would aid drug discovery and drug toxicity testing.

The activation/inactivation of ion channels is referred to as 'gating'. This implies mechanisms for channel opening and closing (Kung & Blount, 2004). In addition to carrier and transporter type channels there are three main types of ion channels, this is shown in Figure 1.4. These are distinguished by the method by which they activate and inactivate (H. Ti. Tien, 2003). 10^4

- Voltage-gated ion channels – activation/inactivation depends on the voltage gradient across the membrane.
- Ligand-gated ion channels – activation/inactivation depends on binding of ligands to the channel.
- Mechanosensitive ion channels – activation/inactivation depends on mechanical stimuli of the protein channel.

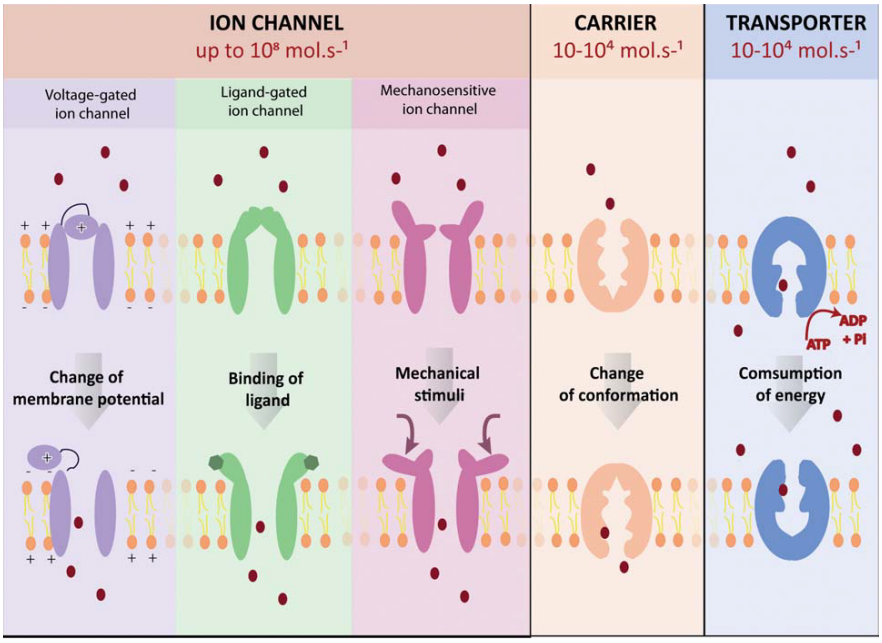

Figure 1.4 Types of translocation mediating proteins
Three classes of proteins capable of translocation across cell membranes are shown: ion channel, carrier and transporter. Ion channels and carrier proteins are involved in passive transport where ions cross the membrane down the concentration gradient. In contrast, active transport is achieved in transporter proteins through the consumption of energy, e.g. by ATP hydrolysis to allow transport up the chemical gradient. Mechanisms and stimulations that bring about changes in protein channel structure to permit translocation as well as typical transport rates are also indicated in the figure. Ion channels can move ions up to 10^4 times faster than carrier and transport proteins. Figure taken from (Demarche et al., 2011)

1.3.2.2 Proteins anchor in the bilayer

As seen in Figure 1.2 membrane proteins span across the lipid bilayer and acts as a conduit connecting the cytoplasm to cell exterior. The protein is shackled to the cell membrane by its nonpolar segments. The section of the protein that traverses through the lipid bilayer, in contact with the nonpolar interior of the bilayer, is hydrophobic and consists of one or more nonpolar helices or several β -pleated sheets of nonpolar amino acids. Any movement of the protein out of the membrane, in either direction, brings the hydrophobic nonpolar regions of the protein into contact with water, which pushes the protein back into the interior and locking it into position (Raven & Johnson, 2002).

1.3.2.3 Active and passive transport

Signal transduction, energy conversion and transport of molecules between the intracellular and extracellular environment can be carried out by the membrane proteins. When considering the translocation mechanism of ions or molecules as a main criteria of classification, passive and active translocation mechanisms (Demarche et al., 2011).

- Passive translocation is driven by concentration gradients between the intracellular and extracellular environment.
- Active translocation occurs against the described gradient. This is associated with the consumption of energy. This can be chemical energy, oxidation or the absorption of light.

There are two types of passive transporters: carriers and ion channels. As the name suggests passive translocation by a carrier is energy-independent. Ion channels are characterised by their ion type selection and the mechanism by which it achieves the

gating function. The selectivity is achieved by the design of amino acid deposits at the entrance of the ion channel which acts as a filter and restricts the flow of ions other than its intended type.

When comparing the rate of translocation between ion channels and the carriers, the ion channel is generally regarded as higher. This is because during translocation of the ions by the carriers, the path of the ions across the membrane can be restricted with some interactions between the amino acid residues.

The most abundant groups of signalling molecules in humans are protein kinases, the G-protein coupled receptors (GPCRs) and voltage-gated ion channels respectively (Demarche et al., 2011). Voltage-gated ion channels high abundance make them important drug targets for biochemists and pharmacologists (Harmar et al., 2009).

When voltage-gated ion channels undergo changes from a closed to an open state, they allow cells to begin and propagate action potentials. This trait makes them crucial for neuronal and cardiac function. Neuronal activity can lead to gene expression regulated via Ca^{2+} influx across the calcium channels (Barbado et al., 2009). This means that they can also be involved in gene regulation as well as signalling pathways. The three most important families of voltage-gated ion channels in humans are Sodium (Hervé Duclohier, 2009), Potassium (Wulff et al., 2009) and Calcium voltage-gated ion channels (Perret & Luo, 2009)

1.3.2.4 Drug Market relevance

A significant portion of drugs with a total market value of more than $15 billion target ion channels (Clare, 2010; Molokanova & Savchenko, 2008; Rask-Andersen et al., 2011; Tiefenauer & Demarche, 2012).

It has been reported that membrane proteins account for up to 70% of all known drug targets and 50% of potential new drug targets. This is due to their intimate involvement in a wide variety of diseases (Wang & Tonggu, 2015). Ion channels are highly relevant in medical therapies, and currently represent almost one fifth of all drug targets (Tiefenauer & Demarche, 2012). Ion channels malfunction can lead to diseases such as muscular dystrophy, cystic fibrosis and osteoporosis. The general term used to describe this is channelopathy. Ion channels are also becoming important in cancer therapy (Arcangeli et al., 2009).

1.4 Electrical characterisation of ion channels

1.4.1 Electrophysiology

1.4.1.1 Ion channel recording methods

Membranes and ion channels are studied by various techniques, however, electrophysiological measurements with cell patch clamping allowing single channel recordings is considered the gold-standard technique.

1.4.1.2 What is Electrophysiology?

The study of the electrical properties of tissues and cells is referred to as electrophysiology. With the discovery of bioelectricity by Luigi Galvani in the 18th century (Piccolino, 1998). The study of this topic has now been greatly expanded (Terlau & Kirchhoff, 2001). In the 1940s and 50s research was conducted on squid axon. This allowed for the study of ionic theory of membrane conduction as well as electrophysiology of action potentials. One of the most significant outcomes from these studies was the understanding that the movement of ions responsible for changes in membrane potential. It was also found that the permeability of the

membrane to sodium ions changes during the action potential. This was the first time this behaviour was recorded and observed (Curtis & Cole, 1940; Hodgkin & Huxley, 1945).

Voltage clamp technique was invented in the late 1940s. This allowed for ionic currents to be measured under known membrane potential (Hodgkin et al., 1952; Marmont, 1949; Terlau & Kirchhoff, 2001). In 1963 Hodgkin and Huxley received the Nobel Prize in Physiology and Medicine for their work. They were able to outline the ionic basis of the action potential by keeping the membrane potential constant (Terlau & Kirchhoff, 2001).

One of the most effective methods for characterising ion channel function is the electrical measurement of ion permeation. This method is so effective that it even allows for single channel resolution (Terlau & Kirchhoff, 2001).

Patch clamping of cell membranes is one of the most widely used methods for studying the currents flowing through the ion channels, carried out after cellular protein expression (Trapani & Korn, 2003). A schematic of a whole cell patch clamp is shown in Figure 1.5.

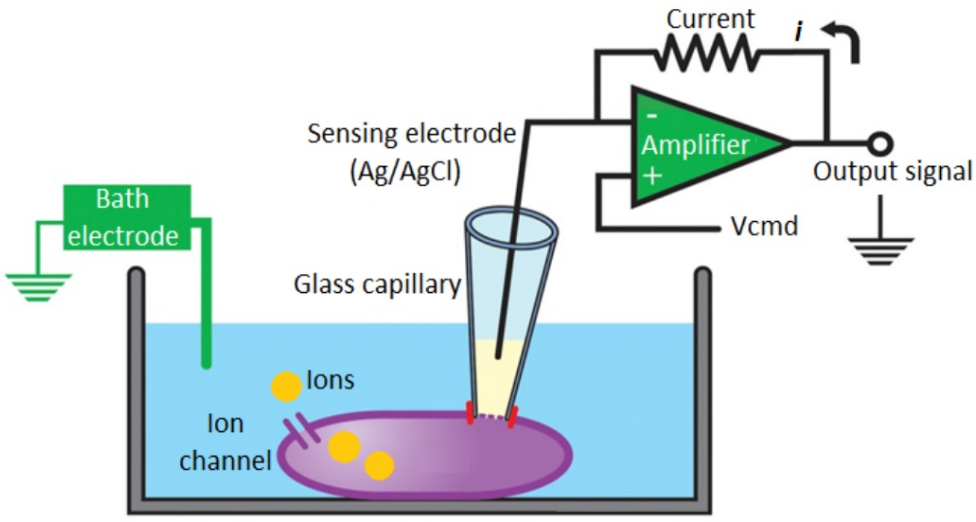

Figure 1.5 Schematic of a typical whole-cell patch clamp
In this configuration, macroscopic currents and action potentials can be measured. First the glass capillary tip is positioned onto the cell memrbane to form a giga-ohm seal. Then negative pressure breaks the membrane patch yeilding electrical continuity between the sensing electrode and the cell cytoplasm. The membrane voltage is set by the command voltage (Vcmd) and membrane potentail is "clamped" by injecting an appropriate amount of current into the cell to maintain the command voltage. The current injected into the cell is equal to and therefore represents the overall currents passing across the entire cell membrane. This current is recorded with reference to the bath electrode. Figure taken from (Clare, 2010)

This configuration will allow for the study of ionic currents through ion channels in the membrane. The glass capillary is pushed onto the surface of the cell which results in a seal. Negative pressure is then applied to break part of the membrane. This gives access to the environment inside the cell, allowing for whole cell ion channel recordings to be made (Zhao et al., 2008). The glass capillary contains electrolyte fluid and the electrode is positioned inside it. The circuit is completed by the grounding electrode that is placed in the solution outside the cell.

A system like the one shown in Figure 1.5 will allow electrical stability between the sensing electrode and the inner cell for better signal recordings. The measurements of quick membrane potential changes can be complicated due to the accumulation of charge on one side of the membrane and its depletion from the other. This can be referred to as reflect currents through the membrane capacitance C_m. This can

compete with the detection of the movements of ions through ion channels I_{ionic}. The total membrane current I_m, therefore, is the sum of these two components and can be represented by the following equation (Aidley & Stanfield, 1996):

$$I_m = I_{ionic} + C_m \frac{dV}{dt}$$

To measure the ionic current, It would be necessary to remove the capacitance current from the equation. By holding the membrane potential at a constant value, $\frac{\mathrm{dV}}{\mathrm{dt}}$ would equal zero, therefore, there would be no capacitance current. This would result in the measured current to be purely the ionic current. The voltage clamp technique allowed for this to be achieved. The silver electrode inside the glass capillary is attached to a trans-impedance amplifier that will allow the detected current to be converted into a voltage signal.

Many investigations on ion channel behaviour have been reported in the literature. There is a great intrest in gating mechanisms and channel selectivity (Atsuta et al., 2004; Terrettaz et al., 2003). Two techniques that are commonly used for ion channel studies are the patch-clamp and artificial black lipid membrane (BLM) systems (Berg et al., 2012; Fertig et al., 2002; Sigworth & Klemic, 2002)

1.4.1.3 Cell patch clamping configurations

There are four main configurations for patch-clamping (Molleman, 2002; Terlau & Kirchhoff, 2001) as illistrated in Figure 1.6.

- Cell attached – The capillary is placed in close proximity to the cell membrane. Weak suction is applied to achieve a tight seal between the capillary and the membrane. The main advantage of this method is the

structure of the cytoplasm is not compromised. The disadvantage of this method is that the intracellular environment cannot be controlled.

- Whole cell – A strong suction is applied. This results in a disruption to the membrane patch and access to the cytoplasm. The interior of the capillary becomes continuous with the cytoplasm. As the name suggests, this method can be used to make recordings of the currents and the electrical potentials from the whole cell.
- Inside out – Once the cell is attached to the capillary, it is retracted and the patch is separated from the rest of the membrane. The cytosolic surface of the membrane is then exposed to air. This method is used to examine single channel activity. The main advantage of this method is allowing modifications to the medium, which the intracellular surface is subjected to.
- Outside out – Once the cell is attached to the capillary, it is then retracted. This resuls in two small pieces of membrane. These pieces then reconnect and form a small vesicular structure with the cytosolic side facing the capillary solution. This method is used to study the effect of extracellular cues such as neurotransmitters.

To ensure the success of the patch-clamp techniques, it is important to have high resistance between the two electrodes that are separated by the membrane bilayer (Hamill et al., 1981)

Studying Ion channels in planar BLMs, as explained later, has the advantage of both inside out and outside out configurations because there is access and control over both interior and exterior surfaces of the membrane.

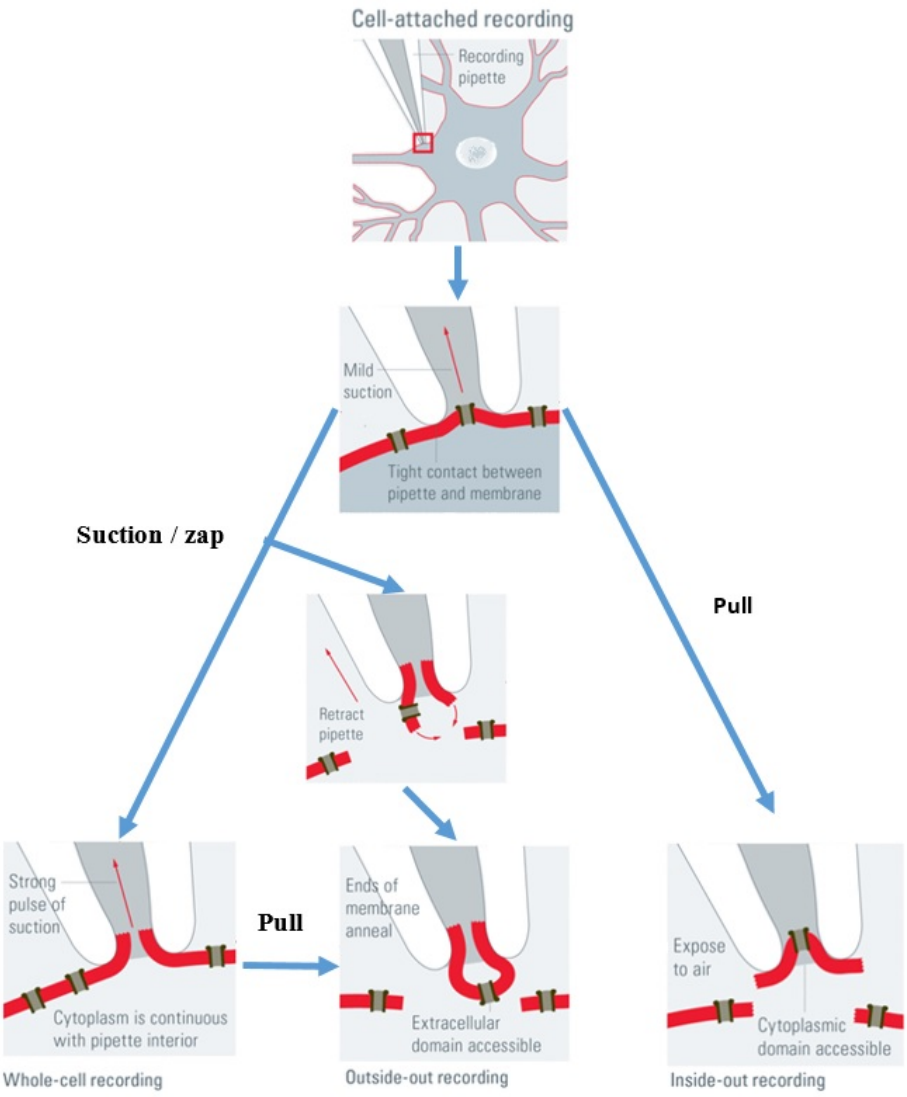

Figure 1.6 The four recording methods for patch-clamp technique
Figure taken from (Sciencelab, n.d.)

1.4.1.4 Automated patch clamp

An ever-increasing cost in time and resources to test a growing number of drug compounds is a driver for constant innovation and automation in the drug discovery industry. It is important to reduce resource waste whilst identifying targets accurately; especially in the early stages of testing where large numbers of drug compounds are tested.

Both drug discovery and side effects detection are important. Serious and unacceptable side effects by drug compound that can block a specific potassium ion channel that is coded by the human ether-à-go-go related gene (hERG) (Masetti et al., 2008), must be detected which necessitates drug testing laboratories routinely carry out hERG-tests (Zou et al., 2010) using high throughput screening (Dunlop et al., 2008).

Several companies (Demarche et al., 2011), have shown the capabilities of automating the once labour-intensive manual patch clamp techniques on cells. An approach that has shown to be effective is the automated array patch clamp technique. This method combines some of the reliability and precision of manual patch clamp technique with a significant increase in throughput.

In these automated patch clamps, live cells in suspension are positioned over patch-size apertures. Similar to the manual patch clamp process, suction is applied to form gigaseal patches. In these configurations, there are often multiple planar apertures that are used to trap the cells.

In recent years many systems for electrophysiological study automation have been developed and brought to market (Dunlop et al., 2008). These commercial systems can have 384 amplifiers and pipets and run hundreds of tests simultaneously. The latest systems can, in theory, test several thousands of compounds per day, but in reality the forming of a gigaseal is still challenging and can reduce test success by as much as fifty percent (Y. Liu et al., 2009).

Some examples of automated electrophysiological systems include the QPatch and Qube 384 from Sophion Biosystems, SyncroPatch 96/384/768PE from Nanion

technologies and Ionworks barracuda from Molecular Devices. The gigaseal reliability issue is quite well known in the pharmaceutical industry. Manufacturers with good gigaseal systems specifically emphasise on this as one of their strong selling points.

As well as expensive setup costs, another disadvantage includes difficulties in guiding the cell to the recording site. Moreover these systems are designed to work with the whole cell patch configuration and therefore unsuitable for examining single ion channels (Zhao et al., 2008). Another limitation of patch clamp technique is that it is very difficult to record channels of endogenous membranes such as cell organelles like mitochondria.

It may be necessary to look at alternative technologies for conducting high throughput studies on ion channels as the relative high start-up cost, combined with increasing demand for experimental throughput, can be a limiting factor.

1.4.1.5 Studying ion channels in Black Lipid Membrane (BLM) systems

Manual cell patch clamping of single cells is expensive, require highly skilled operators and has limited throughput. Automated cell patch clamping is an alternative to conventional patch clamping offering higher throughput, however, this introduces other requirements such as maintaining optimal well-regimented culture conditions for successful assays (Dunlop et al., 2008).

Investigating membrane proteins *in vivo* presents its own difficulties. The complex mixture of proteins can result in aggregation of the recording, which can give rise to errors or misunderstanding. Artificial membrane with selectively implanted proteins systems lend themselves better to characterisation of individual components.

It would be useful to develop an automated high-throughput platform, which enables the study of ion channel activity and behaviour in a live cell-free manner. Systems based on artificial lipid bilayers also known as black lipid membranes (BLMs) - which are a simplified model of the cell membrane, but are capable of incorporating protein channels (Kreir et al., 2012) - are a good candidate for this objective. They offer the prospect of being cost efficient and automatable, but they also present challenges.

These systems retain the essential lipid bilayer structure of biological membranes, but are more suitable for the characterisation of individual components (Reimhult & Kumar, 2008; van Meer et al., 2008). Simplification of the system has led to development of model membranes such as monolayers, bilayers and liposomes (Shen et al., 2013). These have resulted in the capacity for detailed study of membrane protein structure in lipid membranes.

The artificial lipid bilayer membrane resembles the cell membrane patch at the tip of the glass capillary in patch clamp technique that was described earlier. Ion channels can be reconstituted into a membrane but firstly need to be incorporated into liposomes. The ion-channel containing vesicles are then placed into the aqueous electrolytes (Blake et al., 2006). Incorporation of the ion channels occurs as a result of the fusion of the vesicles with the bilayer. Once this has taken place then the tests on the ion channels can be conducted. The system can be treated similar to traditional patch clamp studies.

Single channel recordings can be carried out by the application of voltage clamp across the bilayer membrane (Kongsuphol et al., 2013). This will allow the changes

in ion channel gating to be recorded. Electrical measurements of ion channel activity are directly comparable to those obtained in patch clamp studies. Artificial lipid bilayers have been used to study ion channel activity in many physiologically relevant ion channels. Examples include sodium channels (Neumcke, 1990), big conductance potassium channels - BK or Slo1 (J. Liu et al., 2013), mitochondrial-ATP sensitive potassium channels - mitoKATP (Bednarczyk et al., 2005), acetylcholine receptor (GORE, 1978), as well as others ion channels.

1.4.1.6 Advantages of BLM devices

There are a number of difficulties in creating artificial membrane bilayers. One of the first and most challenging requirements is controlling of nanometre-sized molecules in a micrometre scale environment (Sandison et al., 2007). Depending on biological and chemical requirements of a system, additional limitations may also apply. The surface of the device and its geometry can play a big part in its success. In terms of the material used to produce the system, its wettability and surface roughness are crucial (Zagnoni, 2012). Artificial bilayers in architectures that poorly address these factors are more difficult to form and those that do tend to easily rupture resulting in low success rates.

Although artificially creating and imitating biological systems can be challenging, but the advantages that can be gained from achieving this are significant. The factors that drive the research and development in this field are:

- The reduction of experimental costs
- Highly efficient and sensitive molecular sensors
- Alternative technologies for the study of cellular functions

Advantages of such a system could be the retention of the functionality of freely mobile membrane proteins, achieving single molecule detection levels with Giga-ohm-sealed bilayers and the possibility of integrating microfluidic devices into the system (Suzuki & Takeuchi, 2008). As a result bilayer systems have been employed in various studies to help understanding of different channels including intracellular ca^{2+} regulation (Laver, 2001) and Cystic Fibrosis Trans-membrane Conductance Regulator (CFTR) (Moran & Zegarra-moran, 2008).

1.4.1.7 Electrical properties of BLMs

The lipid bilayer membrane is a dielectric structure formed by the hydrocarbon interior sandwiched between the two polar head regions (H. T. Tien & Ottova, 2003). The simplest equivalent model consists of a capacitor in parallel with a high resistance resistor. The capacitance, C, is proportional to the BLM area and inversely proportional to its thickness. The resistance, R, is inversely proportional to the conductance, G, of the BLM. The specific capacitance can be described as the BLM capacitance divided by its area.

The measurement of the capacitance and the resistance of a lipid bilayer across an aperture can be used for confirming the presence of an optimal BLM. Applying a linear voltage ramp (triangular wave) to a bilayer, should result in a square wave (Bezanilla, 2008). This is due to the differentiating action of the bilayer. This method is used for electrical validation of bilayer formation in an aperture.

The link between BLM specific capacitance and the chain-length of the alkane oil present in the bilayer has been reported (Gross et al., 2011). As the smaller alkane molecules embed themselves between the two monolayers of a BLM, they produce a

thicker membrane. Solvent containing bilayer lipid membranes have a specific capacitance characterisation of 0.4–0.7 μF cm^{-2} depending on the solvent (short or long chain alkanes) (Zagnoni, 2012). The specific capacitance for solvent free bilayers is usually greater and is typically reported as >0.8 μF cm^{-2}. Although capacitance can be measured in a system, it does not necessarily indicate the presence of a successful bilayer formation on its own and must be confirmed by measuring leak current across the membrane.

Ion channel conductance varies with electrolyte salt concentrations. However, typically ion channels add just a few pA (pico amp) to the baseline transmembrane current. Achieving a high giga resistance seal between a BLM and aperture results in a low base-line which aids the detection of low conductance single-channel steps in electrophysiology readings.

1.5 Model membrane systems

The 1930s saw the beginning of cell membrane studies (J. ~F. Danielli, 1936; J. F. Danielli & Davson, 1935). As the understanding of these membranes increased so did the need for bilayer models. In the 60s and 70s new techniques and tools were developed to artificially form these membranes (Montal & Mueller, 1972; Mueller et al., 1962a). The first BLMs were formed across a partition that was coated in Teflon. Electrophysiology measurements were carried out on the membrane positioned between the two aqueous phases.

To create planar artificial lipid bilayers representing a patch of cell membranes, which are roughly spherical in shape, requires lipids dissolved in organic solvent such as decane and a hydrophobic surface, which favours contact with the lipid

hydrocarbon chains (Montal & Mueller, 1972). Bilayer formation in these devices is confirmed electrically by measuring the capacitance of the BLM. Conventionally BLMs were formed by painting (Mueller et al., 1962b), Langmuir Blodgett films (Zasadzinski et al., 1994) and vesicle rupture (Esumi & Yamada, 1993).

Self-assembly of lipid molecules into lamellar lipid bilayers is key to the success of BLM. This is true for the suspended, supported and alternative methods.

1.5.1.1 Modern BLM methods

More modern approaches such as free standing bilayers (Pantoja et al., 2001), droplet interface bilayers (DIB) (Funakoshi et al., 2006; Heron et al., 2007; Hwang et al., 2008; Zagnoni et al., 2009) and tethered bilayers (Andersson et al., 2008) can produce BLMs that are more stable than conventional techniques and can be used in small scale devices.

1.5.2 Suspended BLM

Suspended BLMs are lipid bilayers that have been formed across an aperture with a diameter of several hundred micrometres between two aqueous chambers. There are two main microsystem-based approaches. These are the Mueller-Rudin and the Montal-Mueller method. An illustration of the two methods is shown in Figure 1.7.

- Mueller-Rudin – also known as the "Painting" method, was developed by Mueller in 1962 (Mueller et al., 1962b). In this method, a brush is used for depositing a solution of lipid and hydrocarbon solvents across the aperture. The chambers are then filled with an aqueous solution until the aperture is covered. This results in a monolayer forming in the hydrocarbon-water interface. The solvents mentioned previously, starts to drain and thin to the

edge of the aperture (Mueller et al., 1962b). The monolayers on the two sides of the aperture encounter one another to form a bilayer. This method is referred to as black lipid membrane because, when the two monolayers encounter each other, they appear to optically blacken. The solvent used in this method can cause a few problems. The presence of some solvents can have an effect on the activity of ion channels, therefore, requires careful consideration. The solvents can also affect the thickness of the bilayer, which can in turn have an effect on the activity of the ion channels (Olaf S. Andersen & Koeppe, 2007; Rudnev et al., 1981).

- Montal-Mueller – also known as the "Folding" method was developed by Montel in 1972 (Montal & Mueller, 1972). This method was designed to shorten the time it took to form a bilayer. The edges of the apertures are pre-treated with an apolar solvent. An aqueous solution is then added to the chambers, but only filled below the aperture level. A drop of lipid dissolved in a solvent is added to each aqueous solution. The solvent used is a volatile solvent (such as pentane or hexane) and can evaporate. As the solvent evaporates, a monolayer is formed on the surface of the solution (at the air and water interface). The level of the aqueous solution is then raised passed the aperture in one of the chambers. The lipid monolayer that was formed then bends with the phospholipid tails being orientated vertically. The process is then repeated on the other side of the chamber (White et al., 1976). This results in a bilayer forming very quickly.

A planer bilayer that is attached to the aperture is achieved by using both methods but the Montal-Mueller involves the use of smaller quantities of solvents and can be used to give more reproducible bilayer forming results (Ogden, 1989) . Both sides of

the membrane can be accessible in a BLM configuration, therefore, a variety of test conditions such as asymmetric buffers and perfusion systems can be examined.

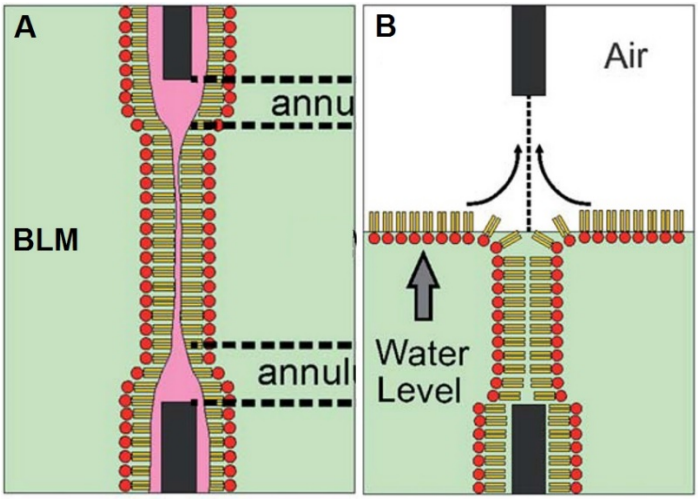

Figure 1.7 Conventional bilayer formation techniques
A) Mueller-Rudin method, B) Montal-Mueller method. Figure taken from (Zagnoni, 2012)

1.5.3 Supported BLM

Supported BLMs are lipid bilayers that were formed on a solid planar support. These solid supports can be gel, glass, silicon or polymer. Using Langmuir-Blodgett transfer Tamm and McConnell characterised the formation of lipid bilayers, which were supported on a range of substrates (Tamm & McConnell, 1985), such as polymers, metals and ceramics (Dong et al., 2006; Groves & Boxer, 2002; Holden et al., 2004; Kreir et al., 2008; Lenz et al., 2004). Supported BLMs can be made from natural lipids as well as synthetic ones. These can be created in a number of configurations such as close contact with the solid substrate or with a space between the substrate and the bilayer.

There is greater interest on horizontal bilayers on solid substrates – collectively referred to as supported lipid bilayers (SLBs) – due to some of the imaging and

analysis limitations of planar bilayers (Alessandrini & Facci, 2011). Supported bilayers are more stable than the suspended bilayers due to the added mechanical stability granted by the solid surface (Belegrinou et al., 2011).

Unlike the suspended methods discussed previously, supported BLMs do not require solvents. These bilayers are produced on the solid surface when there is spontaneous rupture of liposomes or vesicles (Kresák et al., 2009). There have also been BLMs formed on gels (Wiegand et al., 2002), where the gel acts as an ion reservoir. The sturdiness of lipid bilayers can also be increased by encapsulating them between two gel layers (Dong et al., 2006; Mayer et al., 2003; Roerdink Lander et al., 2011).

As mentioned previously, the supported membranes are more stable, but there are also some drawbacks. In SLB, the space between the membrane and substrate is greatly reduced. This results in a reduction in the function and lateral mobility of transmembrane proteins that are incorporated in the bilayer (Salafsky et al., 1996). Electrophysiological measurements can also become more difficult due to the reduced amount of aqueous phase beneath the lower leaflet of the lipid bilayer (Reimhult & Kumar, 2008). To overcome this limitation, polymer supports were integrated into the SLB to increase the space beneath the membrane (Tanaka & Sackmann, 2005). Improvements have also been made in the methods of decoupling the bilayer from the support substrate (Achalkumar et al., 2010).

1.5.4 Droplet interface bilayers (DIB)

Another method for creating artificial bilayers is known as Droplet Interface Bilayer (DIB). In this method, the lipid bilayer is created when two aqueous droplets, each surrounded by lipid/solvent mixture, encounter one another. Each of these droplets

are bound in a lipid monolayer (Funakoshi et al., 2006; Gross et al., 2011; Heron et al., 2007; Hwang et al., 2008; Zagnoni et al., 2009). The Lipid-out technique can be used to create DIB (Bayley et al., 2008) and is shown in Figure 1.8. The principal behind this is two aqueous droplets are deposited into a lipid-solvent mixture. Lipid monolayers then surround the aqueous surfaces of the droplets. As described previously lipid polar heads attach to the aqueous surface and the lipid tails points out into the solution. Bilayers are formed when these lipid monolayers surrounding the droplets come into contact with one another. The simplicity of bilayer formation, which mainly relies on droplet positioning, is one of the main advantages of this method (Lu et al., 2014). There are five main methods for the monolayers to come into contact and become a bilayer:

- Dropping them in close proximity to one another (Ide & Ichikawa, 2005)
- Moving the electrodes that are attached to the droplets (Holden et al., 2007)
- Electro Wetting On Dielectric (Jason L. Poulos, Nelson, et al., 2009)
- Gravity (Jason L. Poulos, Jeon, et al., 2009)
- Controlled fluid flow (Le Pioufle et al., 2008)

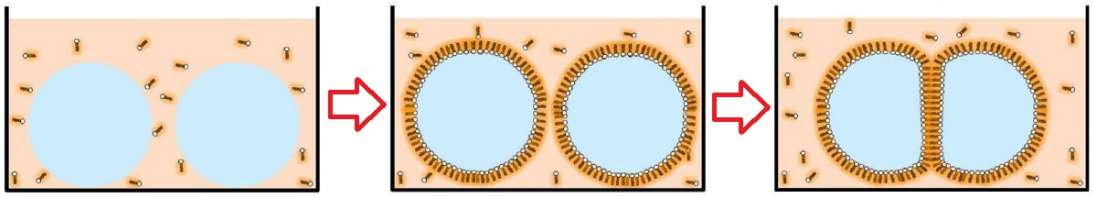

Figure 1.8 The stages of lipid-out technique to form a bilayer
Two separate aqueous droplets are deposited into a lipid-solvent mixture. The polar heads of the lipid molecules attach themselves to the aqueous surface whilst the hydrophobic tails point away and into the solvent mixture. Lipid monolayers spontaneously form around the droplets. Two lipid covered droplets are then brought together and the surrounding monolayers zip together to form a bilayer. Figure adapted from (Kongsuphol et al., 2013)

Tsofina et al published a paper in the mid-60s looking into the production of protein-lipid membranes in aqueous solution (Tsofina et al., 1966). About 40 years later there was great interest in this method again as researchers started to explore and develop methods of creating bilayers (Bayley et al., 2008; Funakoshi et al., 2006; Gross et al., 2011; Heron et al., 2007; Hwang et al., 2008; Zagnoni et al., 2009).

As well as these side by side models, it has also been reported that it is possible to create lipid bilayers using a vertically connected setups (El-Arabi et al., 2012; Zagnoni et al., 2009). These setups are slightly different but achieve the same goal. The lower sections are filled with aqueous solution but the upper section contain the lipid solution. A bilayer is formed once an aqueous droplet is added to the upper section of the device. Same as before, lipid monolayer forms on each side of the two droplets and zip together to form a bilayer when brought close to each other at the intersect.

Forming lipid bilayers using the DIB methods is relatively fast, simple and can be preformed repeatedly. It is also possible to incorporate ion channels into the DIBs by adding the proteoliposomes into the droplets. The ion channels are inserted once the bilayer is formed.

An important feature for a DIB device is the ability to exchange solutions on one side of the bilayer to study the effect of blockers and promoters of the reconstituted ion channels for drug discovery (Tsuji et al., 2013). Although there are number of published DIB platforms, the systems have been used to record bacterial protein activities, which are not pharmacologically relevant to human ion channels. Only recently (Friddin et al., 2013; Hirano-Iwata et al., 2016; Kawano et al., 2013;

Portonovo et al., 2013) have DIB devices been employed to study physiologically relevant ion channels and thus the portfolio of ion channels studied in this way are limited. Therefore, it is useful to develop a reliable methodology to express, purify and reconstitute a variety ion channels into DIBs.

1.6 Objectives

This project had two overarching aims; firstly, to develop a scalable artificial lipid bilayer architecture and secondly, to identify a reliable protein reconstitution method for basic ion channel electrophysiology research in the constructed biomimetic platform.

1.7 Motivations

Ion channels are important pharmacological targets and comprise 1.5% of the human genome (Venter et al., 2001) and play a crucial role in physiological processes (Clapham, 2007; Gouaux, 2005; Okuse, 2007). Thus, a better understanding of their function would aid drug discovery as well as drug toxicity testing. Single ion channel activity is interrogated by electrophysiology techniques which can be broadly categorised into traditional patch clamping and lipid bilayer systems. In patch clamping a glass pipette is attached onto the surface of the cell and a giga-seal is formed. In lipid bilayer constructs ion channels are purified from cells and reconstituted into artificial bilayer setups. The former technique is expensive and requires a skilled operator to carefully position the glass pipette over an individual cell. Systems based on artificial lipid bilayer constructs solve these problems by offering the prospect of being cost efficient and automatable. Although we have seen considerable advancements in automation, miniaturisation and parallelisation of

bilayer systems, the literature remains thin with regards to systematically targeting the problem of functional protein incorporation. Two main approaches are taken for proteins reconstitution, these are detergent solubilisation followed by purification and native/expressed vesicle reconstitution. Detergent solubilisation requires specialist equipment, can be expensive and is not trivial. In the majority of the literature where native/expressed vesicle are leveraged, reconstitution is accompanied by wicking, which is manual (Costa et al., 2013; Kawano et al., 2014) and not scalable. Given these limitations, it would be useful to develop an artificial lipid bilayer platform and methodology which, in tandem, could tackle the above-mentioned challenges and make ion channel electrophysiology more feasible and accessible. The downstream impact of this could potentially be advancement in membrane protein studies at cost-effective rates.

1.8 Novelty

To address the issues discussed previously for ion channel studies, a droplet interface bilayer (DIB) platform capable of simultaneous bilayer formation has been designed and developed. A protocol to form stable synthetic lipid bilayers in this multi-chamber system was therefore identified. The platform was successful in recording single peptidic channel activities as well as channel blocking events. For these peptidic channels, the reconstitution time was shortened by varying the timing of peptide insertion. A relatively simple detergent-free channel isolation and reconstitution method from recombinant overexpressing cell membranes was employed to study a pharmacologically relevant eukaryotic channel, BK STREX. A reconstitution success rate of 29% was achieved by devising a technique based on the ratio of bilayer area to droplet surface area. To the best of our knowledge this is the

first-time recombinant expressing cell fragments have been reconstituted in this way in a DIB system. The platform and procedures laid out in this thesis are likely to be applicable to other eukaryotic ion channels leading to new approaches for drug discovery and drug screening.

2 Chapter 2: General Materials and Methods

2.1 Chip Design and Fabrication

The Droplet Interface Bilayer (DIB) chip and multi electrode holder, attached to the electrode positioning system in Figure 3.19, were designed in PTC Creo CAD software and fabricated by stereolithography 3D printing (Aureus, envisionTEC, Germany) using photopolymer R11 (envisionTEC, Germany). The stereolithography machine was calibrated as per the manufacturer's instructions every time before use. As shown in Figure 2.1, the 3D objects were printed layer by layer in a bat configuration (Bhattacharjee et al., 2016), at a resolution of 25µm in the Z-direction, by using selective light exposure to photo-polymerise the resin. 14 devices as listed in Table 3.1 were fabricated.

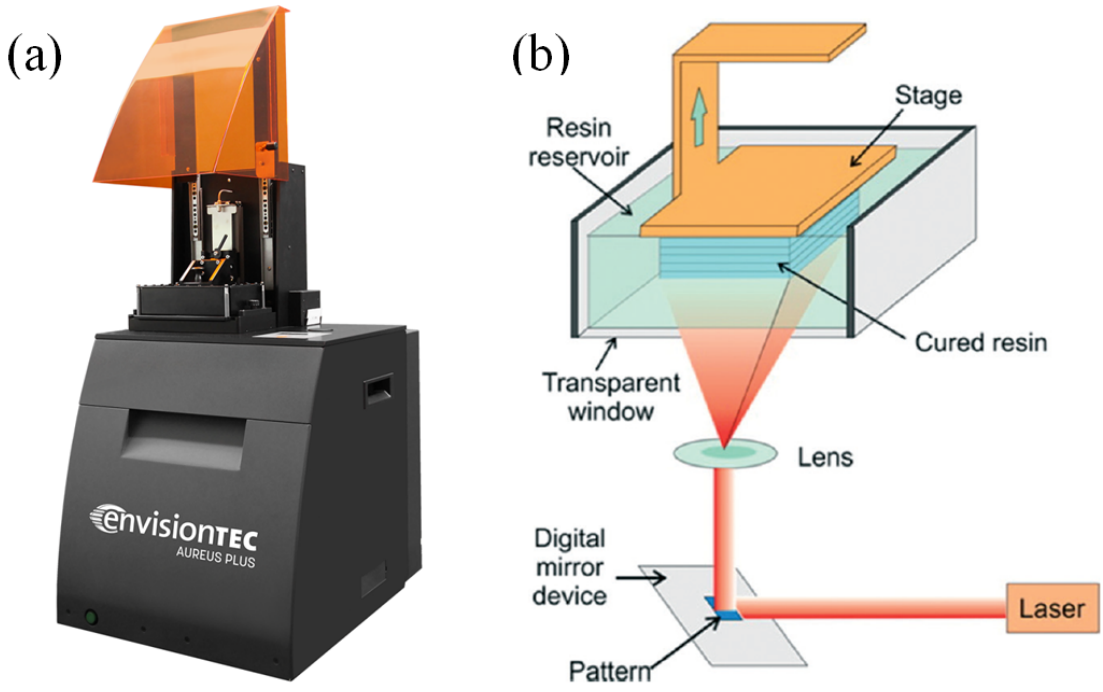

Figure 2.1 Stereolithography machine and configuration
Overview of (a) stereolithography machine and (b) fabrication principle. Light is projected onto the stage causing photopolymer curing plane-by-plane realising rapid prototyping. The stage on which the 3D object is formed is raised by 25µm after each projection. Figure taken from (Bhattacharjee et al., 2016).

2.2 Lipid Preparation

Lipid solution 1,2-diphytanoyl-sn-glycero-3-phosphocholine (DPhPC) (Avanti Polar Lipids, US) in chloroform, known concentration, was taken from freezer and pipetted to a glass vial. Subsequently the chloroform was carefully evaporated using a stream of nitrogen until a waxy film was visible. The vial was then placed under vacuum for 30 minutes to ensure complete evaporation of chloroform. Decane was then added to the desired final concentration. The waxy film was dissolved by vortexing. The sample was used immediately and was kept at room temperature.

2.3 Electrophysiology Reagents

Electrolyte solution for bilayer formation (chapter 4), alpha hemolysin and gramicidin experiments (chapter 5): 100mM KCl, 10mM HEPES buffer, deionised water and KOH were mixed together to achieve a final buffer pH of 7.4.

Alpha Hemolysin (Sigma Aldrich, UK) was made up to a concentration of 20 μg/mL in the above mentioned KCl buffer. Gramicidin (Sigma Aldrich, UK) was made up to a concentration of 1 pg/mL in ethanol (Fisher Chemicals, UK).

Electrolyte solution for Bk experiments (chapter 6), cis side: 300mM KCl, 10mM HEPES, 1.1mM HEDTA ($[Ca^{2+}]_{free} \approx 50\mu M$), 1.05mM CaCl2, deionised water to achieve a final buffer pH of 7.2.

Electrolyte solution for Bk experiments (chapter 6), trans side: 30 mM KCl, 10 mM HEPES, 0.1 mM HEDTA, deionised water to achieve a final buffer pH of 7.2.

2.4 Bilayer Formation

A schematic of the double well chamber and bilayer formation procedure is shown in Figure 3.4. Bilayer formation procedure takes place in the faraday cage. Empty chambers are initially washed with 70% ethanol and water three times and dried under a stream of nitrogen. Depending on well geometry, an appropriate amount of lipid/decane mixture, 30 μL in the case of Device 4, is pipetted into the chambers. Then a droplet of electrolyte solution, 31 μL in the case of Device 4, was injected into one well, given a few minutes to stabilise (Hwang et al., 2008) where a monolayer of lipids quickly forms around the droplet with lipid hydrophilic head attached to the water surface and tails sticking out towards the oil solution. Then a second symmetrical droplet was added to the remaining well. Upon droplet contact, self-assembled monolayers at the oil-water interfaces of the aqueous volumes 'zip' together to form a stable bilayer at the interface of the two wells.

2.5 Electrode Preparation

Ag/AgCl electrodes were used as voltammetric sensors to measure current flowing through the electrode-solution junction for a given applied potential (DEMPSTER, 2001).

Silver electrodes, 99.99% purity and 1.2 mm in diameter, were chlorided by both electrical and chemical methods to make Ag/AgCl electrodes. In both methods, the silver electrodes were cleaned with ethanol and rinsed with water before proceeding. Old chlorided electrodes were first wiped with dilute HCl to remove the previous coating before proceeding with ethanol and water.

Electrical method: The silver wire was connected to positive terminal in a DC source and platinum wire was connected to negative terminal. Both immersed in a HCl /deionised water solution (dilution 1 acid: 10 water) and current was passed. The silver electrode rapidly darkened to a grey/purple colour due to precipitation of insoluble AgCl salt on the anode surface while small bubbles of hydrogen gas emerged from the platinum cathode as a result of the dissociation of HCl.

Chemical method: The silver wire was immersed in household bleach for 15 minutes until a grey colour appeared.

2.6 Faraday Cage and Contents

For electrical measurement of BLM capacitance and electric current a patch clamp amplifier (Pico 2, Tecella, USA), multi-channel patch clamp amplifier (Triton, Tecella, USA) and a personal computer with WinEDR (version 3.3.7, Strathclyde University, Dempster, 1996-2015) and WinWCP (version 4.5.8, Strathclyde University, Dempster, 1996-2015) softwares to capture data were employed. WinWCP was used to confirm bilayer formation, as shown in Figure 2.2, whilst WinEDR was used to capture single channel activity. A triangular input signal of +100mv with a half periods of 10ms and 100ms was applied and current was measured. The amplifiers were calibrated first by connecting to a parallel RC circuit consisting of a 5G ohm resistor and a 1nF capacitor. In bilayer and electrophysiology experiments the Ag/AgCl electrodes were inserted into separate aqueous compartments as depicted in Figure 3.5. The bilayer capacitance was calculated using the following relationship:

$$C = I/(\frac{dV}{dt})$$

C is capacitance, I is current and (dV/dt) is the change in voltage over time. To minimise electrical noise the entire set-up excluding the personal computer was housed in a Faraday cage, show in Figure 3.19, which was grounded by connecting to a common ground to reduce electrical noise and AC interference. The common ground on the patch clamp amplifier was connected to the faraday cage. To dampen the effects of noise caused by surface vibration the set up was raised from the surface of the bench and placed on heavy metal blocks.

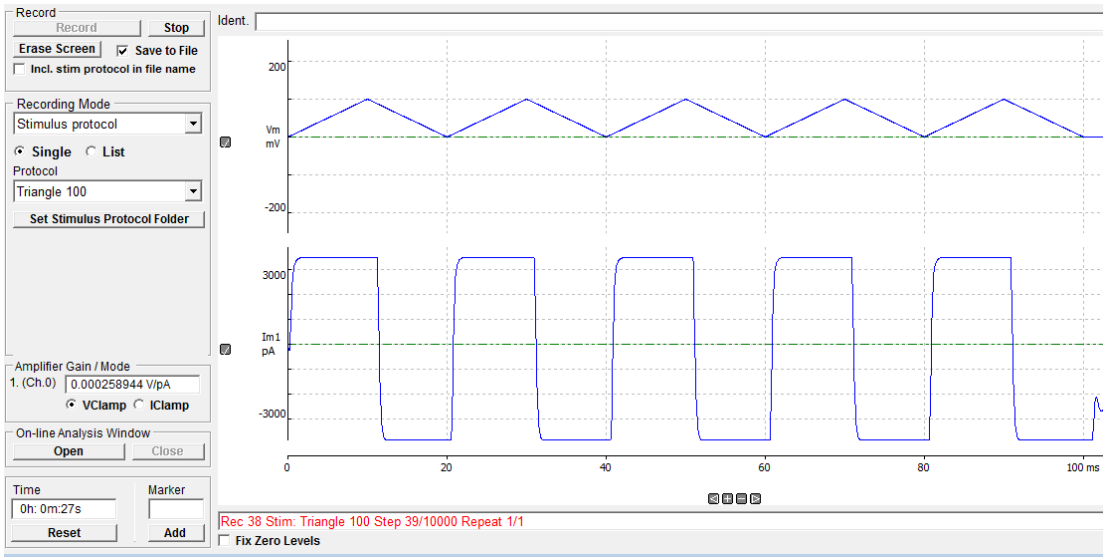

Figure 2.2 Bilayer formation confirmation with WinWCP software
An example of a fully formed bilayer using Pico 2 amplifier as captured by WinWCP software. As demonstrated a triangular voltage is applied and a square current output is observed as expected in the case of a bilayer. Bilayer formation was further confirmed by WinEDR software to observe almost zero current across the bilayer in the absence of reconstituted ion channels and peptides.

2.7 Cell Culture

2.7.1 Cell line

Human Embryonic Kidney (HEK-293) cell line heterologously expressing STREX splice variant of the BK potassium protein channel were (a gift from Dr E Rowan) grown to confluence. HEK-293 cells do not endogenously express BK STREX. The presence of the cloned BK STREX channels expressed by stably transfected HEK-293 was confirmed by traditional patch clamp electrophysiology by Dr E Rowan (unpublished data). The HEK-293 cell line was robust and easily maintained. The cell line grew as monolayers with an epithelial morphology and exhibited contact inhibition.

2.7.2 Culture preparation and medium

A sterile hood (class II biological safety cabinet), was prepared by spraying and wiping with 70% ethanol. All items in the hood including tissue culture flasks, solutions, wrapped pipette tips, pipette and beaker were sterile and sprayed with 70 % ethanol. Solutions were equilibrated at 37% in a water bath prior to use. A sterilised incubator at a temperature of 37 °C and humidified at 95% air / 5 % CO_2, provided the growth conditions.

Cells were maintained in Roswell Park Memorial Institute (RPMI) 1640 medium. The medium contained: DMEM (GibCo-BRL, UK), 10% foetal calf serum (FCS) (Sigma-Aldrich, UK), 1 % sodium pyruvate (Sigma-Aldrich. UK), 1% l-glutamine (Sigma-Aldrich. UK), 1% non-essential amino acid and 1% gentamycin antibiotic.

2.7.3 Cell recovery from frozen and maintenance

The HEK-293 cells were received in cryopreserved format. It is vital that the cells are recovered correctly from frozen to maximise viability and cell recovery. It is standard practice to thaw cells quickly as cryoprotectants, such as DMSO, may be toxic above 4 °C.

The cryovial of cells frozen in liquid nitrogen was thawed rapidly at 37 °C and distributed in 150 cm^2 culture flasks, prepared with RPMI 1640 medium equilibrated at 37 °C. The medium was replaced once the cells had attached. The flasks and cells within were regularly examined under the inverted microscope and colour of growth medium was noted as it indicated medium pH. The medium was replaced when the cells were passaged and when required to propagate the cells, as indicated by changes in the pH of the medium. Yellow medium indicated all the nutrients in the media had been used, while pink coloured media indicated that the environment was alkaline and the cell growth inhibited. This may have occurred due to cell death and/or contamination. If cells required no attention then the flasks were returned to the CO_2 incubator.

2.8 Gel Electrophoresis (SDS PAGE)

Sodium dodecyl sulphate polyacrylamide gel electrophoresis (SDS PAGE) is a technique used to separate proteins according to their electrophoretic mobility which is a function of the length of the polypeptide chain or molecular weight (Kutzbach, 1997). SDS is an anionic detergent which denatures secondary and non-disulfide-linked tertiary structures, and applies a negative charge to each protein in proportion to its mass. Proteins are subsequently loaded onto a polyacrylamide gel immersed in

buffer. An electric potential applied across the gel induces the migration of proteins down the gel by electrophoresis. The polyacrylamide matrix causes smaller proteins travel faster through the pores of the gel whilst larger proteins move slower, leading to protein separation. The proteins are usually visualised by staining using Coomassie Brilliant Blue which reveals a series of bands. Ladders with known protein molecular weights are added in adjacent lane to target proteins and are used to identify the protein of interest, in our case BK STREX. An overview of the method is shown in Figure 2.3.

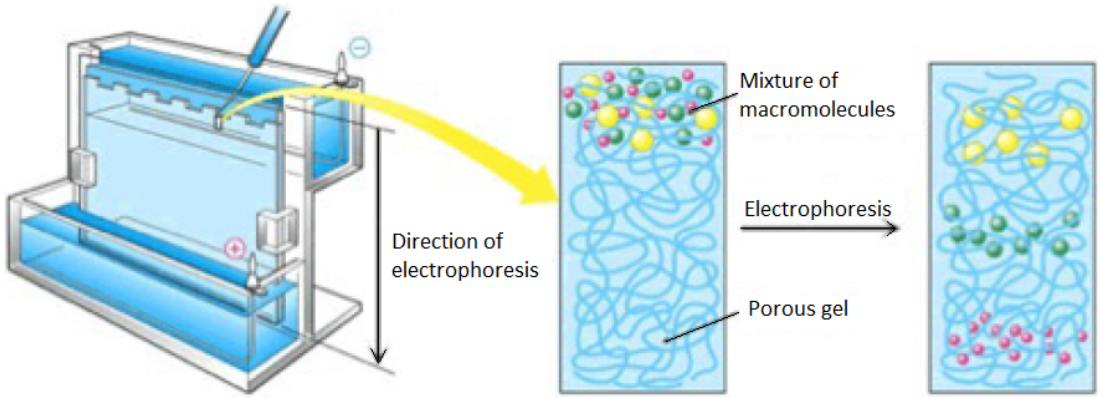

Figure 2.3 SDS PAGE technique for protein separation.
(left) Denatured protein mixed with SDS is loaded onto a polyacrylamide gel immersed in electrolyte buffer. The SDS applies a negative charge on the denatured proteins, causing them to travel down the gel in unison in the presence of a voltage potential. (right) Porous polyacrylamide gel matrix causes slower large proteins to remain at the top of the gel while smaller proteins move to the bottom. Figure taken from (Bertoni & Hardin, 2015).

SDS PAGE was carried out using standard techniques. Briefly, 12% SDS PAGE resolving and stacking gels were prepared using the mini-PROTEAN system (Bio-Rad Laboratories, UK). Resolving gel comprised of 1.5M Tris base, 10% SDS and distilled water, final pH 8.8. Polyacrylamide was then added followed by TEMED and APS. The gel was cast inside the fume hood and left to set for 50 minutes underneath a small volume of isopropanol, used to create a smooth interface for the adhesion of the stacking layer. Stacking gel comprised 0.5M Tris base, 10% SDS and

distilled water, final pH 6.7, polyacrylamide, TEMED and APS. The stacking layer was cast on top of the resolving gel once the isopropanol was removed and a gel comb was inserted for the creation of the wells. The comb was removed once the gel had set and the gel was transferred to the gel tank. Gel tank was filled with 1 L of running buffer containing 150g glycine, 30g Tris base, 10g SDS in 1 L of dH_2O at final pH 8.3. Protein samples were denatured by heating at 99 ºC for 3 minutes and loaded onto the gel. Prestained molecular weight marker (Sigma Aldrich, UK) was loaded in the first lane and used as molecular weight standard. The gels were allowed to run at 160 V for 90 minutes.

2.9 Western Blotting

Western Blot was performed after SDS PAGE gel fractionation of the BK STREX sample to visualise the protein and therefore confirm the presence of BK channel following protein purification and isolation steps as described in chapter 6. This immunoblotting technique attaches antibodies to the target protein in a given sample. The proteins fractionated by SDS-PAGE are transferred to a membrane sheet. The membrane is then treated with blocking buffer, fat-free dried milk or bovine serum albumin (BSA), in order to block the binding of antibodies to non-specific sites. Primary-antibodies are next added to the membrane sheet to bind the specific proteins followed by secondary antibodies, containing a detectable signal, that attach to the primary-antibody. Finally, the protein of interest is visualised by either an infra-red dye for detection by infra-red or horseradish peroxidase for detection using chemiluminescence. The observed signal allows the presence of the expressed ion channel to be verified.

There are a number of advantages and disadvantages to this method. The technique allows for a better separation and detection of proteins in a mixture on the basis of size, charge as well as conformation. The option of stripping of primary antibodies from the proteins of interest, means many different proteins can be detected in one assay. As SDS PAGE is carried out as part of the process, the molecular weight of the proteins is determined as well. The main disadvantage of western blotting is that it is time consuming. In order to get precise results, both the theoretical and practical knowledge of the process, the role of the involved material and the properties of the protein of interest are very important. The antibodies used in this technique can be expensive which pushes up the total cost of the experiments. Also, the non-specific binding of the antibodies to other proteins sometimes produces confusing results.

In this study, following the completion of SDS PAGE step as described in previous section, BK protein channels were electro-transferred to nitrocellulose membrane. To do this a piece of nitrocellulose paper was cut and dampened with transfer buffer together with two sets of sponge-filter paper. As shown in Figure 2.4, the gel sandwich was constructed in this order: support grid, sponge/pad, filter paper, gel, transfer membrane, filter paper, sponge/pad, support grid. The nitrocellulose paper was situated on the anode facing side of the gel. The setup was immersed in a transfer tank filled with transfer buffer and connected to a power pack and the Western transfer ran for 2 hours at 100V.

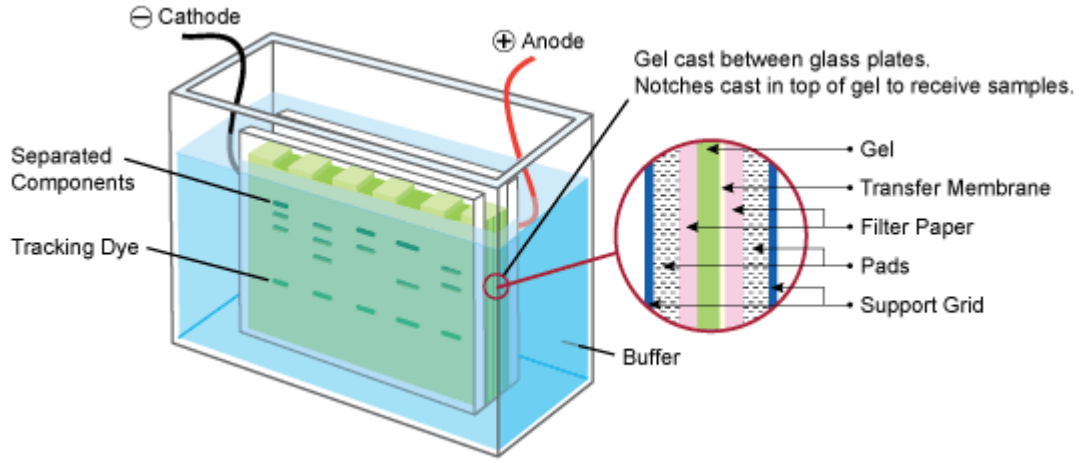

Figure 2.4 Illustration of Western blot setup
A schematic diagram of the fundamental components required for a western transfer. Transfer direction is from cathode to anode. Figure taken from (LeincoTechnologies, 2013)

Subsequently the nitrocellulose paper was blocked overnight on a rotating platform in 0.1% (v/v) tween, 5% (w/v) milk in TBST at 4 ºC. The nitrocellulose was then washed for 1 hour in a solution containing 0.1% tween (v/v), 5% milk and the primary antibody anti-BK L6/60 (UC Davis/NIH NeuroMab Facility, US) prepared to a final concentration of 1 µg/ml in TBST. The antibody solution was then removed and the nitrocellulose paper was briefly soaked in water, which was then replaced with wash buffer containing 3% BSA in TBST. The nitrocellulose was left soaking in the wash buffer on the rotating platform for 10 minutes before the wash buffer was replaced with fresh solution. This was repeated a total of three times. The nitrocellulose paper was then incubated for 1 hour with a solution containing a horseradish peroxidase (HRP) conjugated anti-mouse raised in rabbit secondary antibody (BioRad, UK), prepared at 1:1000 dilution in TBST containing 3% BSA, 0.1% tween. The nitrocellulose paper was then dried and transferred to a darkroom for chemiluminescent imaging using photographic film. The nitrocellulose paper was developed Thermo SuperSignal West Dura ECL detection reagent (Life

Technologies, USA) for 2 minutes and photographic film was placed on top of the nitrocellulose paper for 30 seconds in a light-proof box. The film was subsequently exposed to X-ray in an X-OMAT imaging machine to visualise the results.

3 Chapter 3: A platform for BLM formation

3.1 Application Considerations for Designing a DIB Platform

3.1.1 Market Segmentation

The drug discovery market is composed of defined segments (Xu et al., 2001) where ion channel assays generate knowledge capital. These are: basic research, primary screening, secondary screening and safety screening. The design of BLM constructs to service each segment would have to satisfy a particular set of technical requirements pertinent to the objectives of that segment. As shown in Figure 3.1 the attributes profile for a Primary screening BLM platform, for instance, differs from a BLM device targeting Secondary screening by placing higher importance on cost, robustness and throughput. The above-mentioned segments are defined as:

Basic research – the objective here is to study the behaviour and functionality of biological components under normal, disease and therapeutic conditions. Ion channel assay technology contributes to target identification and target validation in this area. Basic research calls for technologies with high information content, high specificity and low cost but demands less in system throughput. Common technologies in this segment are radioactive flux assays, patch clamping and ion indicator dyes.

Primary screening – the purpose here is to test a significant assortment of chemical stimuli against ion channels of interest. The data collected from primary screening is analysed to identify lead compounds through compiling structure-activity relationships. High throughput and robustness are key requirements whilst high

information content is not crucial. Traditional technologies in this segment are fluorescence and flux-based.

Secondary screening – the data mined during primary screening is used to compose focused repositories. These libraries are used in secondary screening to identify related chemicals with improved properties. As compared to primary screening, fewer compounds are tested during this phase, however they are inspected further for their chemical and physiological properties as they become more advanced lead pharmaceutical candidates. Preferential assay methods such as patch clamping which offer high sensitivity and specificity are employed in this segment.

Safety screening – this relates to testing drugs that could adversely impact the human Ether-a-go-go (hERG) channel, a voltage gated cardiac myocyte membrane potassium channel, leading to long QT syndrome and torsades de pointes (Finlayson et al., 2004; Masetti et al., 2008; Wible et al., 2005) resulting in potentially fatal cardiac arrhythmias. The requirements for this segment are similar to secondary screening. Patch clamping and fluorescence-based methods are used for HERG toxicological screening.

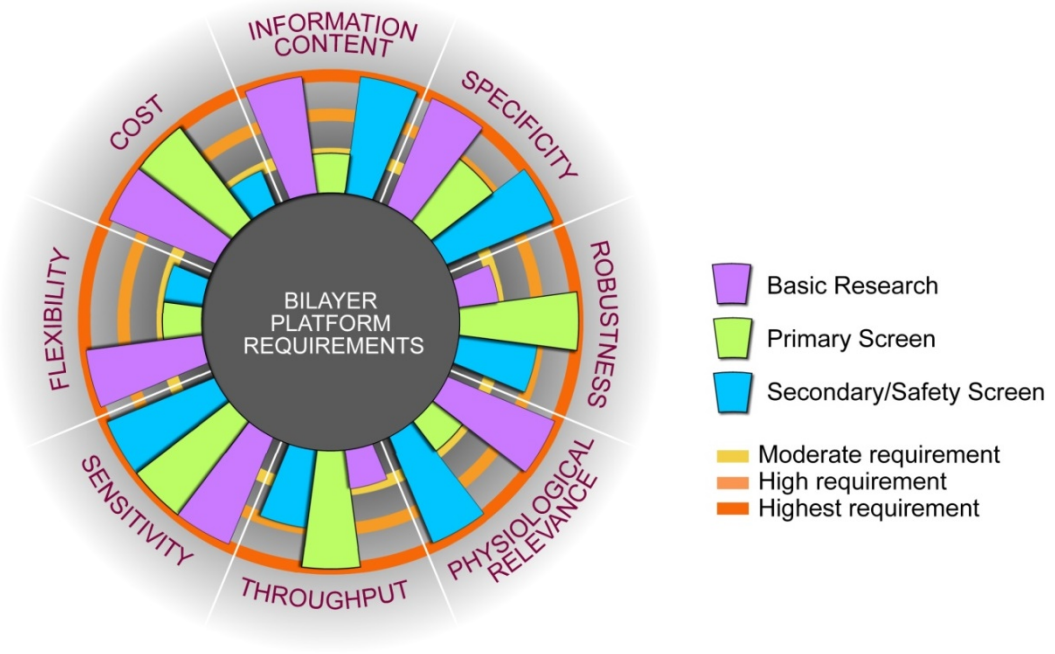

Figure 3.1 Bilayer platform requirements
Illustration of the bilayer platform requirements, ranging from moderate to highest, for each market segment: basic research, primary screening, secondary screening and safety screening.

3.1.2 Platform Requirements

The relevant bilayer platform attributes are captured by Figure 3.1 and are defined as below (Xu et al., 2001):

Information content – is the amount of collectable data from a single test such as temporal resolution and morphological attributes.

Specificity – is the ability of an assay to distinguish between different types of stimuli. A low false-positive rate is an indication of high specificity.

Robustness – is the ability of the assay to withstand changing experimental conditions. High reproducibility indicates high robustness of a platform.

Physiological relevance – describes the relevance of the result of tests to a physiological situation. Relevant assays produce data similar to physiological conditions.

Throughput – is a measurement of test speed and the number of data points acquired in a given time frame.

Sensitivity – describes the minimum change of signal that can be reliably detected. In the context of ion channels studies, it describes the ability of the system to detect channels with small or fast conductance characteristics. A highly sensitive assay will feature a low false-negative rate.

Flexibility – is about versatility and adaptability of the platform to test different ion channels and compounds.

Cost – measures the consumption of resources such as money, manpower, manufacturing time and experiment duration. For example, a platform that can be easily fabricated and is readily operated by a less-skilled operator is desirable. Cost is commonly measured by the cost per data point.

The objective of this project was to develop a novel platform suitable for conducting basic research. With this in mind a sequential waterfall approach to system development was employed by gathering requirements, designing several solutions, fabricating chips, testing built devices and optimising promising candidates and finally scaling out thereby achieving higher assay bandwidth. The cascading engineering evolution is illustrated by the DIB platform funnel in Figure 3.2 and each step is further explained in this chapter.

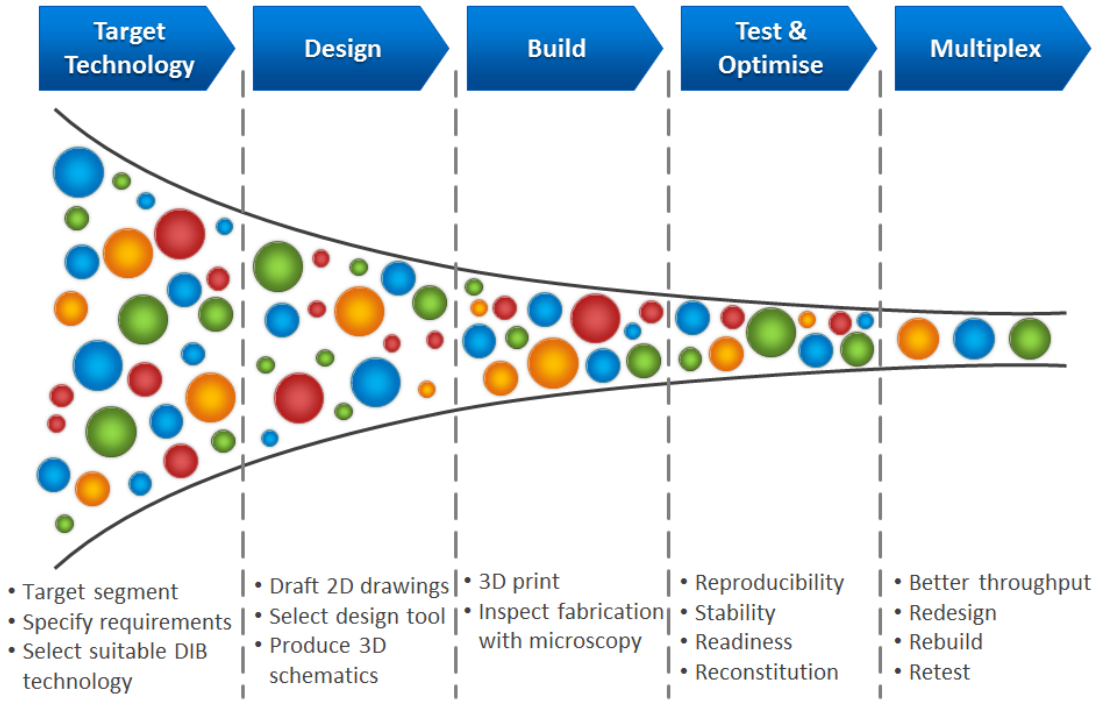

Figure 3.2 Novel DIB Platform Funnel
Illustration of project approach to produce a final DIB architecture solution.

3.2 Technology Selection

Amongst the existing technologies surveyed, the DIB method of BLM formation was selected. Factors driving this decision over other techniques, on top of DIB platform capability to satisfy previously mentioned design criteria for basic research, are practical aspects including the ease of bilayer formation, tight giga-ohm electrical seal, amenability to automation and parallelisation and the potential for simple fabrication methods. Another important feature for a DIB device is the ability to exchange solutions on either side of the bilayer to study the effect of blockers and promoters of the reconstituted ion channels for drug discovery (Tsuji et al., 2013). Electrophysiology was selected as it offers the possibility to investigate proteins at single channel resolution (Fertig et al., 2002; Mayer et al., 2003; Pantoja et al., 2001). Stereolithography, a 3D-printing and rapid prototyping method based on

photopolymerization (Low et al., 2017), was chosen over soft lithography as the suitable fabrication technology due to its automated, assembly-free 3D fabrication, rapidly decreasing costs, and fast-improving resolution and throughput (Bhattacharjee et al., 2016). Moreover, 3D-printing offers the ability to create and quickly redesign almost any geometrically complex structure or feature in a range of materials across different scales. Although there are number of published DIB platforms, these systems have been used to record bacterial protein activities which are not pharmacologically relevant to human ion channels. Only recently (Friddin et al., 2013; Kawano et al., 2013; Portonovo et al., 2013) DIB devices have been employed to study physiologically pertinent ion channels and thus the portfolio of ion channels studied in this way are limited. This demonstrates the difficulties associated with development of a robust high-resolution BLM platform as well as the formulation a reliable protocol for bilayer formation and ion channels insertion in DIB constructs. The proposed solution and experiments described in this thesis aims to overcome these challenges.

3.3 Design

Amongst the DIB architectures studied (Funakoshi et al., 2006; Hwang et al., 2008; Kawano et al., 2013; Lein et al., 2013; Leptihn et al., 2013; Portonovo & Schmidt, 2012; Thapliyal et al., 2011; Tsuji et al., 2013; Zagnoni et al., 2009) a double-chamber chip configuration, visibly similar to the approach taken by Funakoshi et al, as shown in Figure 3.3 was designed.

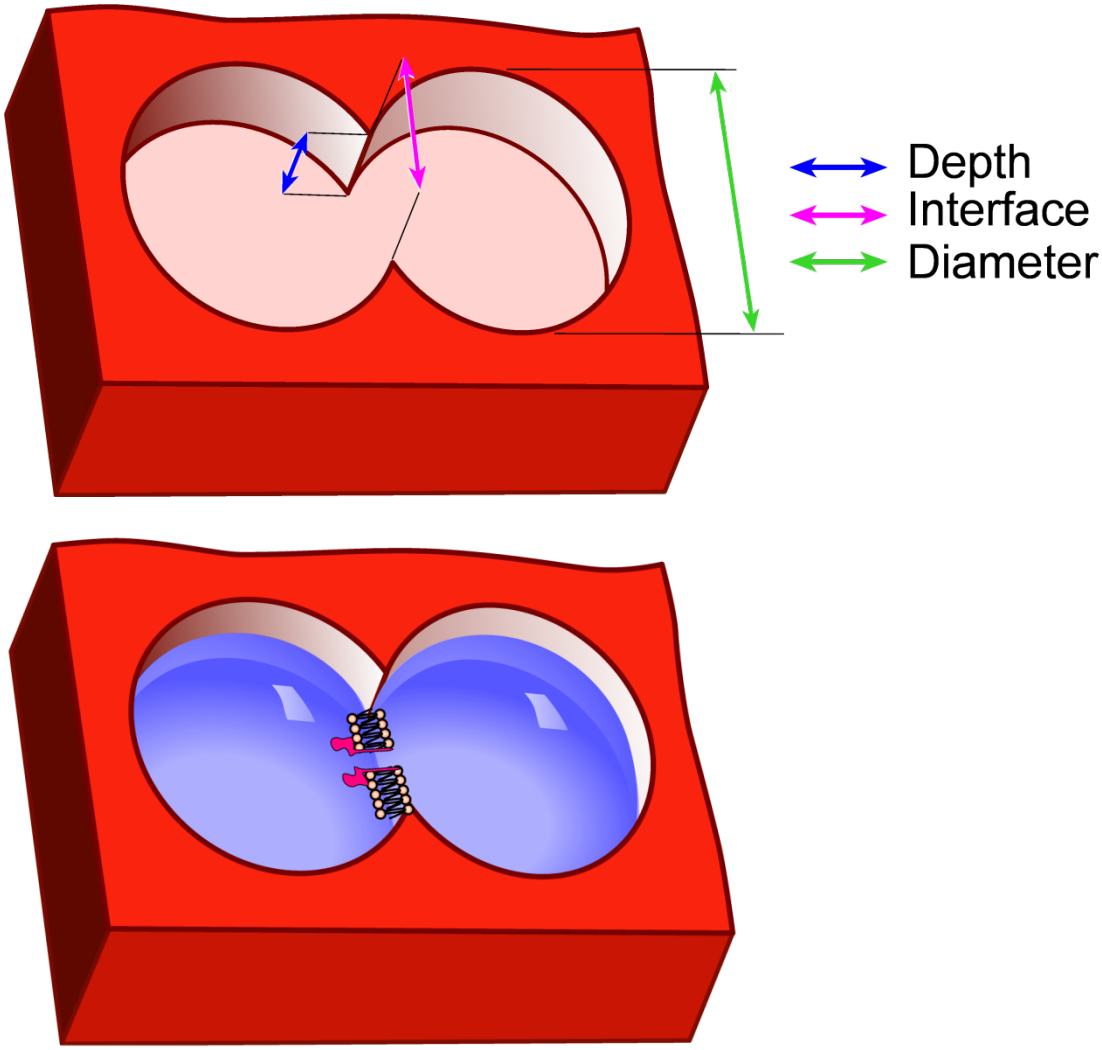

Figure 3.3 Schematic of double chamber chip
The overlapping chambers are open to allow electrode insertion for bilayer formation confirmation and electrophysiological measurements. (Top) The dimensions of the diameter, depth and interface were varied and resulting characteristics were studied to produce a suitable solution. (Bottom) A bilayer forms where the two droplets meet. Protein channels, such as alpha-hemolysin, reconstitute into the bilayer as shown.

This design, in theory, satisfied all the previously mentioned criteria, was amenable to stereolithography, monolayer contact was conceptually straightforward and did not require precise electrode positioning. The steps leading to bilayer formation in this configuration are depicted in Figure 3.4.

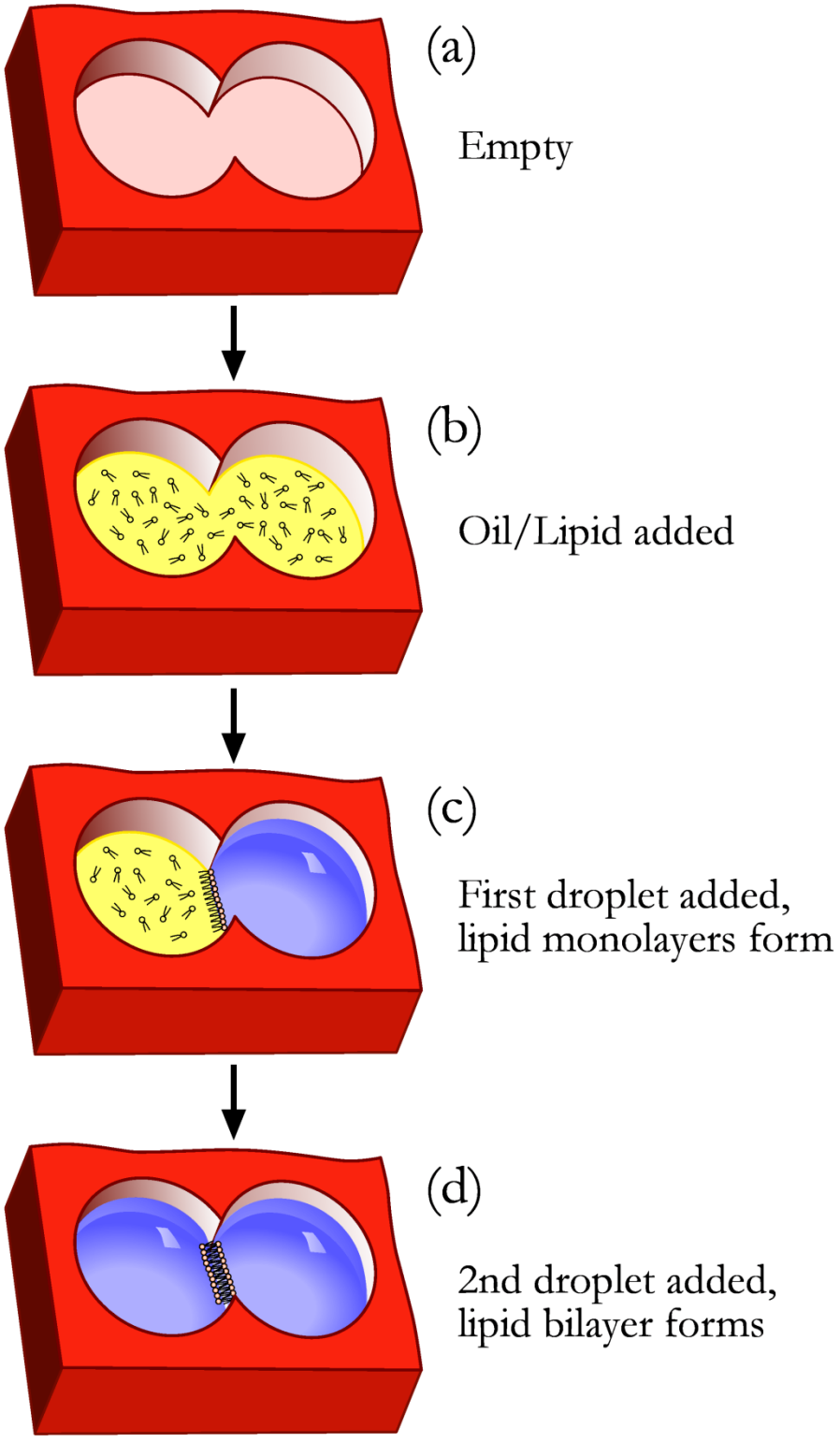

Figure 3.4 Conceptual diagram of Droplet Interface Bilayer (DIB) formation
In the above illustration (a) the chambers are initially empty, (b) an appropriate amount of solution containing lipid in an alkane such as decane is pipetted into the wells. (c) a droplet is deposited into right chamber where a monolayer of lipids quickly forms around the droplet with lipid hydrophilic head attached to the water surface and tails sticking out towards the oil solution. (d) a second droplet is added and upon contact, self-assembled monolayers at the oil-water interfaces of the aqueous volumes 'zip' together to form a stable bilayer.

Table 3.1 A number of permutations of the double-chamber chip configuration were drafted in 3D

Device Number	Diameter (mm)	Depth (mm)	Interface (mm)
Device 1	4	3	2
Device 2	4	2	2
Device 3	5	3	2
Device 4	5	2	2
Device 5	5	3	1
Device 6	5	2	1
Device 7	5	3	0.5
Device 8	5	2	0.5
Device 9	5	3	0.45
Device 10	5	3	0.4
Device 11	5	3	0.35
Device 12	5	3	0.3
Device 13	5	3	0.25
Device 14	5	3	0.2

As shown in Table 3.1 a number of variations in chamber diameter, depth and interface were drafted in 2D and designed in 3D computer-aided design package (Solidworks) in order to understand the relationship between the bilayer area, the droplet volume and the interface area with a view to find a configuration that produces stable, fast forming and reproducible bilayers suitable for protein ion channel experiments.

3.3.1 System Bandwidth

The bandwidth range of the platform was considered at the design stage by identifying and analysing an equivalent electrical model. From an electrical point of view a bilayer is similar to a capacitor as it separates charge over a distance since the hydrophobic tales of the phospholipid molecules are impermeable to charged particles. As illustrated in Figure 3.5 the double-chamber configuration is shown from the top with the equivalent RC electrical components superimposed over the physical parts the electrical component represent. The droplets can be thought of as resistors since the buffer allows electrical charge movement from the submerged electrodes to the bilayer interface. A reconstituted protein channel, such as alpha-hemolysin (α-HL), can also be modelled as a resistor since it permits current flow across the bilayer. The two triangular edges where the chambers overlap also act as a capacitor as they also separate charge over distance.

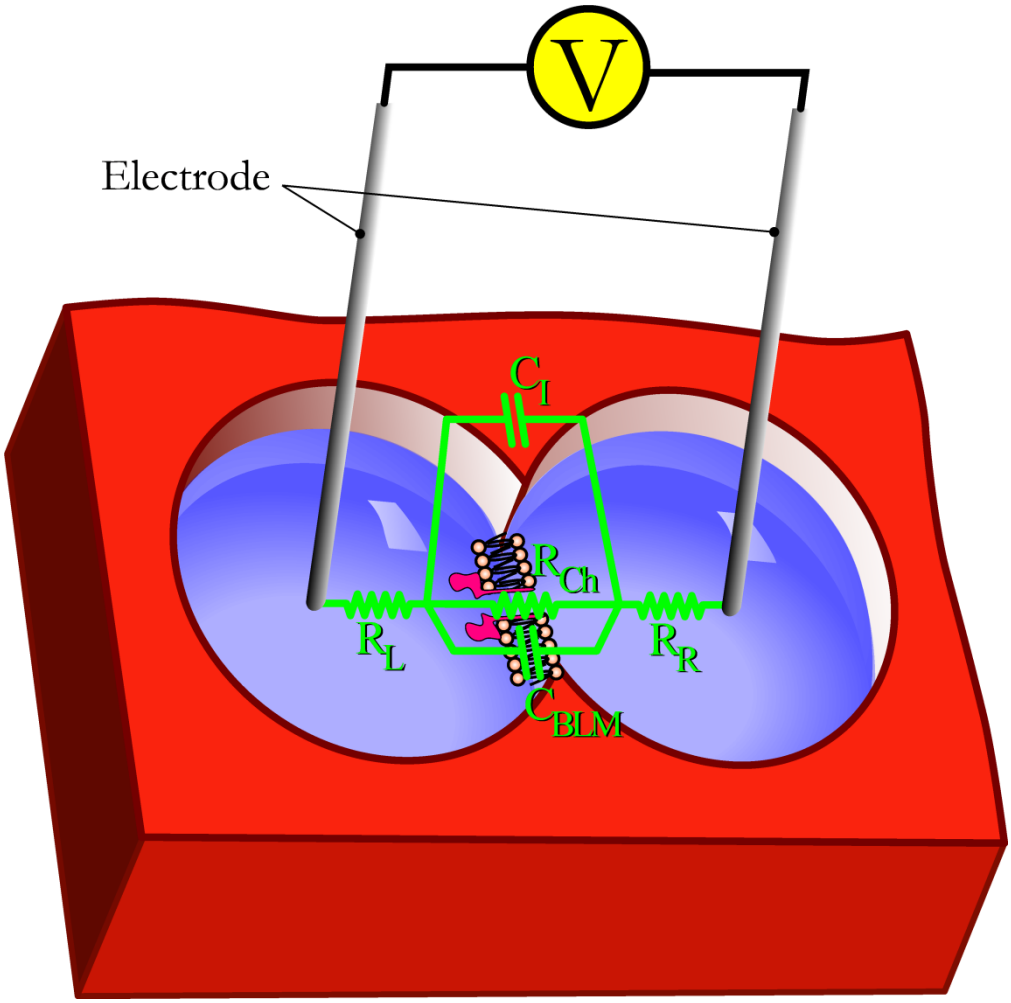

Figure 3.5 Double chamber DIB platform with equivalent RC circuit model superimposed
The resistor elements are the reconstituted protein channel and left and right droplets. The capacitor elements are the bilayer and the triangular edges of the interface.

The electrical circuit from Figure 3.5 can be transformed into a Thevenin equivalent circuit, which yields a simple series RC circuit that can be analysed by inspection. Figure 3.6 depicts the Thevenin transformation of the bilayer RC circuit. An important RC circuit bandwidth indicator is the time constant τ, which measures how fast a system reacts to an input stimulus which in the context of electrophysiology could be a channel opening event or a blocking event. A system with a small time constant settles to a new output state faster than a system with a large time constant, thus a biosensor that supposedly detects molecules traversing the BLM will need a

time constant faster than the molecule's translocation time or detection will not occur.

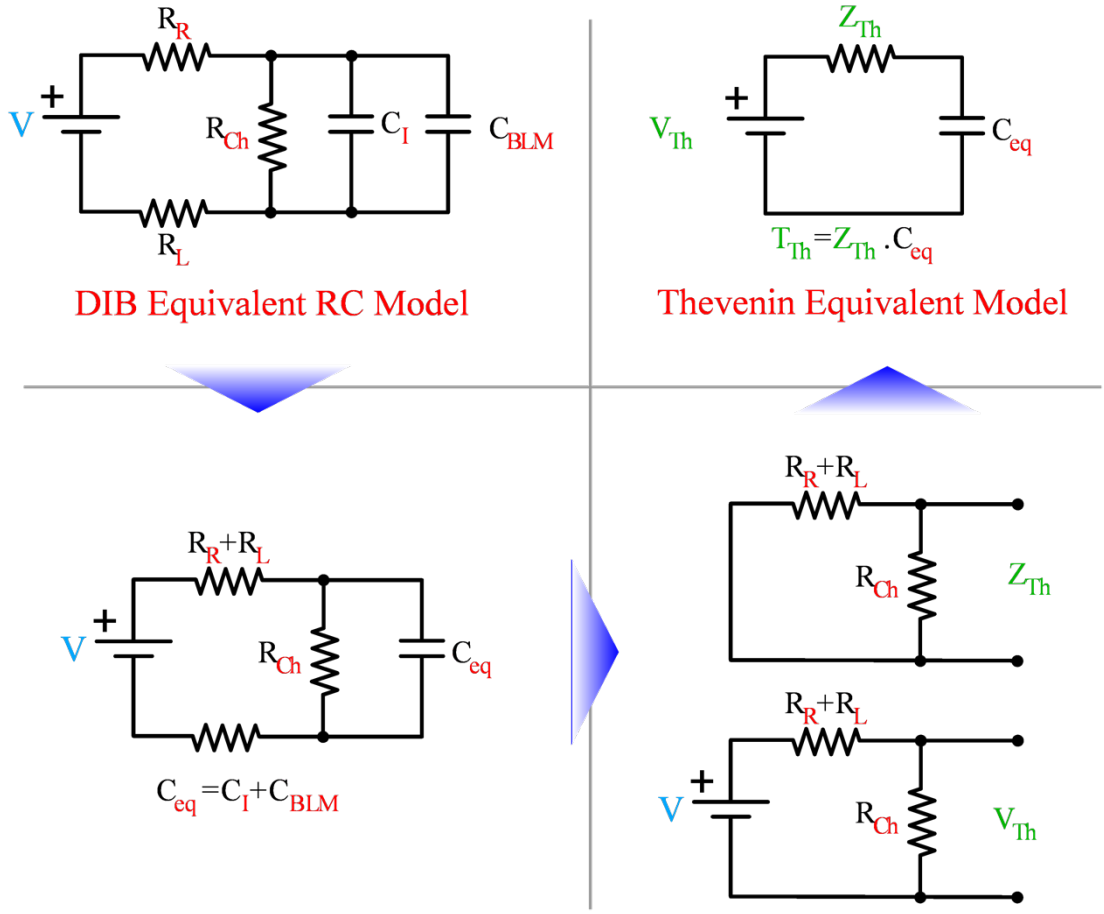

Figure 3.6 Thevenin equivalent model for the bilayer RC circuit shown earlier
R_L and R_R are droplet resistances and are equal for symmetric buffer conditions. R_{ch} is the inserted channel resistance. C_{BLM} and C_I are bilayer and interface capacitances respectively. C_{eq} is the equivalent capacitance and is the sum of C_I and C_{BLM} as they are in parallel. Time constant τ is the product of Thevenin impedance, Z_{th} and C_{eq}.

The equation for the double chamber chip's time constant is provided in Figure 3.6 which is the Thevenin impedance, Z_{th}, multiplied by the equivalent parallel capacitance of the bilayer and interface material, C_{eq}.

Since the bilayer's resistance, R_{Ch}, would be much higher than the droplet resistance in each chamber ($R_{Ch} >> R_R$, R_L), given Equation 1 and Equation 2, Z_{th} can be approximated as just the summation of the droplet resistances.

Equation 1: $$\boldsymbol{R_{total} = R_L + R_R + R_{Ch} \approx R_{Ch}}$$

Equation 2: $$\boldsymbol{Z_{th} = (R_L + R_R).R_{Ch} \,/\, R_{total}}$$

Equation 3: $$\boldsymbol{\tau = Z_{th} . C_{eq}}$$

The system's time constant, τ, from Equation 3, may be improved by minimising the bilayer capacitance, C_{BLM}, the interface material capacitance, C_I, and the droplet resistances R_R and R_L.

The electrical component values of the model circuit can be estimated from first principles as shown in Table 3.2. The following assumptions were made about the resistor and capacitor values:

- Given that each chamber is cylindrical in shape, it is possible to estimate the volume of each chamber. In Table 3.1, chamber radius is between 2mm and 2.5mm and chamber depth is 2mm to 3mm, each well would contain between 25 µl and 59 µl of buffer. Assuming 0.1M KCl buffer is used, then conductivity at room temperature is 12 mS/cm. Since resistivity (ρ) is the reciprocal of the conductivity value (G) and is measured in ohm.cm^{-1} then:

$$\rho = \frac{1}{G} = \frac{1}{12 \times 10^{-3}} = 83\ \Omega.cm^{-1}$$

  Since the diameter of each chamber is around half a centimetre then the resistance of each droplet is 83/2 = 41.5 ohms at room temperature.

- The α-HL resistance (R) is calculated by assuming a cylinder of constant internal diameter of 26 Å and length (l) of 100 Å (Song et al., 1996) filled with 0.1M KCl:

$$R = \frac{\rho l}{A} = \frac{83 \times 100 \times 10^{-8}}{\pi . (13 \times 10^{-8})^2} = 1.56\, G\Omega$$

Where A is channel area and ρ is KCl resistivity.

- The bilayer is assumed to cover the entire cross-sectional area of two chambers. This area varies across the designed chambers, however it is possible to calculate the minimum bandwidth based on the largest bilayer. In Table 3.1, Device 3 possesses the largest cross-sectional area at 6 mm^2. A specific capacitance of 0.5 μFcm^{-2} (Fujiwara et al., 2003) for short-chain decane was used for calculations in Table 3.2.

Table 3.2 Estimated electrical component values for double chamber chip

Component	Description	Estimated Value
$\mathbf{R_L}$, $\mathbf{R_R}$	Left and Right Chamber Resistance	41.5Ω
$\mathbf{C_{BLM}}$	Bilayer Capacitance	30nF
$\mathbf{R_{ch}}$	A-HL Channel Resistance	1.56GΩ

Assuming the estimated bilayer capacitance in Table 3.2, C_{BLM}, is much higher ($C_{BLM} >> C_I$) than the interface material capacitance, C_I, then C_{eq} is simply equivalent to C_{BLM}. Substituting the values from Table 3.2 into Equation 3, the slowest time constant for the test chamber is estimated to be 2.49 μsec as below:

$$\tau = Z_{th} . C_{eq} = 83 \times 30 \times 10^{-9} = 2.49 \times 10^{-6} secs$$

Taking the inverse, the minimum bandwidth is estimated to be 0.4MHz. This is fast enough to record ion channels and blockade experiments as channel dwell times and blocking times typically last in the order of milliseconds (Kawano et al., 2013; Tsuji et al., 2013). This was experimentally verified by successfully recording fast gating channels as shown in the next chapter. Since the bilayer will not cover the entire cross-sectional area of the two chambers from the start, then in reality the bandwidth for any single device will be higher initially and slowly reduce over time in line with the growth of the bilayer and its capacitance. The overall minimum detectable signal will also be limited by noise in the system and the amplifier used in the experimental set up.

3.4 Build

3.4.1 Materials used for BLM systems

A number of physical properties were carefully considered when selecting the fabrication material of choice. The activated photopolymer (R11 envisionTEC, Germany) was observed to be resistant to organic solvents and water absorption was negligible at 0.71%. The cured resin was hydrophobic and this was an important factor as this type of surface has been shown to favour contact with the lipid hydrocarbon chains (Montal & Mueller, 1972). The material was cheap, resulting structures remained stable and allowed for electrochemical detection exhibiting high electrical insulation and low electrical capacitance rendering it suitable for bilayer electrophysiology experiments. A downside of this material was that it was not transparent and thus not suitable for optical detection.

3.4.2 Microscopy

The designs in Table 3.1 were fabricated using stereolithography (Aureus envisionTEC, Germany) with a typical build time of 3 to 4 hours. All three aspects (depth, diameter and interface) of each printed structure were inspected under a microscope (Quick Scope Mitutoyo, United Kingdom) for physical measurements. Depth and diameter results were found to be within 5% of expected values across all fabrications and therefore acceptable. The observed measurements for interface values are shown in Figure 3.7. As shown in the below figure the interface width was measured across three points and the results were averaged for each chip.

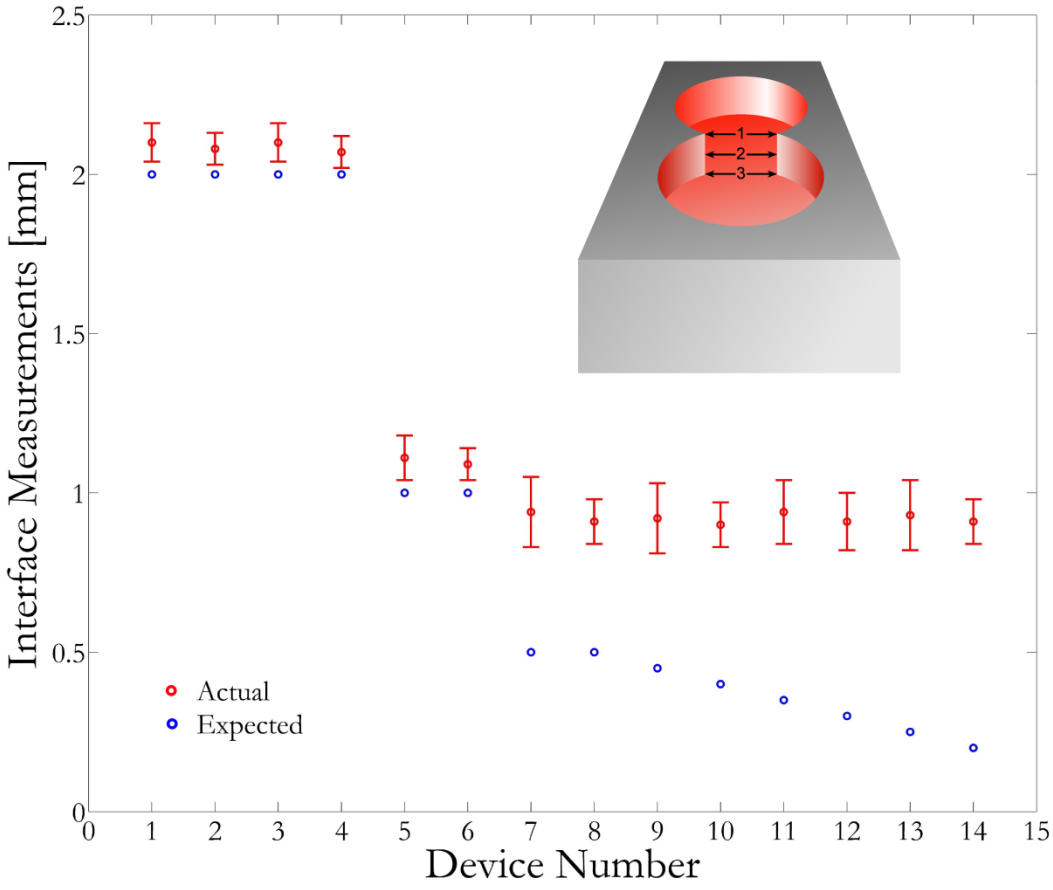

Figure 3.7 Interface measurements: Expected VS Actual
Devices 7 to 14, where designed interface values were below 1mm, were rejected as fabricated designs were not within an acceptable range (±10%) of expected interface values. N = 36 for each device. Error bars indicated ± 1 s.d.

It was found that designs with an interface of lower than 1mm produced deformed apertures. Deformity started as a U-shape interface, as in the case of Devices 7 and 8, which was further exacerbated with shrinking aperture dimensions and resulting in a more V-shape structure, as in the case of Devices 13 and 14. The architectural defect has been exhibited in Figure 3.8 where a 0.5mm interface is compared with a 2mm interface. Consequently Devices 7 to 14 were rejected without further testing as they were deemed unfit for purpose.

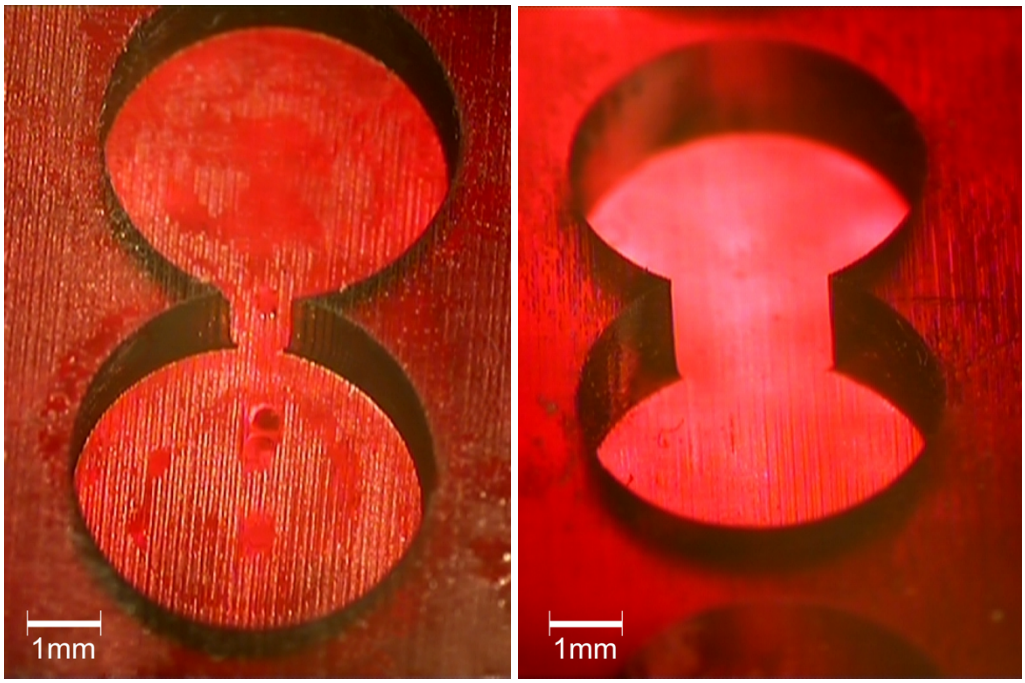

Figure 3.8 Device microscopy
(Left) A close-up of Device 7 displaying a U-shaped interface. (Right) A close-up of Device 4.

3.5 Testing Results and Discussion

The remaining Devices, 1 to 6, were considered for BLM experiments to stochastically determine the most suitable configuration and to develop a robust assay protocol. However, it was soon realised that Devices 1 and 2, due to a smaller chamber diameter of 4mm, made electrode positioning with a manual actuator

practically difficult. Soft silver chloride electrodes would easily arc as soon as the tip collided with the solid part of the device structure in case of alignment error which meant they would have to be manually straightened out. Bending correction often led to electrode surface silver chloride removal which necessitated rechloridisation. Subsequently Devices 1 and 2 were relinquished from further testing.

3.5.1 Bilayer Characterisation

The time for bilayer formation, growth and immediate coalescence after depositing the second droplet to the second well depends on a number of factors, including the incubation time of the first droplet before monolayer contact is made, lipid concentration in the oil and device interface geometry. Bilayer formation can be confirmed by observing a growth in bilayer capacitance, protein channel recording and voltage-induced breakage. Potentials of around 250mV - 400mV were applied to the BLM's formed in devices 3 to 6 to confirm bilayer formation which indicates a sufficiently high stability (Kresák et al., 2009; Mayer et al., 2003).

Di-phythanoyl phosphatidyl choline (DPhPC) was carefully selected as the lipid of choice for the experiments in this chapter as the two phythanoyl-chains present in a lipid molecule allow composed BLM's to be of high stability and sealing resistance (Baba et al., 1999) making it suitable for recording single ion channels. Moreover, DPhPC has been demonstrated to host and permit retained functionality across a range of peptidic channels such as gramicidin (Hwang et al., 2008; J L Poulos et al., 2010) and α-hemolysin (Castell et al., 2012; Funakoshi et al., 2006; Martel & Cross, 2012) as well as eukaryotic membrane protein ion channels such as hERG (Portonovo et al., 2013) and BK (Ide & Ichikawa, 2005).

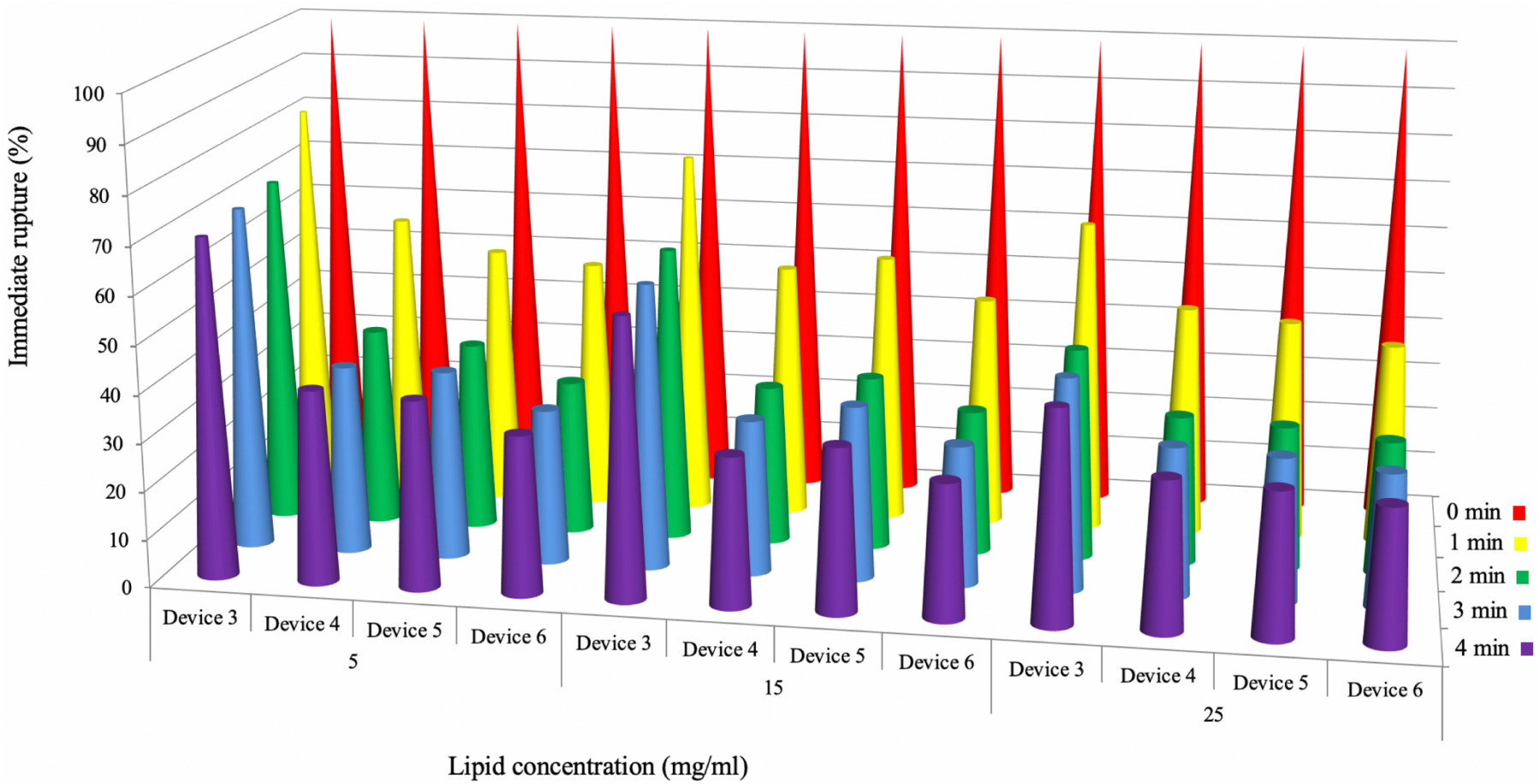

Figure 3.9 Immediate rupture observation across devices 3, 4, 5 and 6
The x-axis represents the four devices under investigation at three lipid mixtures. The y-axis displays the percentage of experiments where droplets coalesced. The z-axis represents the time allowed for the first droplet to rest and stabilise in lipid mixture before the second droplet was added. N = 18 for each lipid concentration-stabilisation time-device combination.

As part of the proposition to find the optimum BLM formation regime, a number of experiments were conducted to minimise the probability of immediate droplet coalescence by investigating lipid concentrations against droplet incubation and stabilisation time for devices 3, 4, 5 and 6. Adequate stabilisation time is required for uniform lipid monolayer formation (Hwang et al., 2008), where insufficient incubation time leads to patchy droplet coverage and subsequently immediate droplet fusion. The data shown in Figure 3.9 are derived from 18 pairs of osmotically symmetrical droplets (0.1 M KCl pH 7.4) conducted at each combination of lipid concentration, incubation time and device. The applied voltage potential was kept consistent across all experiments and successfully formed BLMs survived for at least 5 minutes. In this aqueous system bursting events were visible by eye as well as electrically.

The data reaffirms that rupture is highest if no incubation time is allowed, regardless of lipid concentration or device specific interface area. The data also unveils a number of trends. Immediate rupture in each device diminishes by increasing the lipid concentration from 5mg/ml to 15mg/ml to 25mg/ml and is consistent with other literature (Leptihn et al., 2013). Across each lipid concentration coalescence percentage is correlated to a decrease in interface area where the most significant improvement is seen going from Device 3, 6mm^2 cross sectional area, to Device 4 with a 4mm^2 interface area. Another revealed truth is that the gain in droplet fusion after 2 minutes of incubation is negligible. The conclusion from these sets of experiments is that to form BLMs in this platform a stabilisation time of 2 minutes should be allowed. Another salient point is that Device 3, owing to its large cross-sectional area and droplet volume, is more vulnerable to mechanical perturbation and

thus displays the poorest reproducibility profile regardless of time and lipid concentration when compared with other devices.

Further droplet interface bilayer formation experiments were carried out on all remaining devices at aforementioned DPhPC lipid concentrations in decane where capacitate response of the system was recorded over at least a 20 minute period, however, bilayers were observed to typically live for over one hour. A droplet incubation time of 2 minutes was kept constant across remaining experiments. Capacitance was measured by monitoring the square-wave current output upon application of a triangular-wave input voltage (Gross et al., 2011). The traces in the below figures indicate an increase in capacitance as the bilayer forms. The background capacitance of the platform was digitally removed post data acquisition and thus the traces in the figures have been adjusted for this offset. At the end of the each experiment a fixed 100mv DC voltage was applied to each bilayer to check for low base line currents indicative of a non-leaky bilayer. The bilayer area was calculated by rearranging Equation 4 for area.

Equation 4: $$\boldsymbol{Capacitance = \varepsilon_r \varepsilon_0 \frac{Area}{d}}$$

Where ε_r is relative stative permittivity for DPhPC and is 2.2 (Alonso-Romanowski et al., 1995; Valincius et al., 2008), ε_0 is the electric constant and is 8.854×10^{-12} Fm^{-1}, d is the bilayer thickness and is 3.5 nm (Tristram-Nagle et al., 2010).

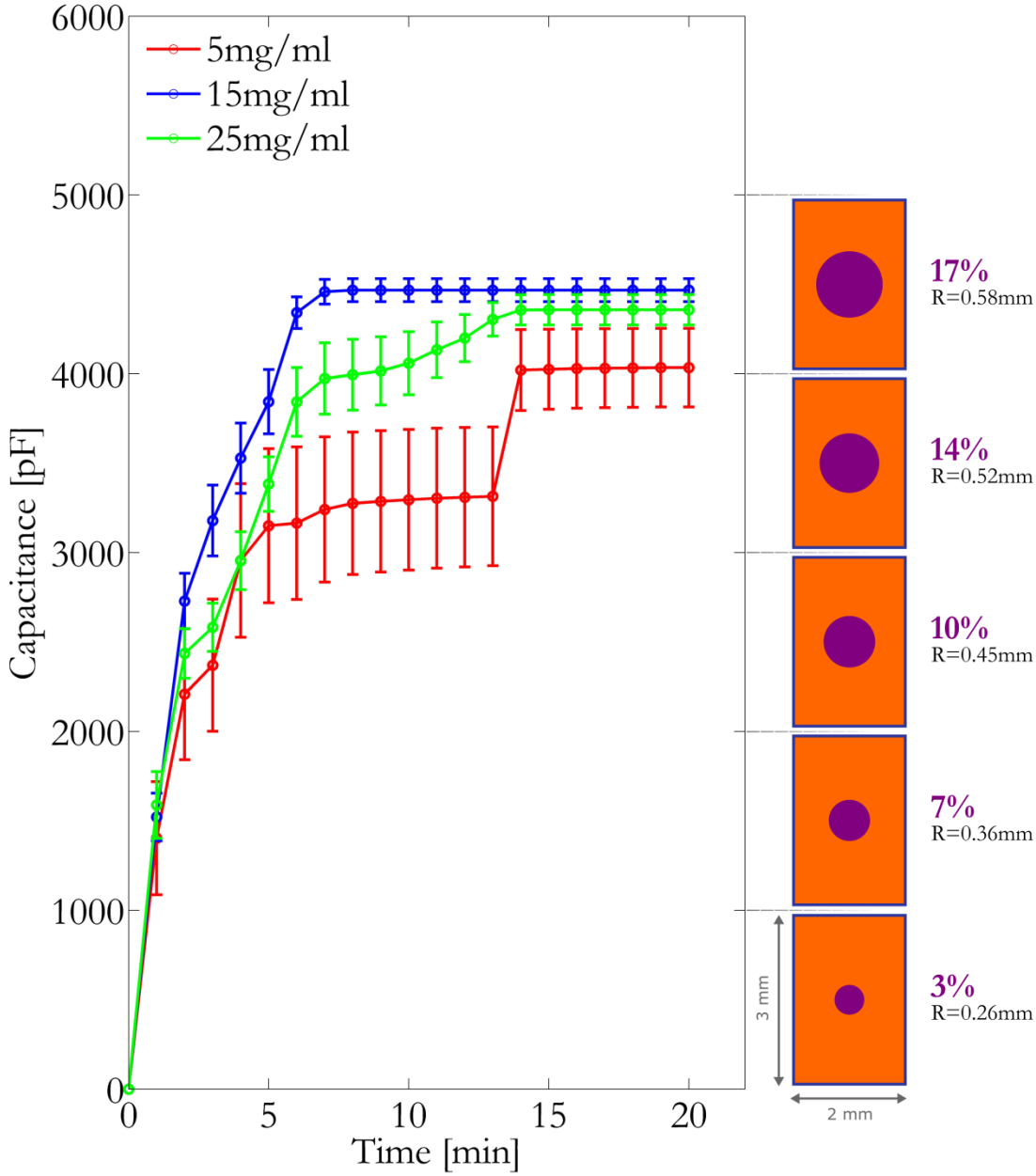

Figure 3.10 BLM formation over time - Device 3
The average capacitance traces of droplet interface bilayers in double chamber platform 3 are shown. Three DPhPC lipid concentrations in decane (5mg/ml, 15mg/ml and 25mg/ml) were tested, where N = 30 for each concentration, and bilayers lifetime was at least 20 minutes. The orange rectangle to the right indicates the device cross sectional interface area (3mm by 2mm) and the purple circles represent the area of bilayer at various capacitances (from bottom to top): 1nF, 2nF, 3nF, 4nF and 5nF. For example, it is estimated that a bilayer capacitance of 5nF indicates that 17% of the cross sectional area is covered by the bilayer. Error bars indicate ± 1 s.d.

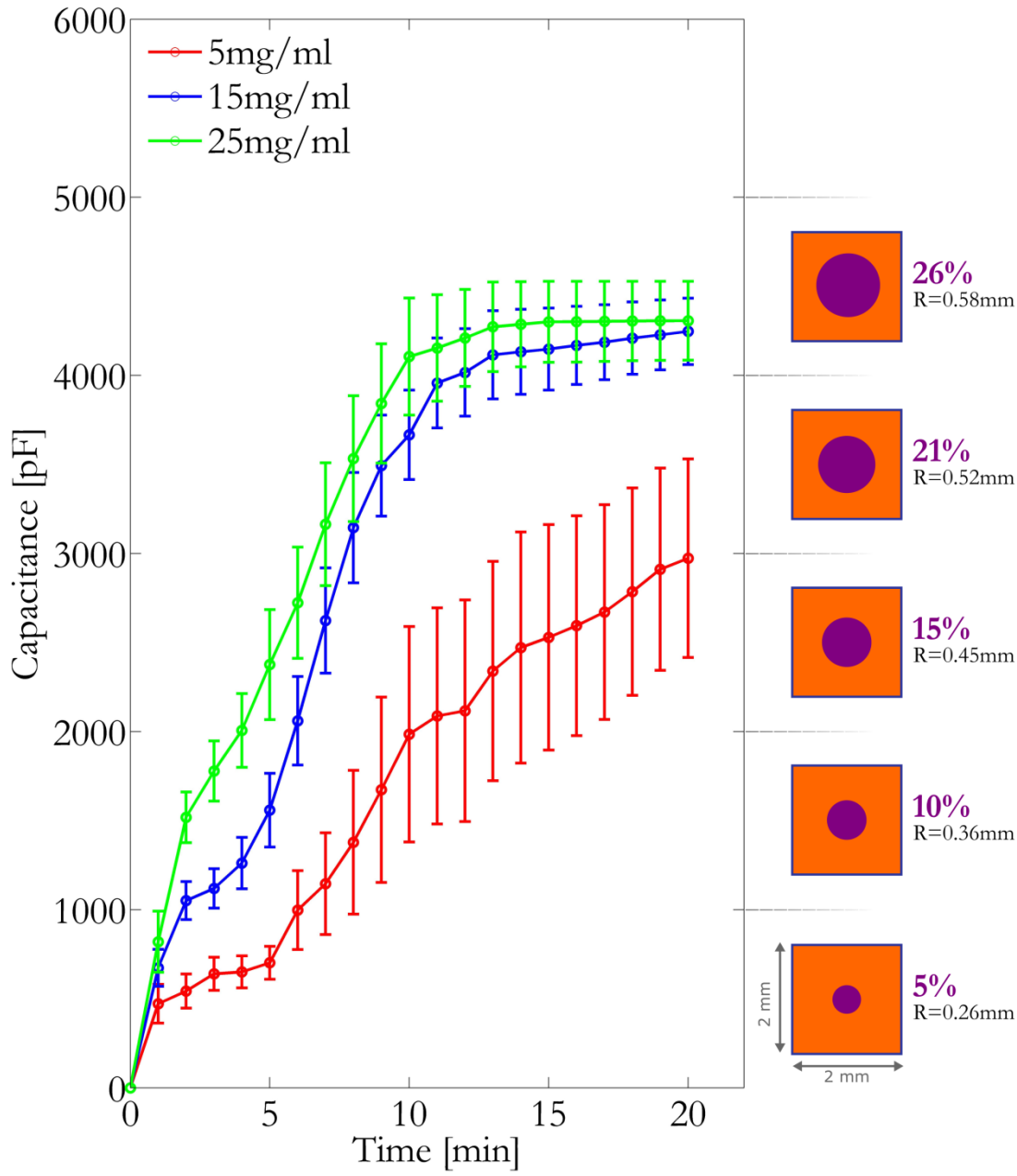

Figure 3.11 BLM formation over time - Device 4

The average capacitance traces of droplet interface bilayers in double chamber platform 4 are shown. Three DPhPC lipid concentrations in decane (5mg/ml, 15mg/ml and 25mg/ml) were tested, where N = 30 for each concentration, and bilayers lifetime was at least 20 minutes. The orange rectangle to the right indicates the device cross sectional interface area (2mm by 2mm) and the purple circles represent the area of bilayer at various capacitances (from bottom to top): 1nF, 2nF, 3nF, 4nF and 5nF. For example, it is estimated that a bilayer capacitance of 5nF indicates that 26% of the cross sectional area is covered by the bilayer. Error bars indicate ± 1 s.d.

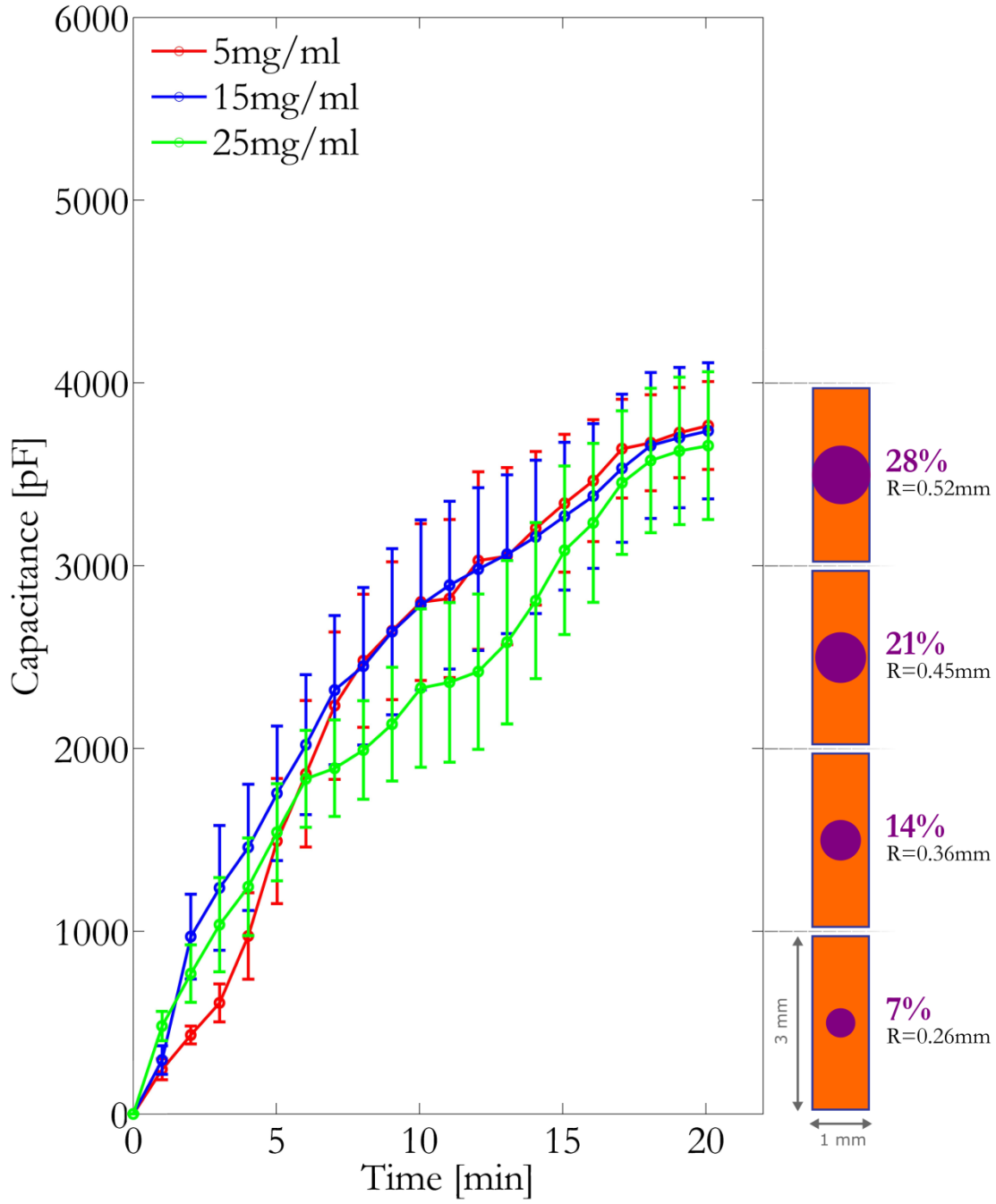

Figure 3.12 BLM formation over time - Device 5
The average capacitance traces of droplet interface bilayers in double chamber platform 5 are shown. Three DPhPC lipid concentrations in decane (5mg/ml, 15mg/ml and 25mg/ml) were tested, where N = 30 for each concentration, and bilayers lifetime was at least 20 minutes. The orange rectangle to the right indicates the device cross sectional interface area (3mm by 1mm) and the purple circles represent the area of bilayer at various capacitances (from bottom to top): 1nF, 2nF, 3nF and 4nF. For example, it is estimated that a bilayer capacitance of 4nF indicates that 28% of the cross sectional area is covered by the bilayer. Error bars indicate ± 1 s.d.

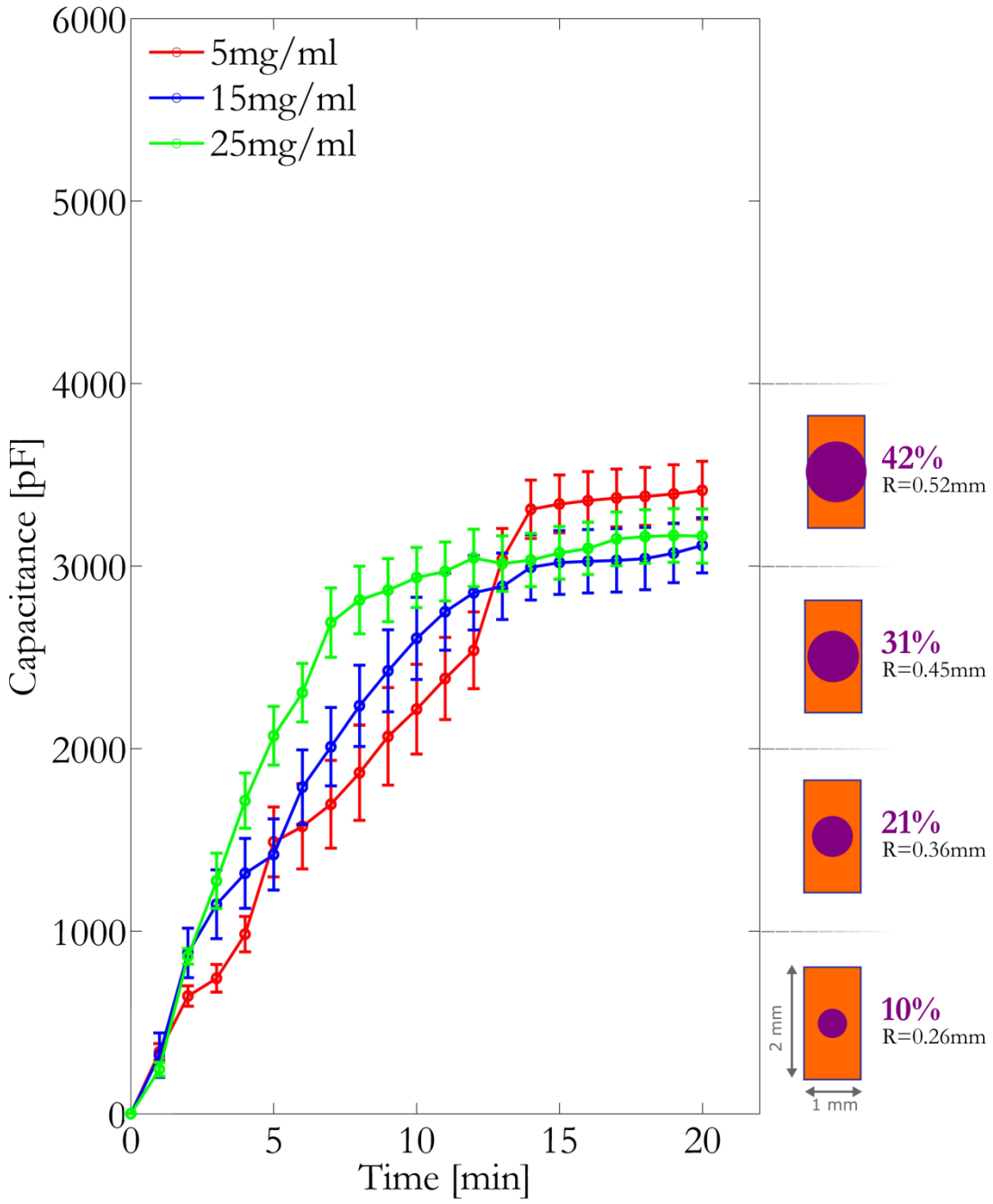

Figure 3.13 BLM formation over time - Device 6
The average capacitance traces of droplet interface bilayers in double chamber platform 6 are shown. Three DPhPC lipid concentrations in decane (5mg/ml, 15mg/ml and 25mg/ml) were tested, where N = 30 for each concentration, and bilayers lifetime was at least 20 minutes. The orange rectangle to the right indicates the device cross sectional interface area (2mm by 1mm) and the purple circles represent the area of bilayer at various capacitances (from bottom to top): 1nF, 2nF, 3nF and 4nF. For example, it is estimated that a bilayer capacitance of 4nF indicates that 42% of the cross sectional area is covered by the bilayer. Error bars indicate ± 1 s.d.

The data helps characterise bilayer formation and suggests that BLMs are stable across all four devices. In Figure 3.10 and Figure 3.11 the capacitance traces plateau

at just under 4.5nF, this is most likely caused by amplifier saturation which implies that bilayer area in devices 3 and 4 are most likely even larger. Larger bilayer area offers both advantages and disadvantages. It has been reported that reducing the BLM formation area allays electrical noise (Mayer et al., 2003; Sigworth & Klemic, 2005) as well as improving BLM stability (Kawano et al., 2013). Although enhancements in signal-to-noise ratio and BLM stability are always desirable, as long as the BLM platform, assisted by filtering techniques, is able to detect single channel activity then the focus should be shifted to another important factor, namely protein incorporation probability which is a common area of difficulty across BLM systems. The earlier system bandwidth calculations estimated that this platform, for all given geometrical configurations, is capable of detecting single ion channel events. In the next chapter, we will see that double chamber platform can record both fast gating and low conductance ion channels.

Although we have seen considerable advancements in automation, miniaturisation and parallelisation of BLM systems (Kongsuphol et al., 2013; Zagnoni, 2012), the literature remains thin with regards to systematically targeting the problem of functional protein incorporation. Only a few methods have been reported to increase the probability and rate of membrane ion channel reconstitution for electrophysiology. One such approach is to vigorously mix the contents of one side of the bilayer using magnetic stirring bars (Cohen et al., 1984). This serves to promote proteoliposomes fusion by increasing chances of vesicle/bilayer collision. However, it also introduces significant mechanical agitation to the system that increases electrical noise in the output tracings and can cause the BLM to pop. Another approach is to introduce osmoticants in the buffer such as glycerol or urea

and create an osmotic gradient. However, as a side effect of increasing fusion rate it adds chemical complexity to the system (Woodbury & Miller, 1990). Another solution is the wicking technique, where a protein-coated glass brush is dragged, whilst in rotation, across a painted bilayer (Costa et al., 2013; Kawano et al., 2014). Although the effectiveness of this method has been demonstrated, it remains a highly manual activity with no scope for automation.

The solution proposed for this practical problem is to boost the chances of protein complex fusion by expanding the bilayer area thereby enhancing the probability of collision with the membrane. This approach should improve the reconstitution rate of both fusogenic, such as alpha hemolysin and gramicidin, and non-fusogenic, such as BK, ion channels. This method is also supportive of studies of transporters. Transporter channels are typically characterised by translocation rates of three to four orders of magnitude lower than ion channels (Gadsby, 2004) which necessitates clusters of transporters to reconstitute to achieve electrical detection as compared to ion channels which only require one successful bilayer insertion (Tiefenauer & Demarche, 2012).

To find the conditions offering the best prospects in this respect the following question was examined: are there statistically significant differences between bilayer capacitance, and therefore bilayer area, mean values at the same lipid concentration level when data are compared across different devices?

To answer this question a one-way analysis of variance (ANOVA) test was used to analyse the data with $p < 0.05$ as the criteria of significant difference. Data was normally distributed as assessed by Shapiro-Wilk's test of normality and the

assumption of homogeneity of variances was violated in all cases, as assessed by Levene's Test of homogeneity of variance. The below figures (Figure 3.14, Figure 3.15 and Figure 3.16) help answer this question. Further analysis on Device 3 has been omitted due to poor bilayer rupture profile and therefore rejection of this geometrical configuration as a viable solution for protein electrophysiological studies.

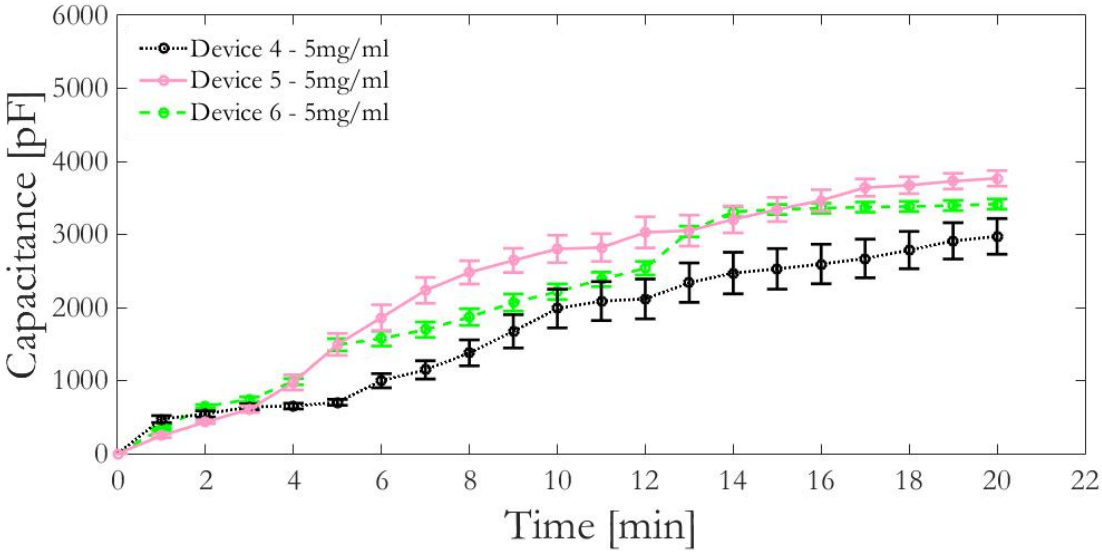

Figure 3.14 Bilayer capacitance comparison at 5mg/ml across Devices 4, 5 and 6
The average capacitance traces of droplet interface bilayers in double chamber platforms 4,5 and 6 are shown. DPhPC lipid concentrations in decane is 5mg/ml. were tested, where N = 30 for each device, and bilayers lifetime was at least 20 minutes. Data suggests that Device 5 produces significantly larger bilayers after 3 minutes when compared to Device 4. In comparison to Device 6, Device 5 produces significantly larger bilayers between 5 minutes and 13 minutes and after17 minutes. Bars indicate ± 95% confidence interval

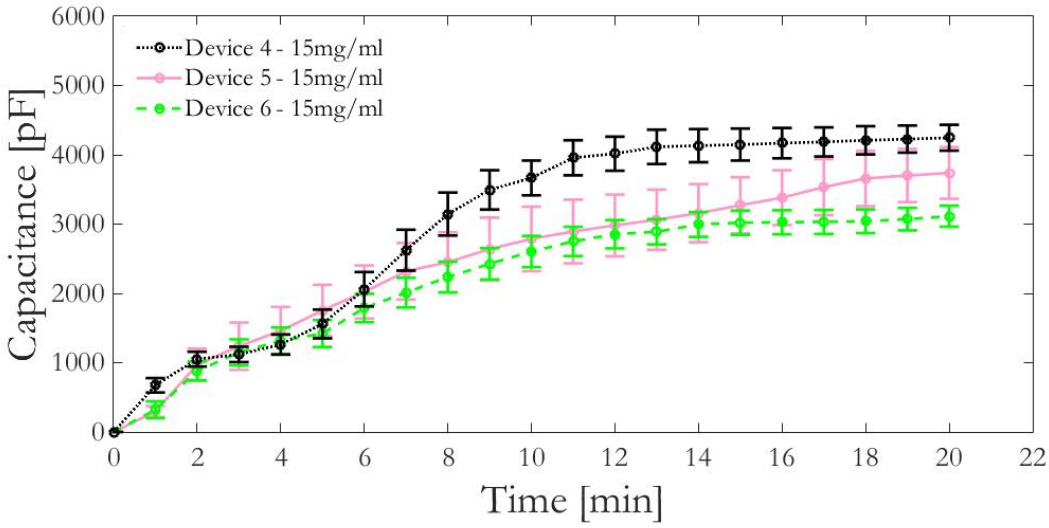

Figure 3.15 Bilayer capacitance comparison at 15mg/ml across Devices 4, 5 and 6
The average capacitance traces of droplet interface bilayers in double chamber platforms 4,5 and 6 are shown. DPhPC lipid concentrations in decane is 15mg/ml. were tested, where N = 30 for each device, and bilayers lifetime was at least 20 minutes. Data suggests that Device 4 produces significantly larger bilayers after 8 minutes when compared to Devices5 and 6. Bars indicate ± 95% confidence interval

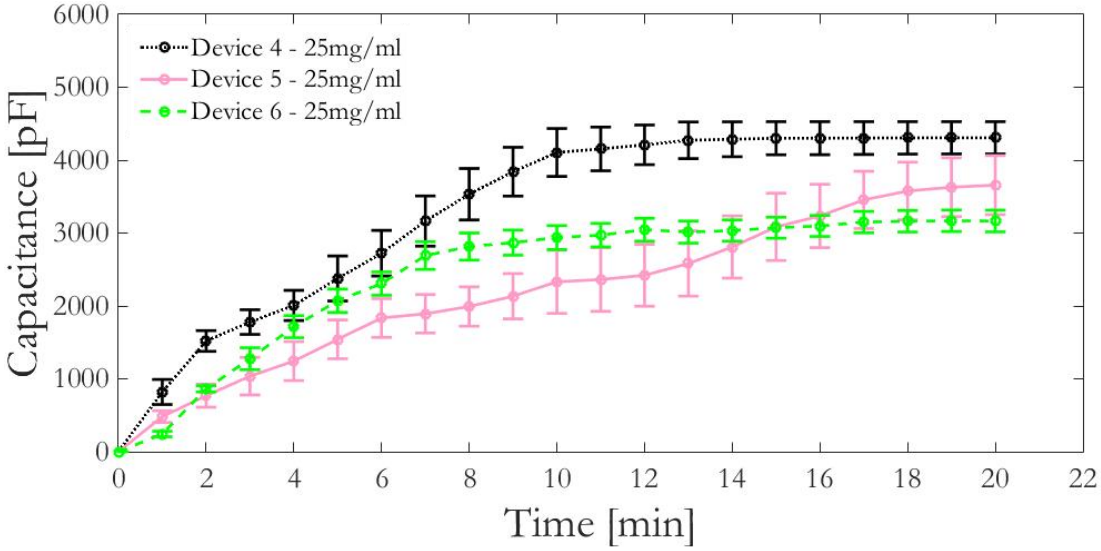

Figure 3.16 Bilayer capacitance comparison at 25mg/ml across Devices 4, 5 and 6
The average capacitance traces of droplet interface bilayers in double chamber platforms 4,5 and 6 are shown. DPhPC lipid concentrations in decane is 25mg/ml. were tested, where N = 30 for each device, and bilayers lifetime was at least 20 minutes. Data suggests that Device 4 produces significantly larger bilayers across all time points when compared to Device 5. In comparison to Device 6, Device 4's bigger bilayers form between 0 minute and 4 minutes and after7 minutes. Bars indicate ± 95% confidence interval

Based on Welch's ANOVA there was significant differences at all DPhPC lipid concentrations. At 5mg/ml Device 5 produced significantly larger bilayers after 3 minutes when compared to Device 4. In comparison to Device 6, Device 3 produced significantly larger bilayers between 5 minutes and 13 minutes and after17 minutes. At 15 mg/ml Device 4 produced significantly larger bilayers after 8 minutes when compared to both Devices 5 and 6. At 25 mg/ml Device 4 produced significantly larger bilayers across all time points when compared to Device 5. In comparison to Device 6, Device 4's bigger bilayers form between 0 minute and 4 minutes and after7 minutes.

Figure 3.9 suggests that bilayer rupture is higher at 5mg/ml when compared with 15 mg/ml and 25 mg/ml lipid concentrations. As a result, only bilayer performances at 15 mg/ml and 25 mg/ml are considered further. As mentioned above and shown in Figure 3.15 and Figure 3.16, Device 4 outperforms others based on rate of BLM formation as well as bilayer size which can be attributed to greater chamber cross sectional area. To find the optimum BLM conditions in Device 4 the following question was examined: is there a statistically significant change in average bilayer size at 15 mg/ml and 25 mg/ml DPhPC lipid concentration?

To answer this question a paired sample T-test was used. For T-tests to be able to provide a valid result, some assumptions must hold true. Data should be checked for normality, homogeneity of variances and existence of any outliers. The normality of the data was also checked using Shapiro-Wilks test and homogeneity of variances was checked using Levene-Test. As illustrated in Figure 3.17 there is generally no significant difference in bilayer size between 15 mg/ml and 25 mg/ml after 7 minutes of monolayer contact.

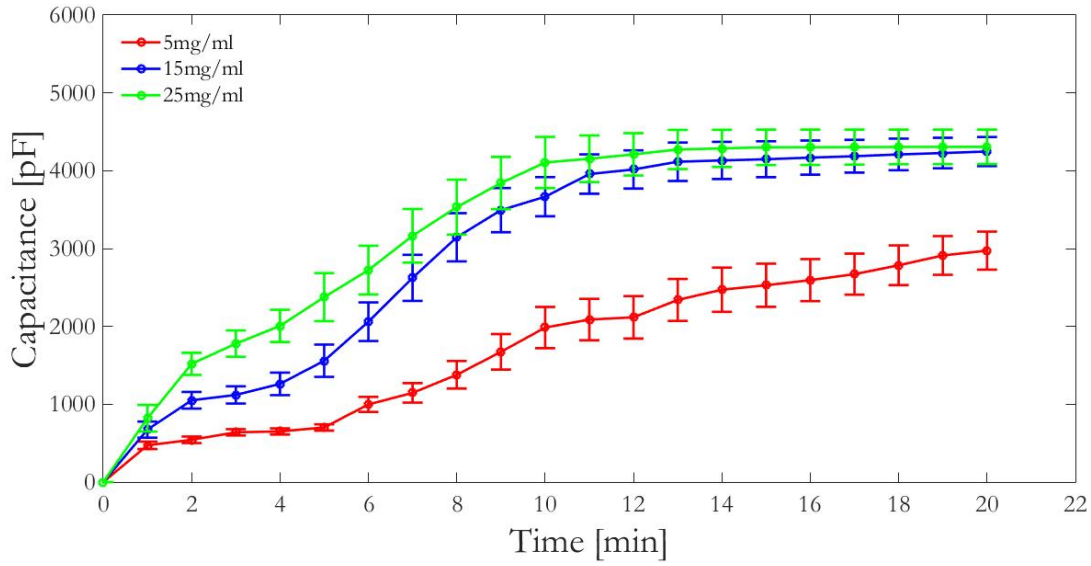

Figure 3.17 Significance bilayer capacitance testing of Device 4
When comparing bilayer size at 25 mg/ml to 15 mg/ml, there are significant differences only between 1 minute and 7 minutes.

To achieve greater protein incorporation probability, it is more meaningful to consider bilayer size in relation to droplet circumference and therefore its volume. Assuming the droplets are spherical in shape and that bilayers cover the total cross-sectional area of the two chambers (Funakoshi et al., 2006), it is possible to use simple volume and area calculations to reveal these relationships for each device.

For Devices 4 and 6, given that the volume of each droplet was the same at 31 µl, the ratio of bilayer area to droplet surface area, in other words the portion of droplet surface covered by the BLM was 8.4% and 4.2% respectively. For Devices 3 and 5, given a droplet volume of 40 µl, the BLM covered 10.6% and 5.3% of droplet surface area respectively. This suggests that the chances of ion channels within a droplet finding their way to the bilayer are highest in Device 4. This conclusion is further supported when inspecting the data in Figure 3.15 and Figure 3.16 along the majority of the observed time points with Device 4's droplet volume in mind.

In the end Devices 3, 4, 5 and 6 were scored against each other, as shown in Table 3.3, on bilayer reproducibility, stability, growth rate and droplet surface coverage and device 4 was selected as the geometrical configuration of choice for multiplexing and protein ion channel experiments.

Table 3.3 DIB platform characterisation matrix. Scoring is out of High (H), Medium (M) and Low (L)

Device Number	Reproducibility	Stability	Growth Rate	Droplet Coverage
Device 3	L	H	H	H
Device 4	H	H	M	M
Device 5	H	H	L	L
Device 6	H	H	L	L

3.6 Noise Analysis

The electrical current noise is an important aspect of a planar bilayer setup as it impacts the minimum detectable ion channel current pulse in the system. Noise can be characterized by its power spectral density or by its variance (Mayer et al., 2003). The sensitivity of the system is limited by three main noise sources, namely amplifier voltage noise (Equation 5), effect of thermal noise in electrode series resistance (Equation 6) and dielectric noise (Equation 7) (Mayer et al., 2003):

Equation 5:
$$S_{vc}{}^2 = 4e_n{}^2\pi^2 C_t{}^2 f^2$$

Equation 6:
$$S_{rc}{}^2 = \frac{16kT^2\pi^2 C_m{}^2 R_a f^2}{1+4\pi^2 C_m{}^2 R_a{}^2 f^2}$$

Equation 7:
$$S_d{}^2 = 8kT\pi DC_t f$$

Equation 8: $$C_t = C_m + C_e + C_a + C_i$$

The summation of spectral components yields the total power spectral density of the system. e_n is the root mean-square (rms) noise voltage in the amplifier. C_t is the total input capacitance as shown in Equation 8 and comprises capacitances of bilayer (C_m), immersed electrodes (C_e), amplifier input capacitance (C_a) and the capacitive contribution of the interface material (C_i). f is the frequency, k is the Boltzmann constant, and T is the absolute temperature (in kelvin). D is the dielectric loss factor and R_a is the access resistance. The access resistance is the sum of several resistances in series, including the electrode/electrolyte interface and the recording solution (Wonderlin et al., 1990). The resistance of the recording solution can be broken down further into three components based on geometrical considerations: the resistance of each buffer droplet on either side of the bilayer, the convergence resistance at each end of the aperture and the resistance of the solution within the aperture.

As shown in Figure 3.18, frequency dependent power spectrum density analysis was carried out for current traces (recorded at 5 kHz with 100 mV potential applied) with just formed bilayer without peptide present. As seen in the Figure 3.18, the peak to peak noise (and thus rms) grows over time in line with bilayer growth as expected.

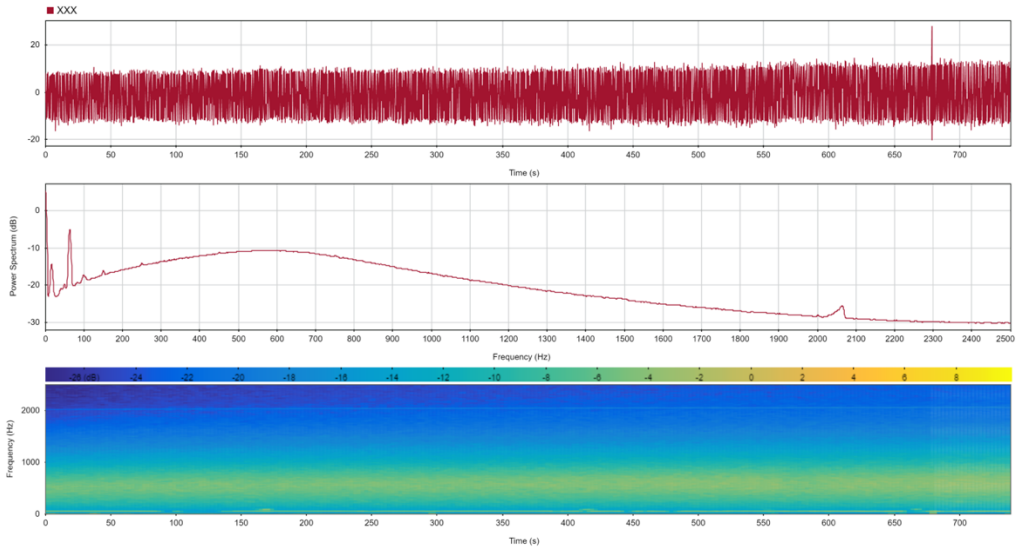

Figure 3.18 Noise analysis of droplet interface bilayers
(Top) peak to peak noise growing in line with bilayer growth (time [s] vs current [pA]). (Middle) frequency dependent power spectrum density analysis of the same current trace is shown (frequency [Hz] vs power spectrum [dB]). (Bottom) heat map of frequencies for the same current trace (time [s] vs frequency [Hz]).

3.7 Multiplexing

To enhance the throughput of the system aspects of the platform were redesigned and reengineered and new components were 3D printed. As shown in Figure 3.19 new features included the electrode positioning system capable of moving in X-Y plane, the perforated multi electrode holder (illustrated in black) and BNC box which connected the multi-channel amplifier to the electrodes via a ribbon cable. Initially the chip was redesigned to fit maximum number of double well chambers. During experimentation, it was realised that after lipid/decane mixture was deposited into a well, it leaked through to the neighbouring double well. This is likely caused by imperfections during the stereolithography process forming unintended micro-channels within the cured photopolymer structure. This issue was resolved by spacing out independent chambers further.

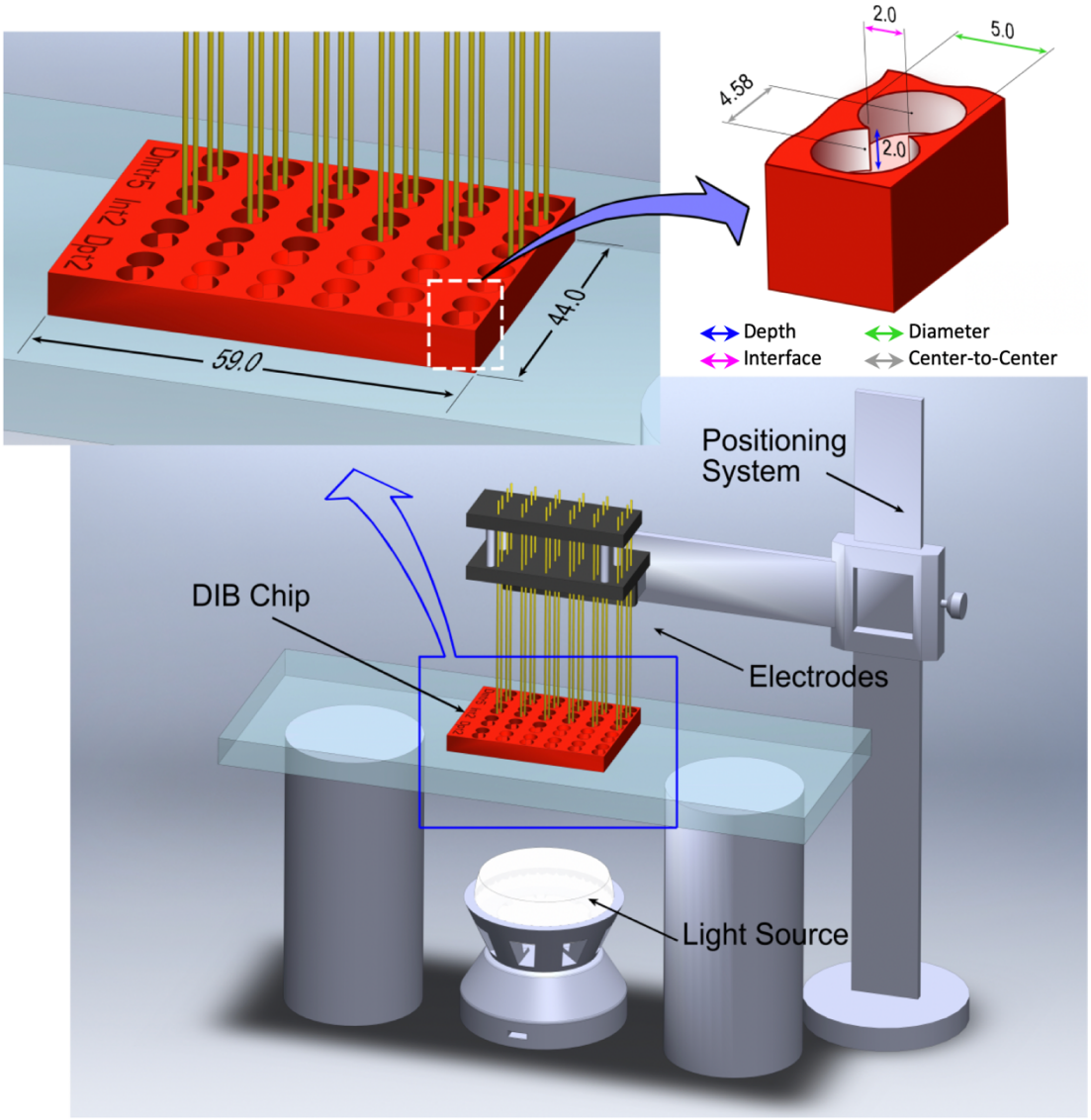

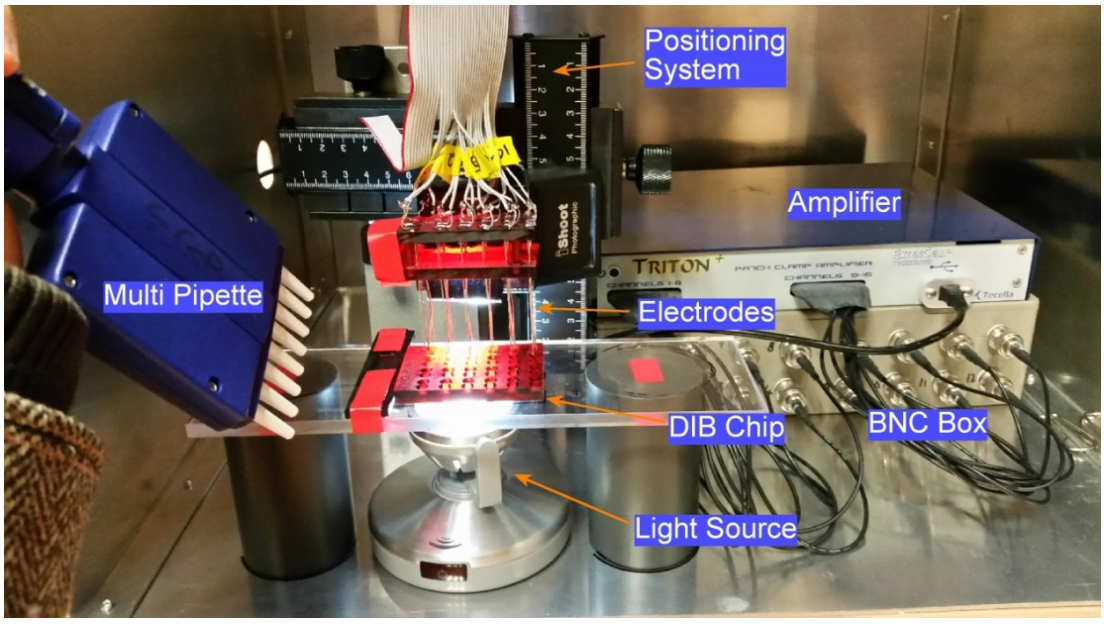

Figure 3.19 Multi-channel DIB platform
(Top) Schematic diagram of the final Device 4 DIB chip and supporting architecture. Dimensions given in *mm*. (Bottom) Experimental rig setup inside the faraday cage. An arrayed 24 double chamber chip connected to a multi-patch-clamp amplifier. The light source allowed for visual inspection of droplets.

In this system, it was possible to add droplets by either pipetting directly into the well or dispensing droplets onto the electrode. The droplet adhered to the electrode and swiftly descended to a resting state at the bottom of the well. Subsequent to successful BLM formation, it was possible to dispense additional droplets on top of existing drops without bursting the BLM thereby allowing for the alteration of buffer composition. This was useful as it meant that proteins, as well as drugs and chemicals, could have been added at a suitable time, for example once bilayer had reached a certain size.

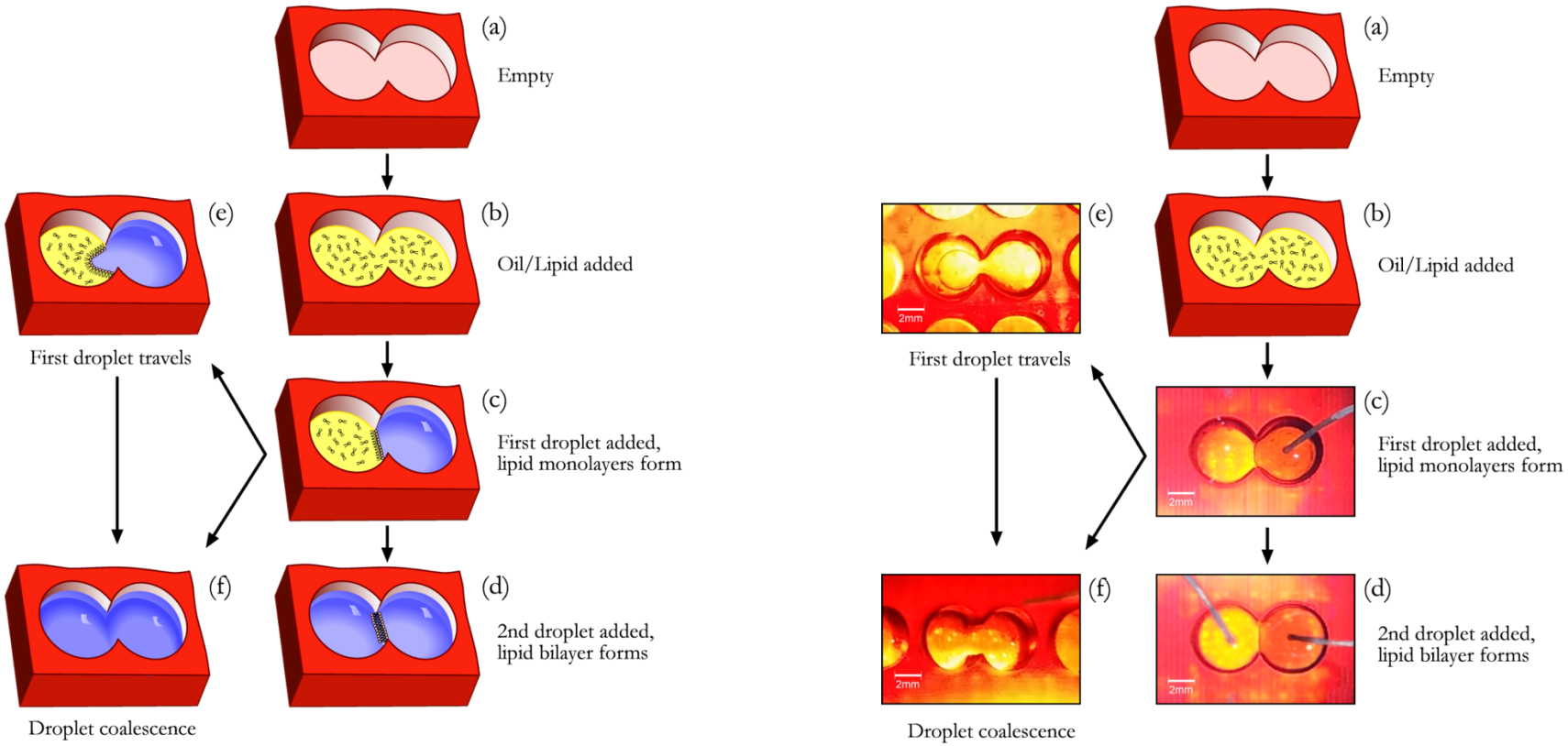

Figure 3.20 Bilayer formation and droplet coalescence sequence
(Left) Sequence diagram of all possible states in the DIB chip where the happy path is:
(a) → (b) → (c) → (d). There are three possible steps after the device is in state (c), occurrence of states (e) and (f) can be minimised by using freshly prepared lipid stock and allowing stabilisation time. (Right) Actual images of the DIB chip in all possible states.

As shown in Figure 3.20, during droplet equilibration, in some instances droplet deformation and travel was observed. This was witnessed at both 15 mg/ml and 25 mg/ml DPhPC lipid in decane mixtures. In almost all these cases droplet merging resulted as soon as the second droplet was added. This droplet travel could have been driven by patchy coverage of lipid on droplet surface, difference in hydrostatic pressure or dated lipid stock. Lessons were learnt and second droplet addition was abandoned in cases of droplet travel to avoid sample material wastage.

3.8 Summary

In this chapter, a logical approach to inventing a novel BLM platform has been presented. The said methodology started by specifying system requirements and targeting a suitable bilayer technology. A droplet interface bilayer (DIB) architecture was chosen as it allowed for a rapid, reliable and simple way of forming suspended lipid bilayers within a millifluidic platform with droplet-droplet monolayer contact. Fourteen configurations were designed in 3D with system bandwidth in mind. The chips were fabricated using stereolithography as a cost-effective way of prototyping at speed. Physical dimensions of built devices were then inspected under microscopy and eight deformed structures were rejected. A further two devices were rejected due to difficulties caused during manual electrode positioning.

Numerous BLM experiments were conducted on the remaining four configurations to identify the most suitable device as well as a robust bilayer formation regime based on reproducibility, stability and growth rate characterisation. Sufficient droplet incubation time was confirmed as a critical step to stable bilayer formation. Lipid concentrations were varied and compared across Devices 3 – 6 and results were analysed for significant differences in bilayer area.

It was hypothesised that the ratio of bilayer size to droplet size could indicate the probability of protein reconstitution for this DIB platform. These ratios were calculated and bilayer to droplet surface coverage was compared as a major factor alongside the aforementioned attributes.

Device 4 with a chamber diameter of 5 mm, depth of 2 mm and interface of 2 mm scored highest in comparison to other architectures and was selected for multiplexing

to enhance platform throughput. The ideal DPhPC lipid concentration in decane was found to be anywhere between 15 mg/ml and 25 mg/ml. It is possible to alter the buffer composition of either side of the bilayer for ion channel studies. The device was capable of being repeatedly used by washing with pure water and ethanol and dried with nitrogen gas.

4 Chapter 4: Proof of Concept with Peptide Channels

Following the identification of an optimised double chamber geometry and enhancement of the DIB platform throughput achieved through multiplexing, the capability of the system to capture the activities of a variety of peptides was investigated to demonstrate proof-of-concept. Small fusogenic peptides, gramicidin and alamethicin, and a larger pore-forming protein, alpha hemolysin, were incorporated into the model membranes by self-insertion. Current-voltage plots of gramicidin are presented as well as observations on the effects of gramicidin addition timing on peptide incorporation delay. The suitability of the platform to carry out drug testing is demonstrated by conducting alpha hemolysin blocking experiments and presenting channel open probability plots.

To demonstrate the feasibility of the platform for medium throughput applications, simultaneous recordings of the mentioned transmembrane pores in a chip with twelve recording chambers and recording electrode pairs were carried out. The chip could be washed and reused repeatedly whilst retaining successful rates of recording. It was possible to achieve protein incorporation after initially allowing for membrane formation and then depositing the peptide of choice into trans/cis side as well as having peptides already present in the second droplet buffer prior to bilayer formation. The peptidic channels adsorbed onto the bilayer and formed pores by spontaneous insertion. Simple peptides serve as a model system to helps us understand the function of protein ion channels, for example, in the past research on gramicidin aided in the appreciation of the selectivity filter of bacterial potassium channel KcsA (Chattopadhyay & Kelkar, 2005).

4.1 Gramicidin Electrophysiology

Gramicidin, a model membrane protein, was the first polypeptide for which single-channel electrophysiology was conducted (Hladky & Haydon, 1970). Gramicidin was chosen for DIB platform experiments for a number of reasons: (a) validates successful formation of a bilayer since gramicidin is assembled from dimers spanning only the thickness of one BLM, (b) confirms the usability of the system for single low conductance ion channel recording, (c) shares an important feature with real ion channels such as the ability to select for specific ions (Kelkar & Chattopadhyay, 2007) and (d) given its well characterised electrical properties (O. S. Andersen, 1983) it was possible to compare observed results to other published work (J L Poulos et al., 2010; Zagnoni et al., 2009).

All experiments start by thoroughly cleaning the double-chamber chip, device 4 from previous chapter, with ethanol (1 wash) and deionised water (3 washes) and dried with a nitrogen air gun. Bilayers were formed by initially depositing 30 µl of a DPhPC/decane mixture at 15 mg ml^{-1} followed by a 31 µl droplet of 0.1M KCl pH7.4 buffer solution containing gramicidin (dissolved in ethanol) at various concentrations. The second droplet of equal volume was added after allowing for a 2 minute monolayer stabilisation time. Symmetric buffer conditions were used and the second droplet contained a mixture of buffer and gramicidin (dissolved in ethanol) at same concentration as the first droplet. At high final concentrations of gramicidin (1 ng ml^{-1}) it was possible to reconstitute gramicidin by adding it to only one side of the bilayer. Sampling was carried out at 5 kHz with 50 mV, 100 mV and 150 mV applied DC potential. A typical gramicidin current recording is shown in Figure 4.1. Dwell times and distinct quantised conductance levels typical of gramicidin channels were

observed which, after correction for salt concentration, were in good agreement with literature (Hirano-Iwata, Aoto, et al., 2010; Hirano-Iwata, Taira, et al., 2010; Le Pioufle et al., 2008; Jason L. Poulos, Jeon, et al., 2009). Dimerization of gramicidin, the transient coming together of two monomers, can be electrically observed where each jump in the recording is representative of a single channel formation. Bilayers with reconstituted gramicidin displayed shorter lifetimes lasting minutes compared to chambers containing only buffer solution lasting at least an hour; this may be due to both the presence of alcohol as well as increased pore surface density causing the bilayer to irreversibly rupture.

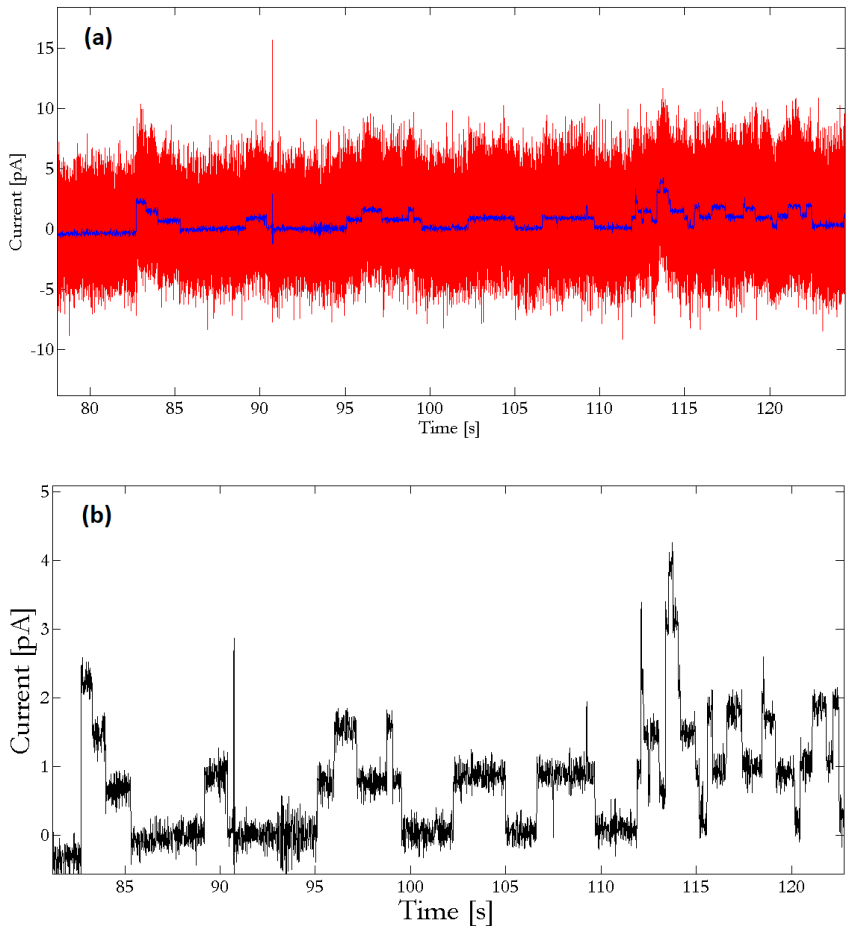

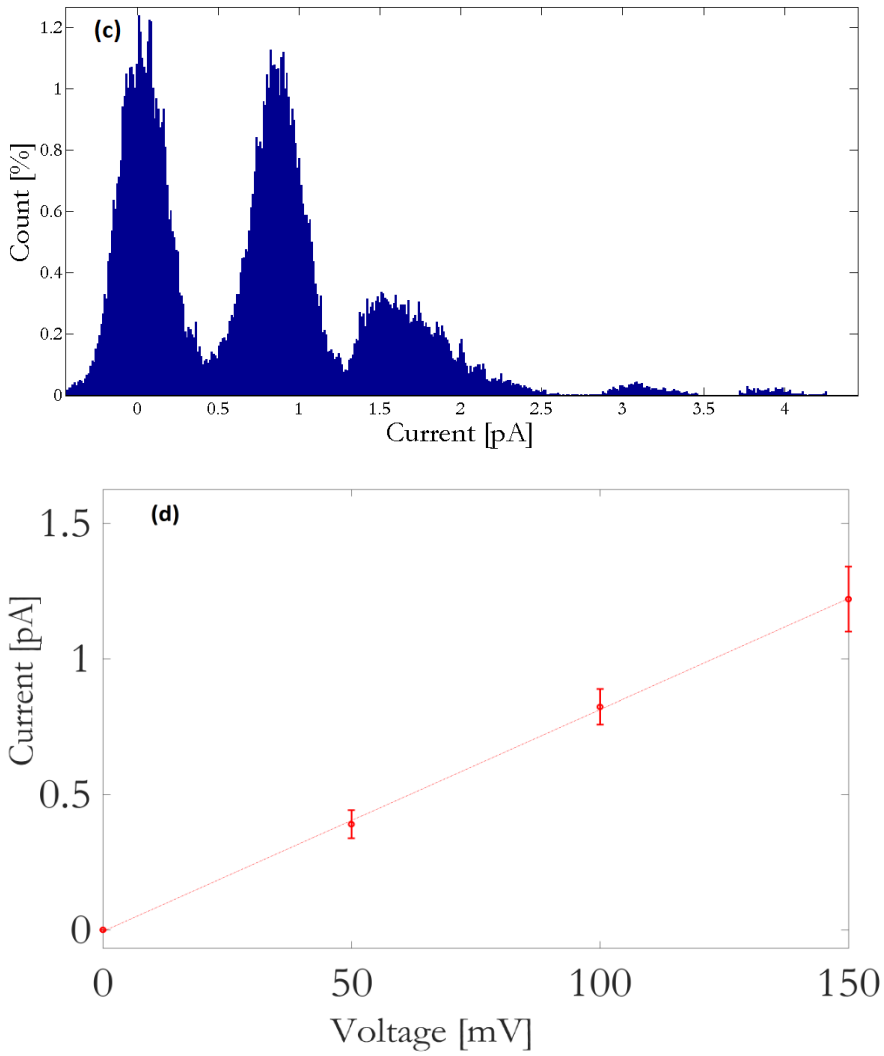

Figure 4.1 Gramicidin channel activity
(a) Monitoring current across the bilayer showing reconstitution of gramicidin channels. Original trace with filtered trace superimposed. (b) Filtered trace of gramicidin channels showing distinct quantised jumps characteristic of gramicidin. Sampling rate 5 kHz, low pass filtered at 100Hz, V_{hold} = +100mV, 0.1M KCl. (c) corresponding point histogram. (d) I-V curves of the gramicidin channel displaying ohmic behaviour. The data are shown as the mean ± s.d. (n > 3 each).

4.1.1 Incorporation Timing of Gramicidin

Given that it was possible to dispense additional droplets on top of existing aqueous compartment post bilayer formation without rupturing the BLM, it was hypothesised that introducing gramicidin to the second droplet in the setup later would improve the protein reconstitution time due to enhanced bilayer area to droplet surface area ratio. To test out this theory, 10 minutes were allowed for the bilayer to grow before

second droplet containing gramicidin was dispensed onto the electrode in the trans side of the bilayer. The peptide containing droplet ran down the electrode and merged with the existing droplet on collision. Based on BLM area analysis in the previous chapter, taking mean bilayer capacitance values, the bilayer area is expected to be 6 to 7 times larger at 10 minutes compared to the first minute. As seen in Figure 4.2 a significant reduction in reconstitution time was observed which confirmed the validity of the hypothesis. To keep the experiments comparable the final concentration of gramicidin was kept consistent across both the fast and slow reconstitution methodologies.

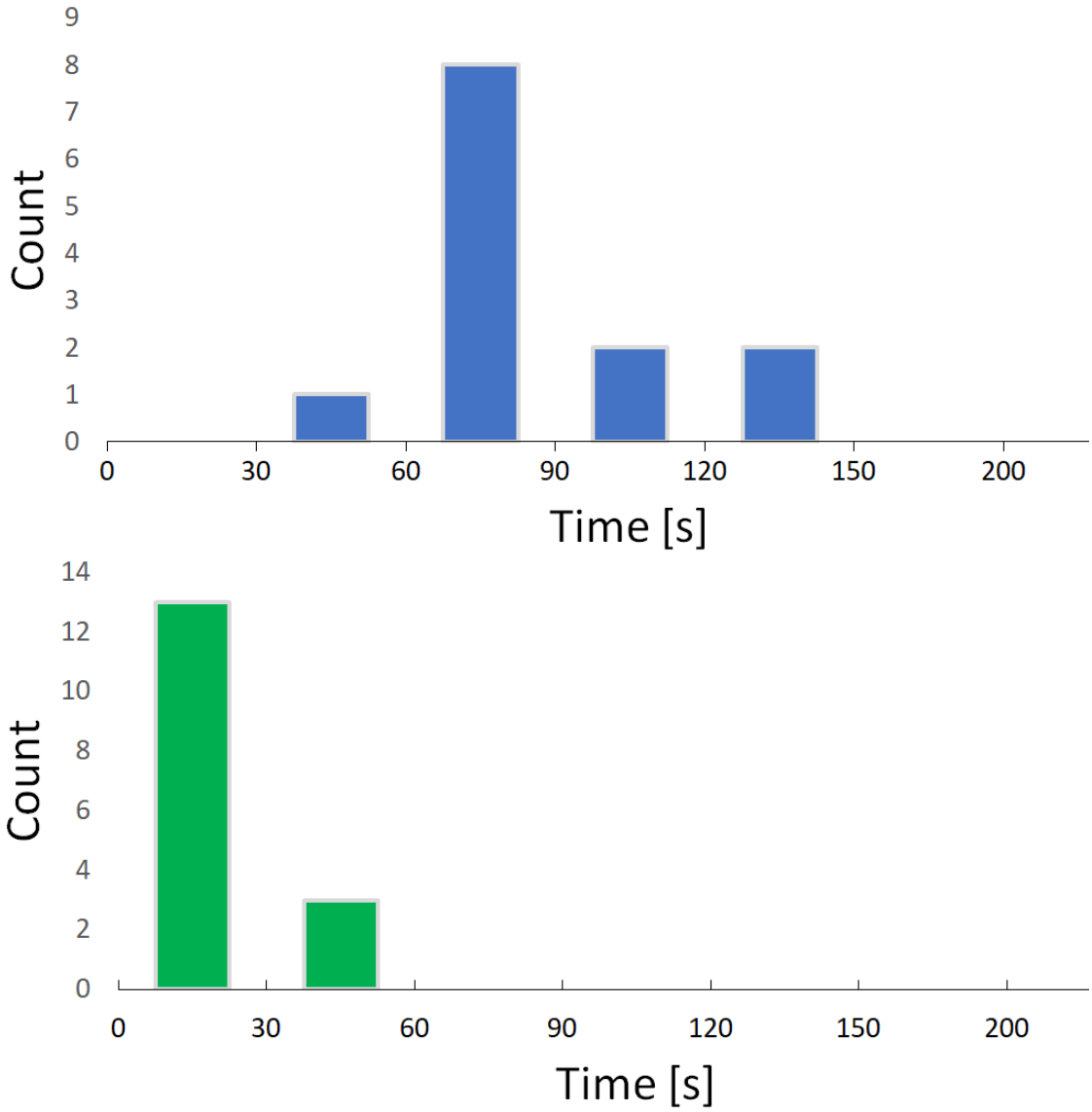

Figure 4.2 Gramicidin reconstitution time
(Top) Time required for gramicidin reconstitution when second droplet contains peptides. (Bottom) Time required for gramicidin reconstitution when peptides are added 10 minutes after adding the second droplet. Count in the vertical axis represents the number of experiments and Time represents the time taken to observe the first instance of gramicidin reconstitution.

4.2 Alpha-Haemolysin Electrophysiology

Alpha-hemolysin (α-HL), a water-soluble channel, is an exotoxin secreted by the bacterium *Staphylococcus aureus*. A number of biosensing solutions employ α-HL as the model pore (Bayley, 2015; Bayley & Cremer, 2001). As a well characterised

channel, α-HL was chosen for DIB platform experiments since its non-gating property allowed for detectable channel inhibition events. The purpose of the blocking experiments were to prove that the system could be utilised to study the effect of drugs on protein kinetics. As seen in Figure 4.3 α-HL displayed sequential stepwise current increase confirming the formation of multiple structurally mushroom-like channels. The observed single pore conductance of 1nS is in agreement with published literature (Thapliyal et al., 2011; Villar et al., 2013)

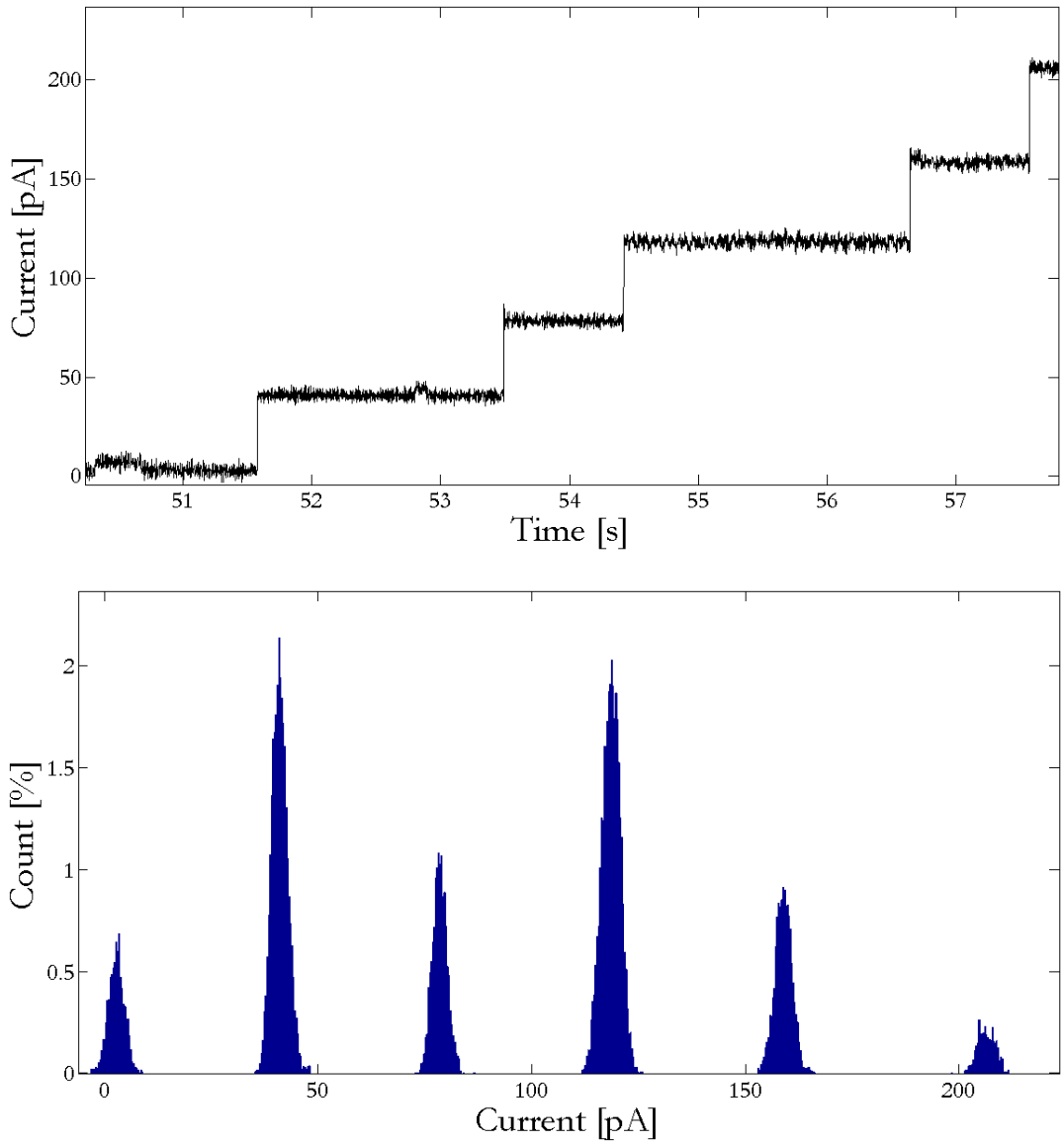

Figure 4.3 Alpha-hemolysin single channel activity in DPhPC
(Top) Alpha hemolysin current trace recorded at 5 kHz sampling rate, low pass filtered at 100Hz, Vhold = +50mV, 1M KCl symmetric buffer conditions. (Bottom) Corresponding point histogram.

4.2.1 Alpha-Haemolysin Blocking

Alpha hemolysin was added to the cis chamber to a final concentration of 10 ng ml^{-1}, which was at ground. The trans compartment was held at 50 mV potential so that the flow of cations was directionally from trans side to cis chamber as indicated by a positive current. Channel blocker β-cyclodextrin (βCD) at various concentrations, shown in Figure 4.4, were added to the trans chamber. All experiments were conducted at room temperature.

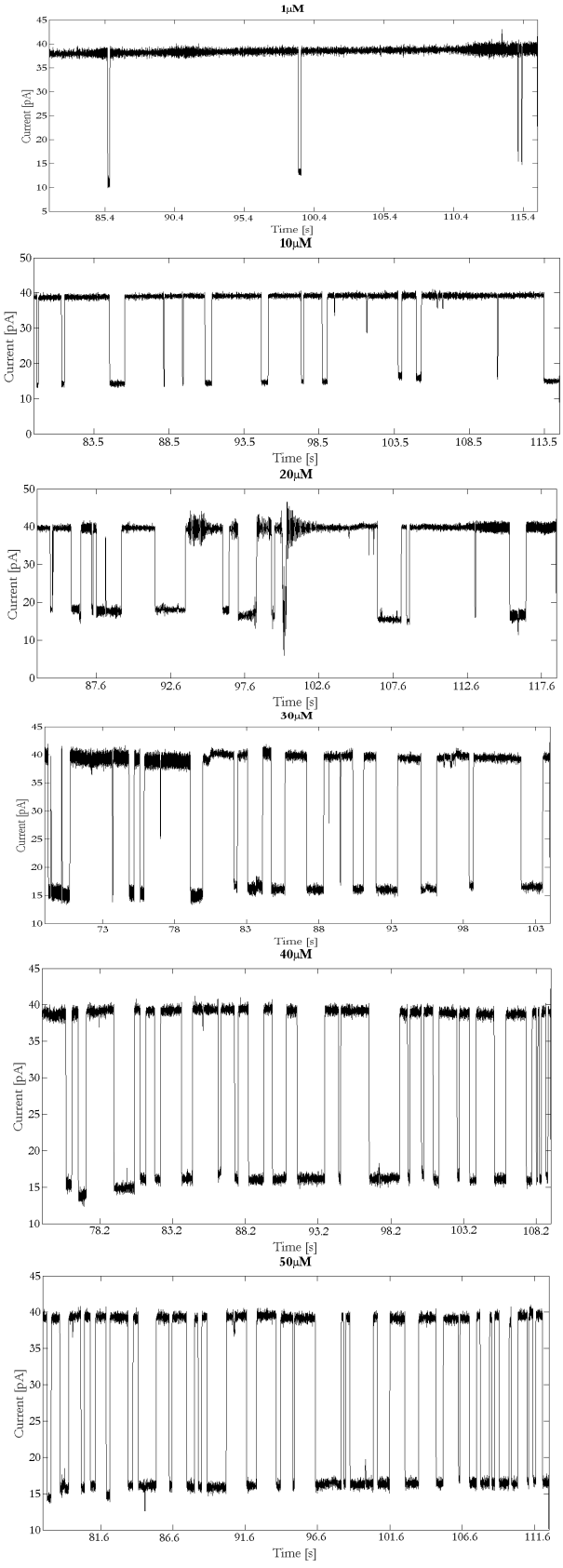
1μM
Current [pA]
Time [s]
10μM
Current [pA]
Time [s]
20μM
Current [pA]
Time [s]
30μM
Current [pA]
Time [s]
40μM
Current [pA]
Time [s]
50μM
Current [pA]
Time [s]

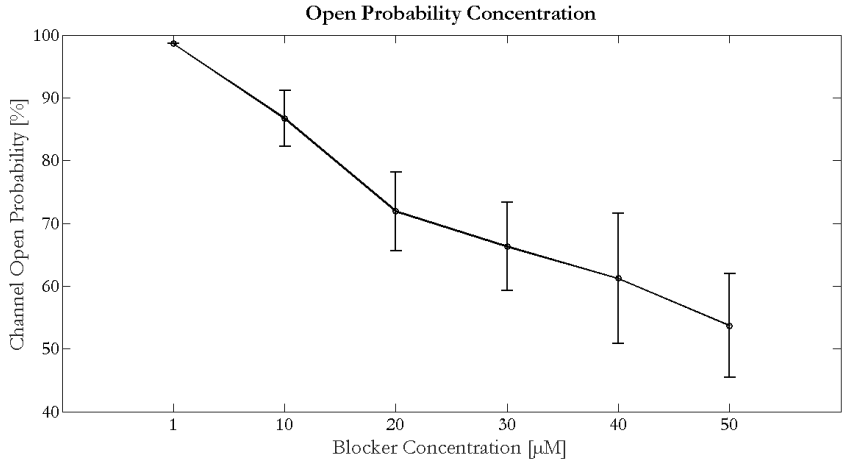

Figure 4.4 Alpha-hemolysin inhibitor experiments
(Top) Short segments of current traces in the presence of β-cyclodextrin at various concentrations (1–50 μM). Traces recorded at 5 kHz sampling rate, low pass filtered at 100Hz, V_{hold} = +50mV, 1M KCl pH7.4 symmetric buffer conditions. (Bottom) Concentration dependence of the inhibition of a single αHL pore by β -cyclodextrin. Channel open probability was plotted versus the concentration of the blocker. Experiments were performed and data acquired for at least 90s were analysed. The data are shown as the mean ± s.d. (n > 3 each).

The inhibitor experiments produced reversible partial blockades of the single channel currents. The kinetics of the interaction show only one current blockade level suggesting one binding site for βCD within the α-HL pore which reduced the conductance of the pore by 60–70% by lodging at a point about half way through the channel, where the diameter is at its narrowest around 14 Å (Gu et al., 1999). In separate experiments βCD was added to the cis side but no blocking events were observed which confirms βCD binds from the trans side of the lipid bilayer even though the cis entrance to lumen is wider than the trans entrance. This observation is consistent with other published work (Gu & Bayley, 2000).

4.3 Alamethicin Electrophysiology

Alamethicin is an antibiotic peptide produced by the fungus *Trichoderma viride*. Alamethicin is one of the best studied peptides (Andrew Woolley & Wallace, 1992; H. Duclohier & Wróblewski, 2001; R Latorre & Alvarez, 1981) that has served as a model pore for voltage gated channels. Typical features of alamethicin are voltage-dependent conductance and the existence of multiple non-equidistant conductance levels of a single channel (Sondermann et al., 2006).

Previous reports stated that both amplitude resolution and bandwidth in a voltage clamp experiment are strongly dependent on the total capacitance of the recording system (Levis & Rae, 1998; Mayer et al., 2003). Earlier in this chapter it was shown that the system was sensitive enough to detect low conductance amplitude events as in the case of gramicidin. In order to show that the DIB platform's bandwidth is sufficient to capture fast gating channels, experiments on alamethicin channels in DPhPC/decane membranes were performed.

Bilayers were formed by initially depositing 30 µl of a DPhPC/decane mixture at 15 mg ml^{-1} followed by a 31 µl droplet of 1M KCl pH7.4 buffer solution. The second droplet of equal volume was added after allowing for a 2-minute monolayer stabilisation time. Symmetric buffer conditions were used and the second droplet contained a mixture of buffer and alamethicin (dissolved in ethanol) at 4 µg ml^{-1} concentration. Sampling was carried out at 10 kHz with +150 mV applied DC potential. A typical alamethicin current composed of bursts of discrete multilevel conductance is shown in Figure 4.5 were in good agreement with published reports (Cafiso, 1994; Hirano-Iwata, Taira, et al., 2010; Kawano et al., 2013). Sojourns in

conductance states with dwell times of 3.5 ms were captured by the setup suggesting a minimum system bandwidth of 285 Hz.

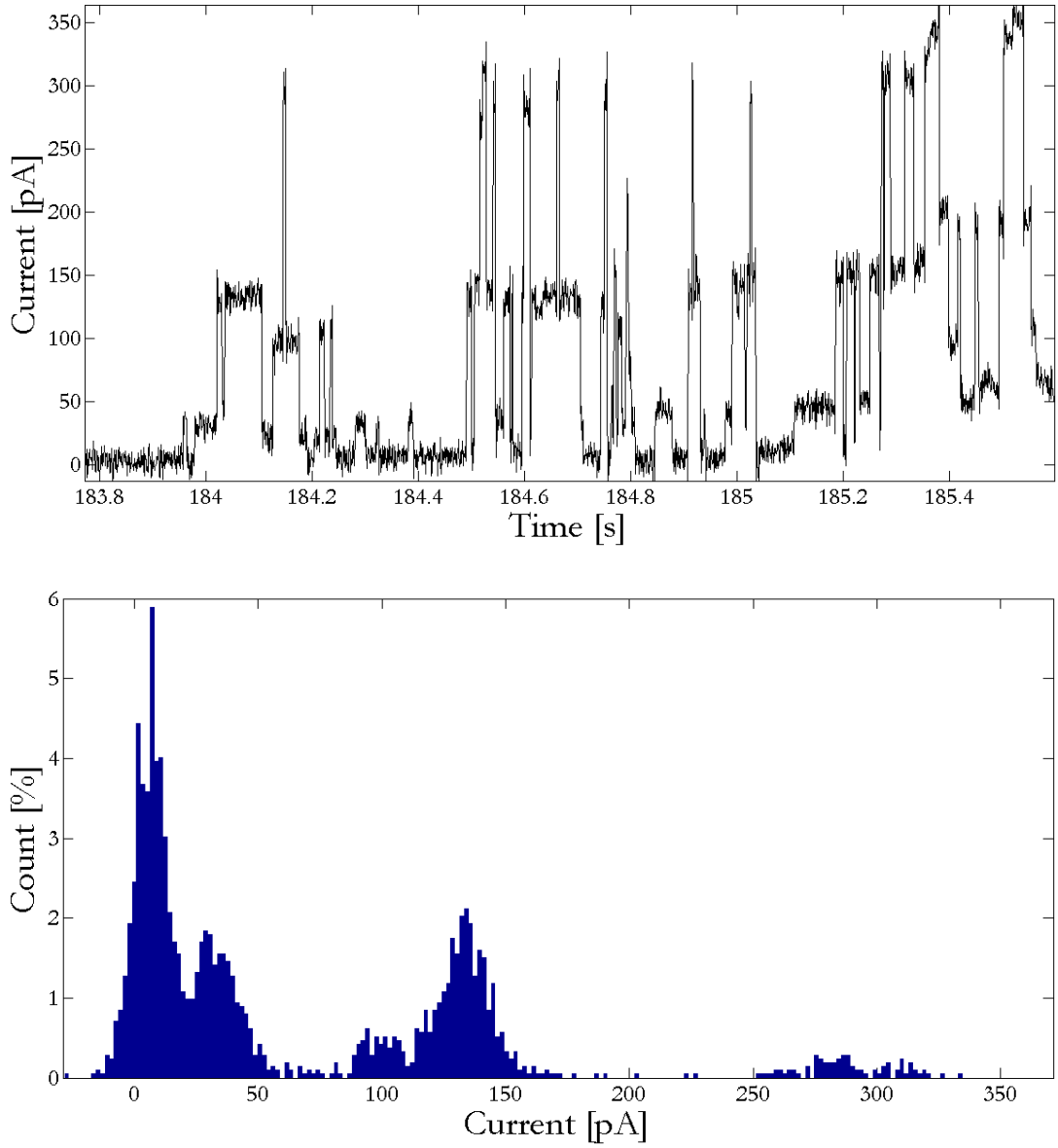

Figure 4.5 Alamethichin single channel activity in DPhPC
(Top) Alamethicin current trace recorded at 10 kHz sampling rate, low pass filtered at 1 kHz, Vhold = +150mV, 1M KCl symmetric buffer conditions. (Bottom) Corresponding point histogram.

4.4 Summary

In this chapter, we succeeded in simultaneous and parallel recording of channel currents through transmembrane pores. Improvements to system throughput is straightforward using automation and increasing the number of double chambers, electrodes and amplifiers. The bilayers in the experiments were formed of DPhPC and the droplets were symmetric, however DIBs can be created with a variety of physiological lipids in both symmetric and asymmetric buffer conditions. The suitability of the DIB platform for protein studies by acquiring single channel activities was demonstrated by reconstituting gramicidin, alpha hemolysin and alamethicin. The conductance and kinetics of the recorded pores were in agreement with published literature. Each of the selected model ion channels revealed a different aspect of the system. Gramicidin reconstitution confirmed the possibility for detecting low conductance channels, whilst alamethicin incorporation verified the suitability for channels with short dwell time. It was observed that bilayer lifetime diminished as a result of increasing transmembrane pore density. The relationship between bilayer size and protein incorporation time was investigated, the data suggests that incorporation time decreases with bilayer size due to enhanced bilayer area to droplet surface area ratio. It was possible to add β-cyclodextrin to the aqueous chamber without rupturing the bilayer in alpha hemolysin blocking experiments proving platform's versatility for drug screening applications.

5 Chapter 5: BK Ion Channel Electrophysiology

In chapter 5 it was demonstrated that the DIB platform was suitable to record peptidic currents. Naturally, the next step is to test more complex ion channels. Thus the aim of this chapter is to investigate the possibility of reconstituting pharmacologically relevant BK STREX ion channels, to examine the applicability of the ion channel reconstitution technique introduced in the previous chapter to BK STREX in order to reduce incorporation time and improve successful reconstitution and to study the voltage dependence of BK STREX ion channels.

Other studies have interrogated BK channels in DIB platforms (Tsuji et al., 2013), however, their reconstitution method necessitated the production of detergent-stabilized ion channels or proteoliposomes which is demanding, time consuming and requires specialist equipment. In the experiments of this chapter a simpler, more cost effective yet reliable channel insertion method from recombinant overexpressing cell membranes was employed thus avoiding a labour intensive reconstitution process (Demarche et al., 2011) whilst retaining full channel functionality.

There are also a number of other studies that have employed the simpler crude membrane method to isolate and incorporate BK channel, however, these have not been in DIB platforms and require stirring to induce ion channel reconstitution (Crowley, 2003; O'Connell et al., 2006). To the knowledge of the author this work is the first to explore BK STREX phenotype channel electrophysiology by combining DIB platform with recombinant expressing cell fragments.

5.1 Introduction

5.1.1 Potassium Ion channels

Potassium-selective (K+) channels are the largest and most diverse group of ion channels represented by some 70 known loci in the mammalian genome (Gutman et al., 2005). Potassium channels have been found in all cell types and show wide ranging structural diversity creating broad physiological functionality. These highly selective cation channels are characterised by an equilibrium potential near the cellular resting potential, making them important determinants in maintaining the resting membrane potential (Salkoff et al., 2006).

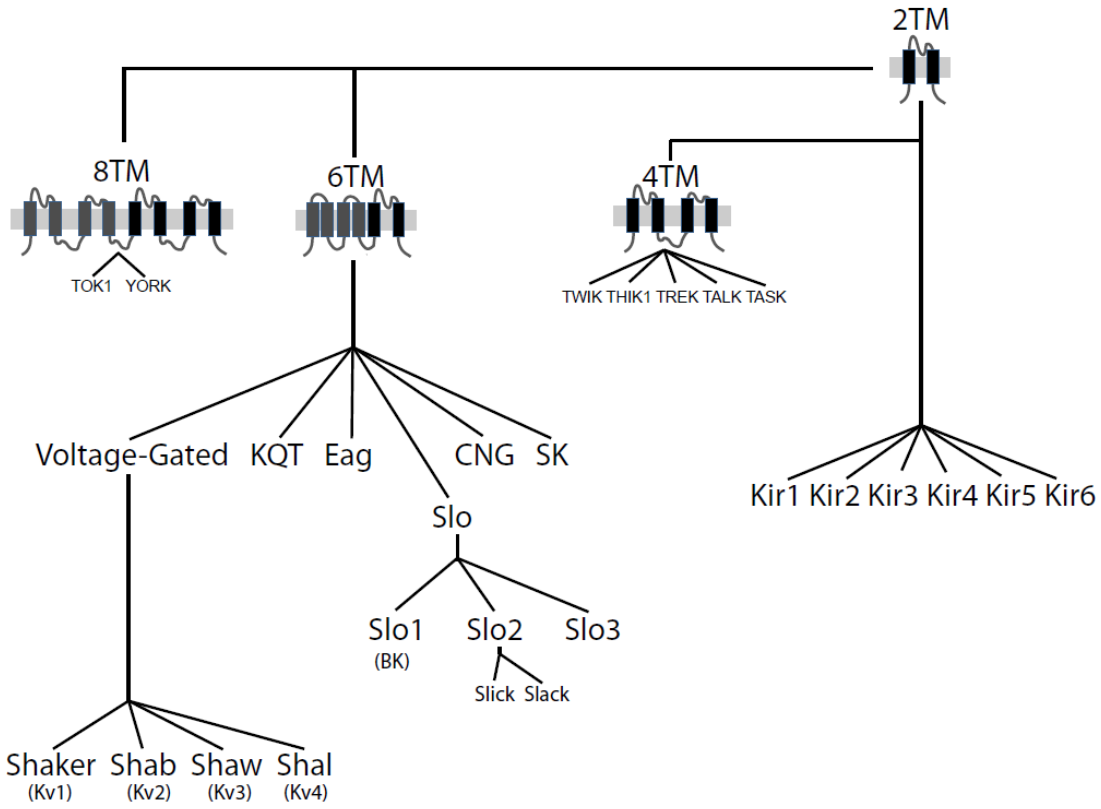

Figure 5.1 The potassium channel family
Potassium channels can be categorised into four main structural classes encoding 2 transmembrane (2TM), 4 transmembrane (4TM), 6 transmembrane (6TM) and 8 transmembrane (8TM) subunits. Within the 6TM class there are a further six families of which the Slo1 subfamily in the Slo multigene family are characterised by high single channel conductance. These big conductance potassium (BK) channels are the ion channels studied in this chapter. Figure taken from (Jeffries, 2010).

As shown in Figure 5.1, the classification of potassium channels is broadly defined by transmembrane topology; those with two transmembrane domains (2TM) around a conserved pore domain, those with four transmembrane domains (4TM) associated with two pore domains, the six transmembrane domains (6TM) associated with one pore domain and the eight transmembrane domains (8TM) with two pore domains. Each class is subdivided into other families which are extended to more structurally and functionally similar subfamilies. The potassium ion channel studied in this chapter, BK, is a member of the Slo1 family under the Slo multigene family. The BK subfamily, also known as maxi-K channels (Ramon Latorre et al., 1983) or Slo1 channels (Atkinson et al., 1991), are identified by a large single channel conductance profile, ranging around 250 pS (Farley & Rudy, 1988; R Latorre et al., 1982; Marty, 1983) which earned it the name big potassium channels (Blatz & Magleby, 1983).

BK channel structure is assembled from pore forming α-subunits and regulatory β-subunits (Garcia-Calvo et al., 1994; McManus et al., 1995). The BK channel pore-forming α-subunit is uniquely encoded by a single gene, KCNMA1 also called Slowpoke (Lee & Cui, 2010), and the regulatory β-subunits are encoded by a family of four genes, KCNMB1-4 (Jeffries, 2010). The BK channel is gated by both voltage and an increase in cytosolic calcium. BK channels are found in most cells throughout the body where they regulate a large variety of physiological processes including smooth muscle tone (Brenner et al., 2000; Matthias Sausbier et al., 2005) and neurosecretion (Robitaille et al., 1993). BK channels have been shown to be responsive to a range of factors including hypoxia (McCartney et al., 2005), protein kinases (Schubert & Nelson, 2001) and growth factors (Weaver et al., 2004).

The importance of BK's physiological role and therefore its study is highlighted by the pathophysiological conditions which occur as a result of BK channel dysfunction in an affected tissue. For example, in smooth muscle of cardiovascular system this malfunction leads to increased blood pressure (Brenner et al., 2000; Matthias Sausbier et al., 2005) . In the bladder BK channel dysfunction causes urinary incontinence (Meredith et al., 2004), in the colon BK dysfunction brings about abnormal loose fecal matter (Hagen et al., 2003) and in penile arterial and corpus cavernosum smooth muscle BK dysfunction causes decline in erectile capacity (Christ et al., 2004; Werner et al., 2005). In the central nervous system (CNS) the BK channel regulates neuronal excitability (Faber & Sah, 2003; Raffaelli et al., 2004; M Sausbier et al., 2004; Womack, 2004). In the CNS, BK dysfunction leads to a number of pathophysiological conditions such as epilepsy and paraoxysmal dyskinesia (Brenner et al., 2000; Du et al., 2005), high frequency hearing loss (Rüttiger et al., 2004) and deficient motor co-ordination (M Sausbier et al., 2004).

5.1.2 BK STREX

The BK channel under study in this chapter is the STREX phenotype. As shown in Figure 5.2, there are a number of splice sites in the intracellular C-terminus (C:1-5) as well as in the N-terminus (N:1-2) and differential splicing impacts functional characteristics of the BK channel (Chen et al., 2005; Saleem et al., 2009). For BK STREX variant (e21 variant), at splice site C2 there is a 58 amino acid insert (exon 21) between exon 19 and exon 23. The e21 variant, first defined in 1997 (Saito et al., 1997), is highly conserved from human to zebrafish and confers an apparent increased Ca^{2+} sensitivity to the BK channel (Jeffries, 2010).

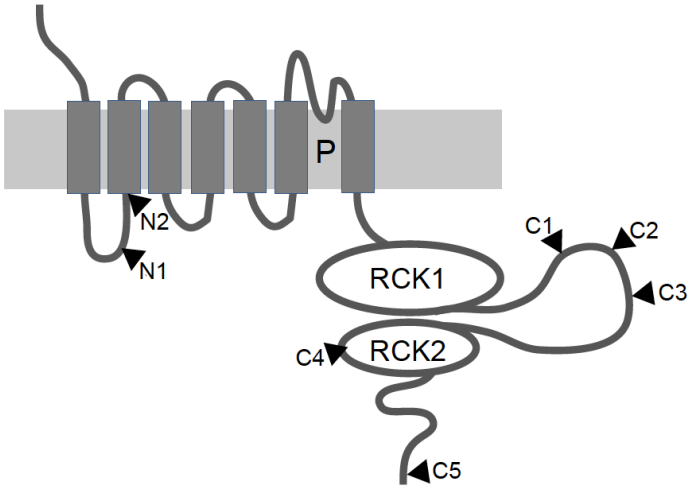

Figure 5.2 Topology of BK channel
Illustration of alternative splice sites in the N-terminus (N:1-2) and C-terminus (C:1-5). Figure taken from (Jeffries, 2010).

It was found that the number of channels containing the exon 21 splice insert relative to channels without an insert at the C2 site could be modulated by the hypothalamic-pituitary-adrenal (HPA) stress axis (Xie, 1998). Following this discovery exon 21 was named the STRess axis-regulated EXon, or STREX. STREX has been shown to be important in modulating BK channel behaviour. For instance, McCartney demonstrated that a cysteine rich motif in STREX confers hypoxic sensitivity to BK channels (McCartney et al., 2005) .

BK STREX can be found mainly in endocrine tissues, the pancreas and pituitary as well as the cerebellum, uterine smooth muscle, and prostate (Chen et al., 2005; Ferrer et al., 1996; Saito et al., 1997; Shipston et al., 1999; Tseng-Crank et al., 1994; Xie, 1998; Zhu et al., 2005). It is largely absent from spinal cord tissue, the majority of smooth muscle cells and skeletal muscle (Jeffries, 2010).

5.2 Isolation of BK Ion Channel

Reconstitution of ion channels from native membranes into lipid bilayers permits the study of single channels with parallel control of internal and external buffers, and possibly with a better control of the microenvironment of the ion channel compared to excised membrane patches in traditional patch clamping (Ertel, 1990). This is chiefly because cytoplasmic remnants are unlikely to be present in reconstituted channels. This accessibility to the internal and external side of the channel protein has proven valuable in modulatory studies (Toro et al., 1990; Reinhart et al., 1991; Chung et al., 1991; Scornik et al., 1993). It has been demonstrated that channels reconstituted from expression systems exhibit functional properties characteristic of native BK channels (Pérez et al., 1994). Prior to reconstitution, ion channels were isolated from HEK 293 cells.

5.2.1 Crude Membrane Preparation

HEK-293 membrane fragments containing BK STREX were isolated using a HEK-293 membrane preparation protocol (Crowley, 2003) with slight modifications. The entire procedure was performed at 4°C. HEK-293 cells stably transfected with BK STREX cDNA (provided by Prof Mike Shipston, University of Edinburgh), covering a total area of 300 cm^2, were grown to confluence, pelleted, and resuspended on ice in 10 ml of buffer: 30 mM KCl, 2 mM $MgCl_2$, 10 mM HEPES, and 5 mM EGTA, pH 7.2 supplemented with 100 µM phenylmethylsulfonylfluoride, 1 µg/ml aprotinin and 1µg/ml leupeptin. The cell suspension was forced through a 27-gauge needle four times using a 10ml syringe and sonicated at maximum power for 60s to lyse the cells. The suspension was carefully layered on a 20% (w/v) and a 38% (w/v) sucrose

density gradient (in 20 mM MOPS, pH 7.1). This was achieved by dispensing the cell suspension first using a 21-gauge needle to the bottom of a 30mL ultracentrifuge tube. The 20% (w/v) sucrose solution was then injected to the bottom of the tube displacing the cell suspension, followed by the 38% (w/v) sucrose solution which displaced the 20% (w/v) sucrose solution. The resulting three layer tubes, illustrated in Figure 5.3, were centrifuged in a swing-out rotor (Optima L-100 XP ultracentrifuge with swing-out rotor SW28 Ti, Beckman Coulter, USA) at 25,000 rpm for 60 min at 4°C. A cloudy white band at the 20% to 38% interface was collected with a syringe, diluted with bi-distilled H_2O, and centrifuged (Optima L-100 XP ultracentrifuge with fixed-angle rotor 50.2 Ti, Beckman Coulter, USA) at 45,000 rpm for 60 min at 4°C. The resulting pellet was resuspended in 200µL of buffer (250 mM sucrose and 10 mM HEPES, pH 7.3) and stored at - 80°C and was used later for electrophysiological experiments.

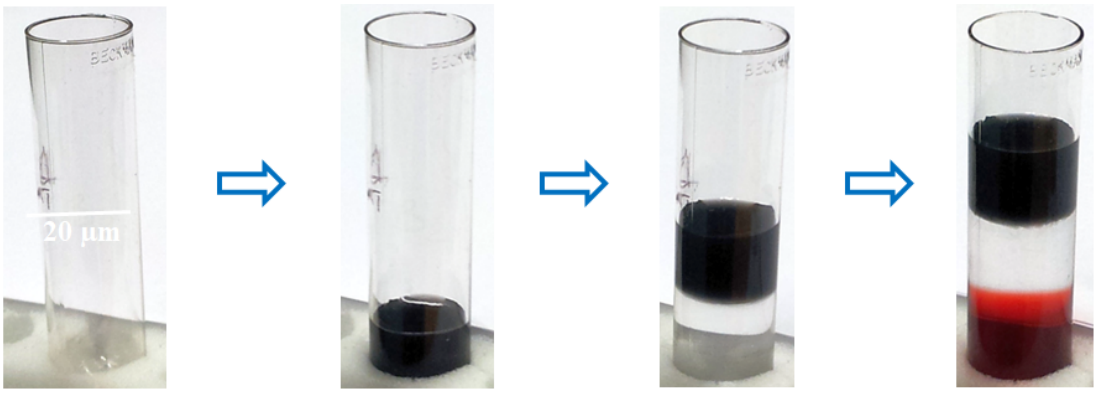

Figure 5.3 Sucrose gradient protein isolation
Illustrating the procedure followed to isolate membrane proteins from HEK-293 cells. The following steps create the appropriate sucrose gradient layers before centrifugation. Dye, not used in real experiments, is used here for visualisation purposes. (Left to right) Sample is loaded first (black dye), then 20% (w/v) sucrose solution (clear solution) is slowly injected to the bottom, finally 38% (w/v) sucrose solution (red dye) is injected to the bottom of tube.

5.2.2 Bradford Protein Assay

A Bradford protein assay is a protein concentration determination procedure involving the binding of dye to protein (Bradford, 1976). The principle behind this technique is a colour change of the solution in response to the binding of the Coomassie Brilliant Blue G-250 dye with protein. Protein standards were prepared from bovine serum albumin (BSA) to establish a correspondence between absorbance values and known BSA concentrations. A standard curve was set up using BSA at a concentration range of 62.5-2000 μg/mL. The results are expressed as mean ± SEM of triplicate readings, compared to a negative control which was only dH_2O. This is plotted by the blue line in Figure 5.4. The below procedure was followed, as per the manufacturer, to measure the concentration of purified BK protein from the sucrose gradient step:

The Quick Start Bradford 1X Dye Reagent (Bio-Rad, UK) was removed from 4 °C and was warmed in a water bath for 30 min. After a gentle mix, 250 μL of the reagent was transferred to each well of a 96-well flat bottom black plate and 5 μL of the BK sample was added to designated wells. A blank was prepared by adding 5 μL of the dH_2O to the 1X reagent. The plate was then incubated for 15 minutes at room temperature and the absorbance was measured at 595 nm on a M5 microplate reader (Molecular Devices, UK). The average sample protein concentrations of purified BK channels were found to be 1.86 mg ml^{-1} which is in agreement with published work (Oshima et al., 2013).

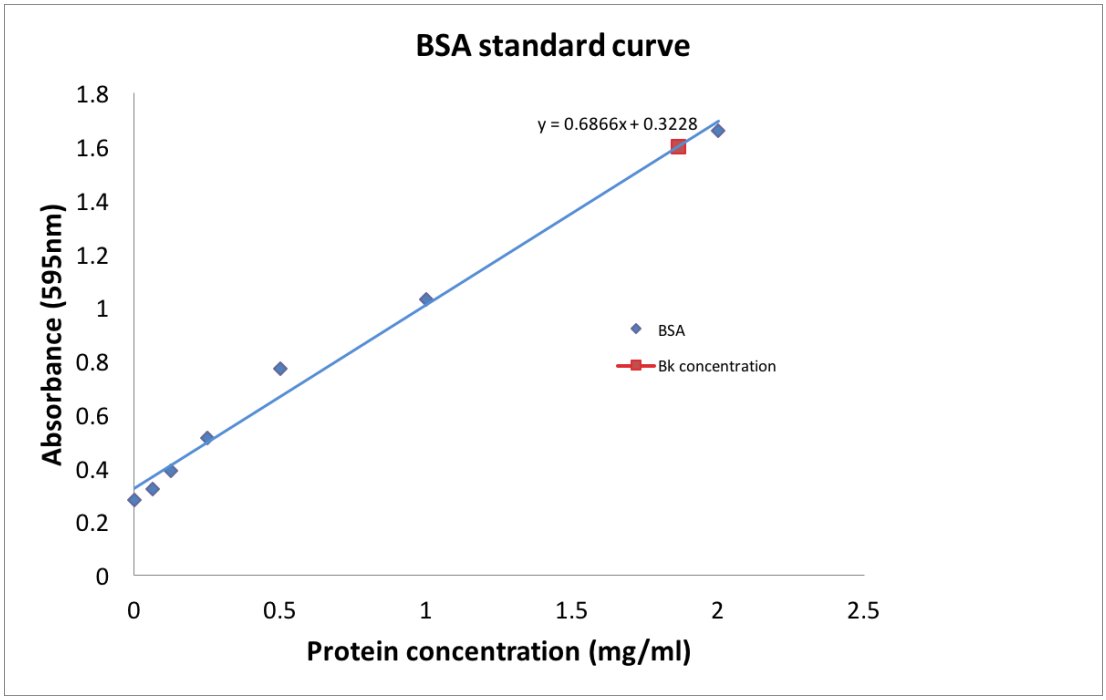

Figure 5.4 BSA standard calibration curve and BK concentration
The calibration curve was plotted against increasing concentrations of BSA (62.5-2000 µg/mL). The values shown here are the mean of triplicate reading ± SEM (SEM bars too small to see). The red square represents the average absorbance of the three extracts of the purified BK channel.

5.3 Confirmation of BK Channel Expression

Before running the necessary procedures to isolate the BK STREX ion channel from the cell for electrophysiology it was necessary to first confirm that the HEK-293 cells were expressing the protein. To do this manual patch clamping was carried out and macroscopic currents were recorded (data not shown). BK expression was also confirmed using reverse transcription polymerase chain reaction (RT-PCR) techniques as explained below. PCR is a technique used in molecular biology to amplify a segment of DNA generating millions of copies of a particular DNA sequence (Mullis et al., 1986).

As shown Figure 5.5, the expression of BK mRNA in HEK-293 cells was determined through the following steps: RNA isolation, cDNA synthesis, reverse transcription PCR, gel electrophoresis, gel purification of the PCR product and DNA sequencing to confirm the identity of the PCR product.

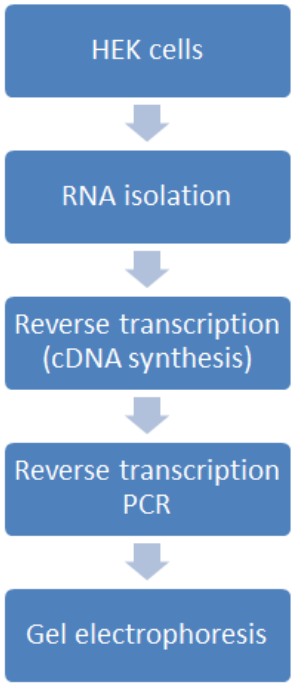

Figure 5.5 Confirmation of BK channel expression workflow

5.3.1 PCR and PCR-related techniques

5.3.1.1 RNA isolation for HEK-293-BK cells

Total RNA was isolated from HEK-293-BK cells to allow to assay for BK channel mRNA expression. Total RNA was isolated from standard T-25 flasks where the cells were grown to 80% confluence. The RNA isolation was carried out using a Isolate 2 RNA Mini Kit (Bioline, UK) as per the manufacturer's protocol The optional DNase treatment included to reduce any carryover genomic DNA contamination which might interfere with the PCR assay. Concentration and quality assessment of the extracted RNA was carried out using NanoDrop 2000C Spectrophotometer (ThermoFisher Scientific, UK). RNA was confirmed to have a A_{260} / A_{280} ratio of 2.1. RNA was stored at -80°C until required.

5.3.1.2 First-Strand cDNA Synthesis of HEK-293 BK RNA

To assess the expression of BK channel mRNA by PCR, the extracted total RNA had to be converted to complementary DNA (cDNA). This cDNA synthesis was carried out using a Tetro cDNA Synthesis Kit (Bioline, London, UK). 5µg of HEK-293 total RNA was used in a 20µl reverse transcriptase reaction as per the manufacturer protocol. The kit supplied oligo dT was used as the primer and the reaction underwent a 45 minute of incubation at 45°C. This sample was marked as RT+. A reaction was set up in parallel with no reverse transcriptase (RT-) and would act as a negative control for the PCR as no template should be present unless genomic DNA was carried over from the RNA isolation. A PCR carried out with an aliquot of this RT- cDNA should not generate an amplicon unless carryover genomic DNA acted as

the template. The reverse transcriptase inactivation step was carried out and the cDNA was stored at -20°C until required.

5.3.1.3 Reverse Transcription PCR

Reverse transcription PCR (RT-PCR) is a technique in molecular biology to detect gene expression through the creation of complementary DNA (cDNA) transcripts and then the amplification of cDNA through traditional PCR. RT-PCR was used here to confirm the expression of BK STREX gene, inferring the expression of BK STREX ion channel in HEK-293 cell line.

PCR primers specific for human BK channel were designed against GenBank accession NM_001014797.2 as seen in Table 5.1.

Primer	Primer Sequence	Primer Tm	Amplicon Size
BK AssayFOR	5′-AACATCCCGAGCTGGAATTGG-3′	57.7°C	256
BK AssayREV	5′-GCTCACAAACAGTAGGGAAGGACAG -3′	59.2°C	

Table 5.1 RT-PCR primer sequences detection of human BK mRNA expression in cell lines
GenBank accession number NM_001014797.2 was used to design the primers but the primers will also detect multiple BK (KCNMA1) transcript variants (NM_002247, NM_001161352, NM_001161353, NM_001271518, NM_001271519) and generate a single 256bp amplicon

The PCR components for a 25µl endpoint PCR reaction followed the Q5 Hot Start High-Fidelity 2X Master Mix DNA polymerase system recommendations (New England BioLabs, UK) , and is detailed in Table 5.2. The components were added to 200ul thin-walled PCR tubes using aerosol-resistant tips.

Reaction Component	25µl Reaction
Q5 Hot Start High-Fidelity 2X Master Mix	12.5µl
10µM Forward Primer	1.25µl
10µM Reverse Primer	1.25µl
cDNA	1µl
Nuclease-Free Water	9µl

Table 5.2 Recipe for Q5 Hot Start High-Fidelity 2X Master Mix PCR reaction setup

The thermal cycling conditions were as shown in Table 5.3 using a Primus 96 thermal cycler, (MWG AG Biotech, Ebersberg, Germany). Once the reaction was completed it was stored at -20°C until gel electrophoresis.

Step	Temperature	Time
Initial Denaturation	98°C	120 seconds
35 Cycles	98°C	10 seconds
	60°C	20 seconds
	72°C	30 seconds
Final Extension	72°C	120 seconds

Table 5.3 PCR Thermo cycling conditions

5.3.1.4 Horizontal Submarine Gel Electrophoresis

Gel electrophoresis was employed for visualisation, sizing and gel purification of PCR products using a horizontal submarine mini-gel apparatus (Bioscience Services,

UK) and electrophoresis power supply (Kodak, UK) and extract PCR product. The PCR product was electrophoresed with a 1% w/v Tris-borate-EDTA (TBE; 89mM Tris-Base, 2mM Na_2-EDTA, 89mM Boric Acid, pH8.3)-agarose gel with a 1× TBE electrophoresis buffer. In order to visualise the DNA 2µl of a 10mg/ml solution of Ethidium Bromide was added to the 50ml agarose gel.

15µl of PCR product was added to 2µl of gel loading buffer (BioLine, London, UK) and total volume was pipetted into gel well. 6µl of BioLine Hyperladder 2 size marker was also deposited into neighbouring well. The fragments were electrophoresed at 50 volts for 1 hour. The resulting PCR products were visualised and recorded on an InGenius UV gel documentation system (Syngene, UK). The PCR amplified a single amplicon in the RT+ reaction of the 256bp as expected.

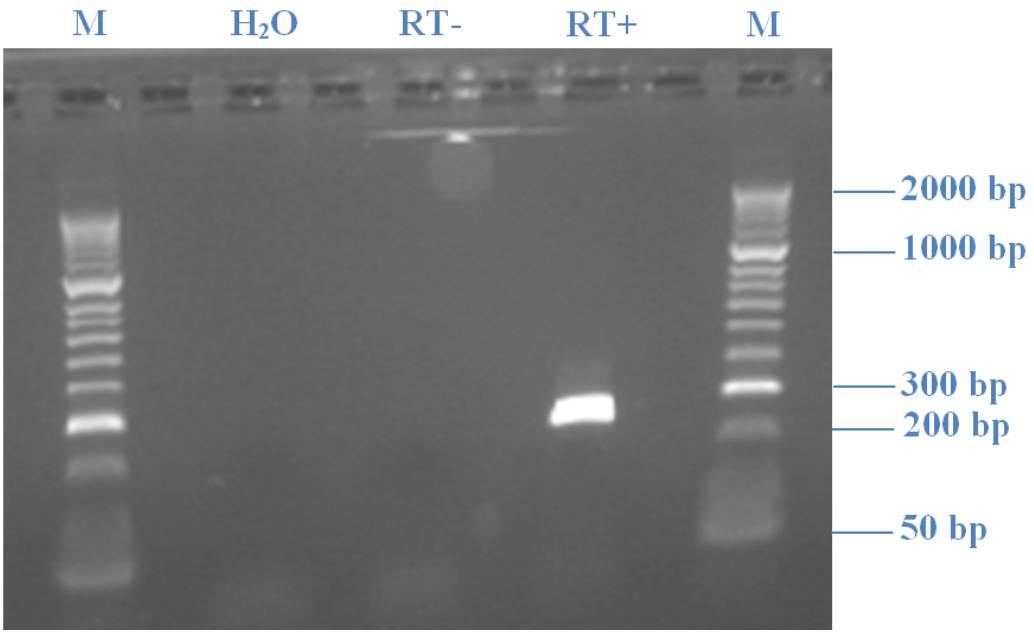

Figure 5.6 Gel electrophoresis result of transcribed PCR product of BK cDNA confirming 256bp on a 1% agarose gel
Lanes from left to right: BioLine Hyperladder 2 (M), deionised water (H_2O), negative control (RT-), transcribed PCR product (RT+), BioLine Hyperladder 2 (M).

5.3.2 Western blot

Western blot was performed to verify the presence of expressed BK ion channels from crude membrane fragments. Western blotting is an analytical procedure used to detect specific target proteins involving running sodium dodecyl sulfate polyacrylamide gel electrophoresis (SDS-PAGE), transfer to nitrocellulose membrane sheet, blocking to prevent non-specific antibody binding, staining with primary and secondary antibody and detection using chemiluminescence. (Burnette, 1981; Ross, 1995).

Western Blot analysis was performed using the primary-antibody anti-BK L6/60 (UC Davis/NIH NeuroMab Facility, US) against the BK channel C-terminus. The secondary antibody used for the channel was anti-mouse raised in rabbit HRP (BioRad). The western blot results (not shown) were inconclusive.

5.4 BK Ion Channel Studies

5.4.1 Ion Channel Reconstitution

The efficiency of protein ion channel studies in bilayer systems are impacted by two important factors, namely bilayer stability and ion channel reconstitution. Optimum bilayer stability conditions for the proposed DIB platform were identified in chapter 4. In order to maximise the chances of channel reconstitution a number of aspects were carefully considered including bilayer lipid composition, protein isolation method, protein concentration, calcium concentration and bilayer area.

A neutral lipid, DPhPC, was selected for the experiments in this chapter since other studies have shown this type of lipid composition to be successful for BK incorporation (Ide & Ichikawa, 2005; Kawano et al., 2013). The crude membrane protein isolation method has also proven widely successful in a number of published literature (Crowley, 2003; de Wet et al., 2009; Leptihn et al., 2011; Oshima et al., 2013; Rosemblatt et al., 1981; Yuan et al., 2004) for purifying and integrating ion channels in BLM electrophysiological experiments. Studies (Leptihn et al., 2011; Pérez et al., 1994) have also demonstrated that another major step is to dilute the membrane-enriched sucrose interface to preserve ion channel functionality, maintain bilayer stability, diminish the interference of unwanted endogenous channels from the membrane and to help with single channel recording. As such, the isolated membrane fragments were diluted to around $1{:}10^6$ (v/v). Increases in intracellular calcium concentrations are detected by BK channel calcium bowl which is known to enhance channel open probability (Crowley, 2003; McCartney et al., 2005; Pérez et al., 1994), thus a Ca^{2+} concentration of 50 μM was used for the cis droplet. Lastly,

given published reports on the dependence of incorporation of an active ion channel on lipid bilayer area (Kresák et al., 2009; Miller, 1986; Studer et al., 2011), two permutations of bilayer area, whilst keeping chamber buffer volumes equal, were investigated as in chapter 5. In these experiments ion channels were added to the cis compartment before bilayer formation, by having protein membrane fragments already mixed with second droplet buffer, and were compared against dispensing membrane fragments to cis chamber 10 minutes after bilayer formation. As estimated in chapter 5, the bilayer area is expected to be 6 to 7 times larger at 10 minutes compared to the first minute. In both cases BK STREX channels fused with the bilayer and formed functional ion channels, however, the reconstitution time differed significantly as shown in Figure 5.7. To keep the experiments comparable the final concentration of BK STREX was kept consistent across both reconstitution methodologies.

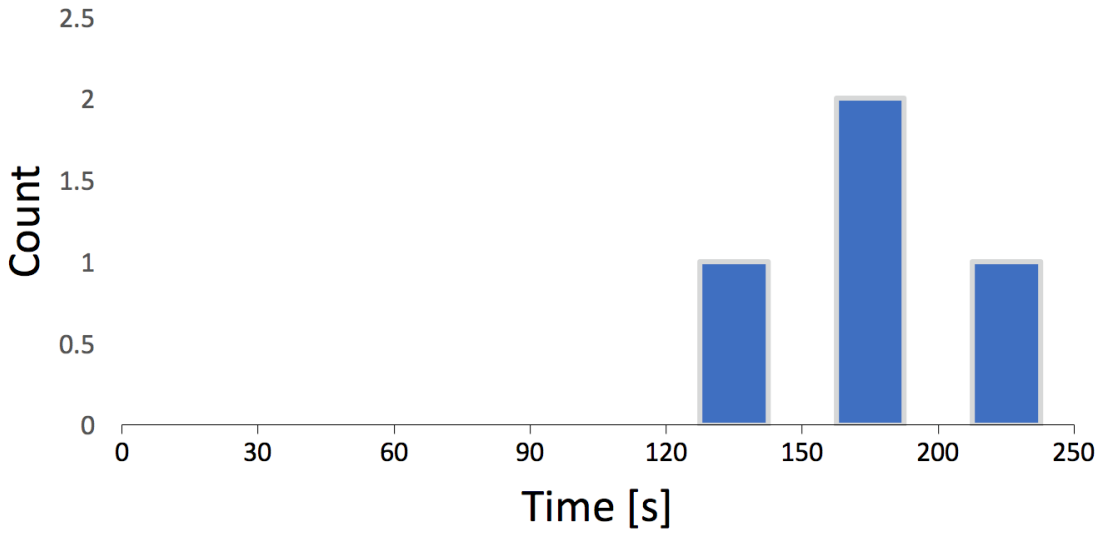

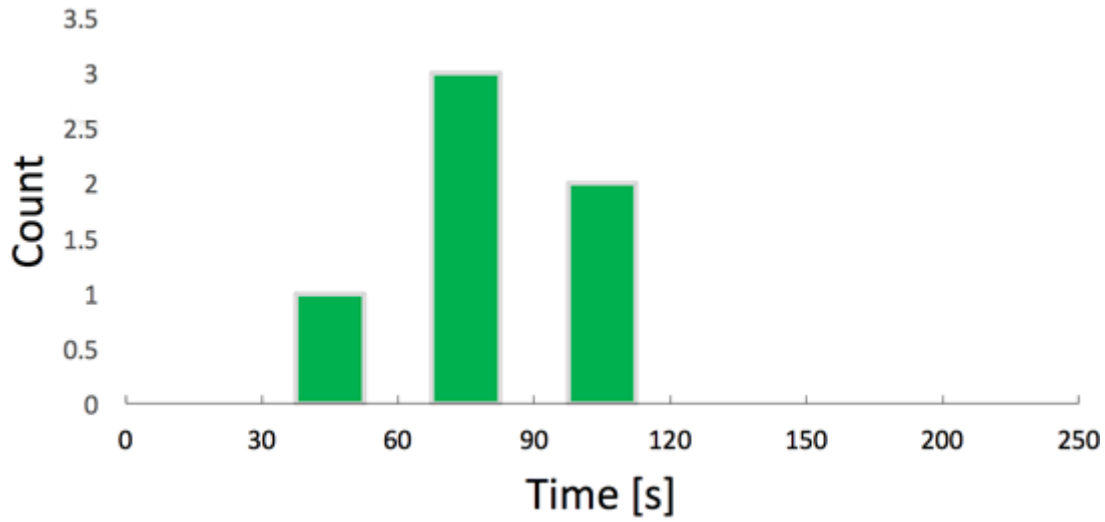

Figure 5.7 BK STREX reconstitution time
(Top) Time required for BK STREX reconstitution when second droplet contains ion channels. Success rate: 7% in formed bilayers (Bottom) Time required for BK STREX reconstitution when ion channels are dispensed 10 minutes after adding the second droplet. Success rate: 29% in formed bilayers. Count in the vertical axis represents the number of experiments and Time represents the time taken to observe the first instance of BK STREX reconstitution.

Enhancing the ratio of bilayer area to droplet surface area accelerates the overall protein fusion process by shortening the time it takes for protein vesicles to reach and attach to the bilayer surface, sometimes referred to as pre-fusion state (Miller, 1986) . Given that in these experiments the trans and cis droplets contained asymmetric buffer solutions, a salt gradient aided actual fusion post vesicle attachment (Miller, 1986).

The success rate of recording BK STREX currents was enhanced and controlled by applying this technique and single ion channel events were successfully recorded in 29% of cases, compared to a success rate of 7%, where bilayers did not rupture.

5.4.2 BK Electrophysiology

Bilayers were formed as previously described in chapter 4. Recordings of single-channel activity were performed at 5 kHz in the DIB platform as described in chapter

3. The trans side was held at ground and only ion channels with the intracellular side oriented towards the cis side were studied.

The voltage dependence of the BK STREX channel was investigated under constant cis calcium concentration of 50 μM. As shown in Figure 5.8, DC potentials of 20 mV, 40 mV and 60 mV were applied to reconstituted ion channels. Channel amplitude was observed to be a linear function of transmembrane potential which is consistent with other published studies on BK (Garcia-Calvo et al., 1994; Ide & Ichikawa, 2005; Kawano et al., 2013; R Latorre et al., 1982; Pérez et al., 1994). The calculated conductance of BK STREX was around 130 pS, based on the slope of the linear fit of the I-V curve in Figure 5.8, which is comparable to traditional patch-clamping experiments of BK STREX (McCartney et al., 2005).

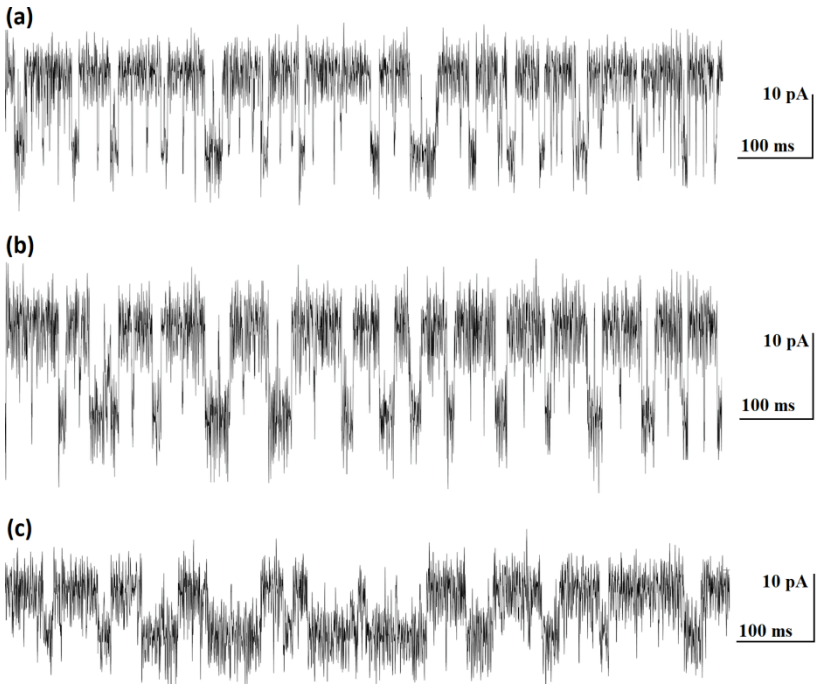

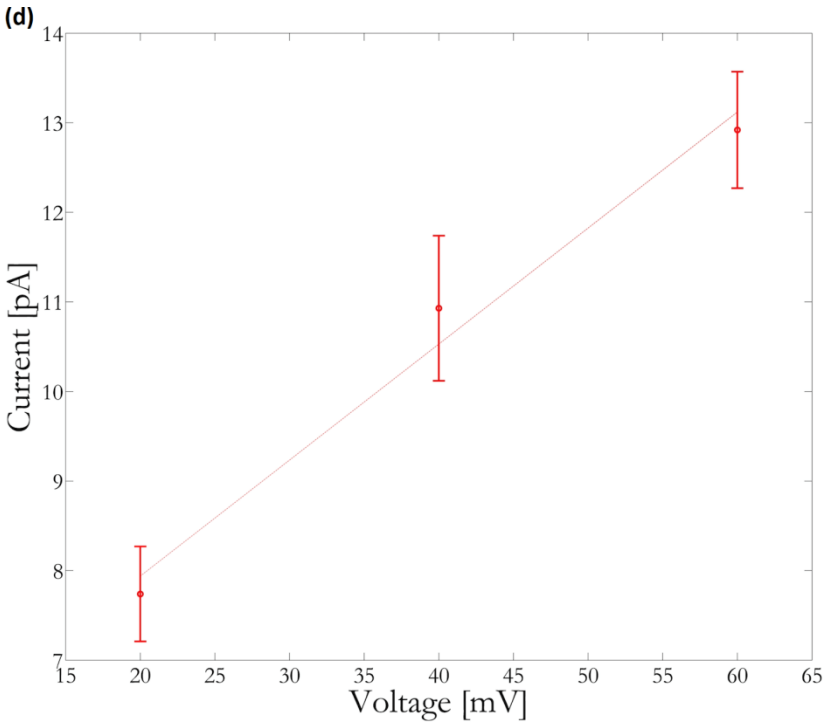

Figure 5.8 BK STREX single channel current traces at varied voltages
Current traces recorded at 5 kHz and low pass filtered at 1 kHz. Various voltages were applied: (a) 60 mV, (b) 40mV and (c) 20mV. (d) I-V curve of BK STREX showing linear relationship between voltage and unitary conductance. The data are shown as the mean ± s.d. ($n \geq 3$ each). Free Ca^{2+} concentration on cis side was kept constant throughout all experiments at 50 µM.

The channel opening and closing events in Figure 5.8 are characteristic of BK and the recordings demonstrate the voltage dependence of the open probability of BK STREX channel as quantified in Figure 5.9 and were in good agreement with literature (Garcia-Calvo et al., 1994; Pérez et al., 1994).

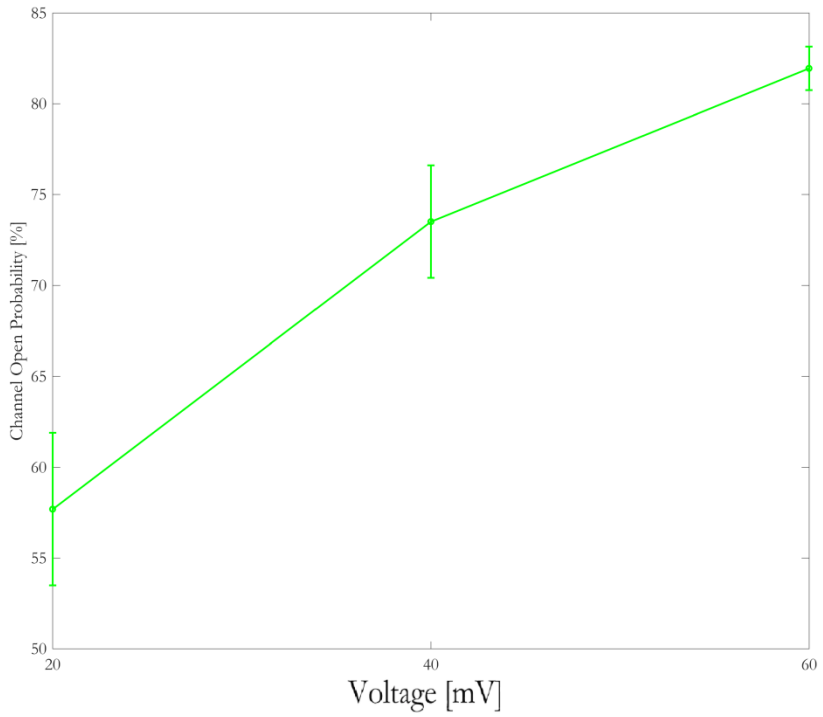

Figure 5.9 BK STREX ion channel open probability
Traces lasting at least 30s were used to calculate open probability. The data are shown as the mean ± s.d. (n ≥ 3 each)

The above experiments demonstrated successful reconstitution and physiological relevance of BK STREX ion channel. Regular everyday lab equipment was used to isolate membrane protein directly from cell membranes which were then reconstituted into DIBs in a reliable repeatable manner. Although detergent-free reconstitution methods are not new by themselves and have been around for a long time (Bean, 1969; Williams, 1985), and even though parallel experiments of BK STREX vesicle fusion in a planar lipid bilayer were not performed, it is the author's opinion based on presented data that acquiring single channel activity using a combination of crude membrane preparations and DIB systems are dramatically simpler than these previous methods and capable of automation as it does not require any manual wicking (Costa et al., 2013) or stirring.

Other advantages of the presented platform and protocol is scalability and thus enhanced throughput, low cost and quantities of material required for ion channel purification and reconstitution and accessibility to both sides of the bilayer for drug studies. Given the above mentioned features the author believes the developed DIB platform and utilised reconstitution method in this study is a suitable alternative to patch-clamping for basic research on other pharmacologically relevant membrane ion channels.

5.5 Summary

Bilayer systems coupled with electrophysiology technology allow functional studies of ion channels. However, these architectures have often been hampered by low success rates stemming from difficulties associated with reconstituting ion channels.

In the electrophysiology experiments of this chapter, a number of key steps were followed to reconstitute BK STREX ion channels into the DIBs which can be extended to other eukaryotic membrane channels. These were:

- BK expressing HEK 293 cells were cultured
- Cells were ruptured
- Membrane ion channels were isolated with sucrose gradient centrifugation
- Ion channel expression was confirmed with RT-PCR
- Isolated ion channel concentration was quantified with Bradford assay
- Artificial bilayers were formed in DIB platform
- Diluted protein sample with natural membrane vesicles containing ion channels were added after allowing for bilayer area expansion
- Vesicles attached onto and fused with the bilayer which was confirmed using electrophysiology

Lessons learnt in chapter 5 were incorporated and the ratio of bilayer area to droplet surface area was manipulated to increase the membrane fusion probability of BK STREX ion channels in DIBs. This observation was consistent with published literature identifying the dependence of ion channel incorporation on lipid bilayer area (Kresák et al., 2009; Miller, 1986). This enhancement led to shorter wait periods for membrane vesicles to reach the surface of the bilayers. Ion channel currents were

recorded in 29% of the bilayers that did not immediately rupture. The characteristic channel properties were retained for BK STREX channels after incorporation into the bilayers as demonstrated by voltage-dependence experiments.

This method for enhancing the probability of ion channel incorporation has the potential to increase the experimental efficiency of bilayer systems, leading to the realisation of a DIB-based, high-throughput platform for ion channel functional assays and thus present a viable alternative to the patch-clamp method for basic research.

6 Chapter 6: Conclusion and Outlook

6.1 Summary

This project had two objectives; firstly, to develop a scalable artificial lipid bilayer architecture and secondly, to identify a reliable protein reconstitution method for basic ion channel electrophysiology research in the constructed biomimetic platform. These objectives were the author's response to the limitations of both conventional patch clamp electrophysiology and popular ion channel reconstitution methods used as outlined in Chapter 1.

To address the first objective, a logical approach to inventing a novel BLM platform was presented in Chapter 4. The said methodology started by specifying system requirements and targeting a suitable bilayer technology. A droplet interface bilayer (DIB) architecture was chosen as it allowed for a rapid, reliable and simple way of forming suspended lipid bilayers within a millifluidic platform with droplet-droplet monolayer contact. A number of configurations were designed and fabricated using stereolithography as a cost-effective way of prototyping at speed. Majority of the built devices were rejected due to deformity and practical difficulties for electrode positioning. Bilayers in the remaining devices were observed for reproducibility, stability, growth rate and droplet coverage. In each device, a number of parameters were considered when forming bilayers, this included droplet incubation time, lipid concentration. The device with a chamber diameter of 5 mm, depth of 2 mm and interface of 2 mm scored highest in comparison to other architectures and was selected for multiplexing to enhance platform throughput.

The suitability of the DIB platform for protein studies by acquiring single channel activities was demonstrated by making simultaneous and parallel recordings of gramicidin, alpha hemolysin and alamethicin peptides in Chapter 5. Each of the selected model ion channels revealed a different aspect of the system. Gramicidin reconstitution confirmed the possibility for detecting low conductance channels, whilst alamethicin incorporation verified the suitability for channels with short dwell time. The relationship between bilayer size and protein incorporation time was investigated, the data suggests that incorporation time decreases with bilayer size due to enhanced bilayer area to droplet surface area ratio. It was possible to conduct alpha hemolysin blocking experiments proving platform's versatility for drug screening applications.

To address the second project objective, a number of key steps to reconstitute BK STREX ion channels into DIBs were identified in Chapter 6, these can in theory be extended to other eukaryotic membrane channels.

Lessons learnt in chapter 5 were incorporated and the ratio of bilayer area to droplet surface area was manipulated to increase the membrane fusion probability of BK STREX ion channels in DIBs. This enhancement led to shorter wait periods for membrane vesicles to reach the surface of the bilayers. Ion channel currents were recorded in 29% of the bilayers that did not immediately rupture. The characteristic channel properties were retained for BK STREX channels after incorporation into the bilayers as demonstrated by voltage-dependence experiments. This method for enhancing the probability of ion channel incorporation has the potential to increase the experimental efficiency of bilayer systems, leading to the realisation of a DIB-

based, high-throughput platform for ion channel functional assays and thus present a viable alternative to the patch-clamp method for basic research.

6.2 Suggestions for Future Work

To test the ubiquity of our method, experiments with a range of ion channels must be carried out. These could be ion channels of smaller organelles and cells such as mitochondria and erythrocytes since these types of ion channels are only accessible to the most skilled patch clampers.

Conducting ion channel experiments with known agonists or antagonists. Although blocking experiments were carried out on alpha hemolysin channels, it would be useful to perform experiments with a range of eukaryotic channels to claim that the platform and proposed procedures are truly suitable for drug screening applications.

It would be useful to add total buffer exchange functionality to the current DIB platform to enable the testing of a range of drugs in one experiment. This would be done by washing out the existing drugs whilst maintaining a stable bilayer.

Another idea could be to reconstitute ion channels from cell free expression systems into the DIB platform. This work was started by the author but was not completed due to time and funding constraints.

The composition of the lipid bilayer could be altered to study the effects of bilayer environment on pharmacologically relevant ion channels. In this study synthetic lipids were used in addition to the native lipids present when reconstituting channels from cell extracts. Although it was not something that was investigated here, slight behavioural modifications could result from different lipid compositions.

Lastly, certain aspects of the setup could be automated to increase throughput by removing the need for manual intervention. These features include DIB chip positioning by a robotic arm or conveyer belt, lipid/oil mixture and buffer droplet dispensing by robotic pipetting, machine vision technology to avoid injecting a second droplet into wells where the first droplet has travelled too far as well as robotic translation of electrode stage.

7 References

Abraham, M. R., Jahangir, a, Alekseev, a E., & Terzic, a. (1999). Channelopathies of inwardly rectifying potassium channels. *The FASEB Journal : Official Publication of the Federation of American Societies for Experimental Biology*, *13*(14), 1901–1910. http://www.ncbi.nlm.nih.gov/pubmed/10544173

Achalkumar, A. S., Bushby, R. J., & Evans, S. D. (2010). Cholesterol-based anchors and tethers for phospholipid bilayers and for model biological membranes. *Soft Matter*, *6*(24), 6036. https://doi.org/10.1039/c0sm00030b

Aidley, D. J., & Stanfield, P. R. (1996). Investigating channel activity. In *Ion Channels: Molecules in Action* (1st editio, pp. 46–52). Cambridge University Press.

Alessandrini, A., & Facci, P. (2011). Unraveling lipid/protein interaction in model lipid bilayers by Atomic Force Microscopy. *Journal of Molecular Recognition*, *24*(3), 387–396. https://doi.org/10.1002/jmr.1083

Alonso-Romanowski, S., Gassa, L. M., & Vilche, J. R. (1995). An investigation by EIS of gramicidin channels in bilayer lipid membranes. *Electrochimica Acta*, *40*(10), 1561–1567. https://doi.org/10.1016/0013-4686(95)00036-E

Andersen, O. S. (1983). Ion movement through gramicidin A channels. Studies on the diffusion-controlled association step. *Biophysical Journal*, *41*(2), 147–165. https://doi.org/10.1016/S0006-3495(83)84416-6

Andersen, Olaf S., & Koeppe, R. E. (2007). Bilayer Thickness and Membrane

Protein Function: An Energetic Perspective. *Annual Review of Biophysics and Biomolecular Structure*, *36*(1), 107–130. https://doi.org/10.1146/annurev.biophys.36.040306.132643

Andersson, M., Okeyo, G., Wilson, D., Keizer, H., Moe, P., Blount, P., Fine, D., Dodabalapur, A., & Duran, R. S. (2008). Voltage-induced gating of the mechanosensitive MscL ion channel reconstituted in a tethered lipid bilayer membrane. *Biosensors and Bioelectronics*, *23*(6), 919–923. https://doi.org/10.1016/j.bios.2007.09.014

Andrew Woolley, G., & Wallace, B. A. (1992). Model ion channels: Gramicidin and alamethicin. *The Journal of Membrane Biology*, *129*(2), 109–136. https://doi.org/10.1007/BF00219508

Arcangeli, A., Crociani, O., Lastraioli, E., Masi, A., Pillozzi, S., & Becchetti, A. (2009). Targeting Ion Channels in Cancer: A Novel Frontier in Antineoplastic Therapy. *Current Medicinal Chemistry*, *16*(1), 66–93. https://doi.org/10.2174/092986709787002835

Atkinson, N. S., Robertson, G. A., & Ganetzky, B. (1991). A component of calcium-activated potassium channels encoded by the Drosophila slo locus. *Science (New York, NY)*, *253*(5019), 551–555. https://doi.org/10.1126/science.1857984

Atsuta, K., Noji, H., & Takeuchi, S. (2004). Micro patterning of active proteins with perforated PDMS sheets (PDMS sieve). *Lab on a Chip*, *4*(4), 333–336. https://doi.org/10.1039/b400774c

Baba, T., Toshima, Y., Minamikawa, H., Hato, M., Suzuki, K., & Kamo, N. (1999).

Formation and characterization of planar lipid bilayer membranes from synthetic phytanyl-chained glycolipids. *Biochimica et Biophysica Acta - Biomembranes*, *1421*(1), 91–102. https://doi.org/10.1016/S0005-2736(99)00114-5

Barbado, M., Fablet, K., Ronjat, M., & De Waard, M. (2009). Gene regulation by voltage-dependent calcium channels. *Biochimica et Biophysica Acta (BBA) - Molecular Cell Research*, *1793*(6), 1096–1104. https://doi.org/10.1016/j.bbamcr.2009.02.004

Bayley, H. (2015). Nanopore sequencing: From imagination to reality. *Clinical Chemistry*, *61*(1), 25–31. https://doi.org/10.1373/clinchem.2014.223016

Bayley, H., & Cremer, P. S. (2001). Stochastic sensors inspired by biology. *Nature*, *413*(6852), 226–230. https://doi.org/10.1038/35093038

Bayley, H., Cronin, B., Heron, A., Holden, M. A., Hwang, W. L., Syeda, R., Thompson, J., & Wallace, M. (2008). Droplet interface bilayers. *Molecular BioSystems*, *4*(12), 1191–1208. https://doi.org/10.1039/b808893d

Bean, R. C. (1969). Discrete Conductance Fluctuations in Lipid Bilayer Protein Membranes. *The Journal of General Physiology*, *53*(6), 741–757. https://doi.org/10.1085/jgp.53.6.741

Bednarczyk, P., Dolowy, K., & Szewczyk, A. (2005). Matrix Mg 2+ regulates mitochondrial ATP-dependent potassium channel from heart. *FEBS Letters*, *579*(7), 1625–1632. https://doi.org/10.1016/j.febslet.2005.01.077

Belegrinou, S., Menon, S., Dobrunz, D., & Meier, W. (2011). Solid-supported

polymeric membranes. *Soft Matter*, *7*(6), 2202–2210. https://doi.org/10.1039/C0SM01163K

Berg, J. M., Tymoczko, J. L., & Stryer, L. (2012). Biochemistry: International edition. In *Biochemistry: International Edition* (6th ed.). W. H. Freeman.

Bertoni, & Hardin. (2015). *Becker's World of the Cell, 9th edition* (8th ed.). Pearson.

Bezanilla, F. (2008). How membrane proteins sense voltage. *Nature Reviews Molecular Cell Biology*, *9*(4), 323–332. https://doi.org/10.1038/nrm2376

Bhattacharjee, N., Urrios, A., Kang, S., & Folch, A. (2016). The upcoming 3D-printing revolution in microfluidics. *Lab Chip*, *16*(10), 1720–1742. https://doi.org/10.1039/C6LC00163G

Blake, S., Mayer, T., Mayer, M., & Yang, J. (2006). Monitoring chemical reactions by using ion-channel-forming peptides. *ChemBioChem*, *7*(3), 433–435. https://doi.org/10.1002/cbic.200500532

Blatz, A. L., & Magleby, K. L. (1983). Single voltage-dependent chloride-selective channels of large conductance in cultured rat muscle. *Biophysical Journal*, *43*(2), 237–241. https://doi.org/10.1016/S0006-3495(83)84344-6

Bradford, M. M. (1976). A rapid and sensitive method for the quantitation of microgram quantities of protein utilizing the principle of protein-dye binding. *Analytical Biochemistry*, *72*(1–2), 248–254. https://doi.org/10.1016/0003-2697(76)90527-3

Brenner, R., Peréz, G. J., Bonev, a D., Eckman, D. M., Kosek, J. C., Wiler, S. W.,

Patterson, a J., Nelson, M. T., & Aldrich, R. W. (2000). Vasoregulation by the beta1 subunit of the calcium-activated potassium channel. *Nature*, *407*(6806), 870–876. https://doi.org/10.1038/35038011

Burnette, W. N. (1981). “Western Blotting”: Electrophoretic transfer of proteins from sodium dodecyl sulfate-polyacrylamide gels to unmodified nitrocellulose and radiographic detection with antibody and radioiodinated protein A. *Analytical Biochemistry*, *112*(2), 195–203. https://doi.org/10.1016/0003-2697(81)90281-5

Cafiso, D. S. (1994). Alamethicin: A Peptide Model for Voltage Gating and Protein-Membrane Interactions. *Annual Review of Biophysics and Biomolecular Structure*, *23*(1), 141–165. https://doi.org/10.1146/annurev.bb.23.060194.001041

Castell, O. K., Berridge, J., & Wallace, M. I. (2012). Quantification of membrane protein inhibition by optical ion flux in a droplet interface bilayer array. *Angewandte Chemie - International Edition*, *51*(13), 3134–3138. https://doi.org/10.1002/anie.201107343

Celesia, G. G. (2001). Disorders of membrane channels or channelopathies. *Clinical Neurophysiology*, *112*(1), 2–18. https://doi.org/10.1016/S1388-2457(00)00496-X

Chattopadhyay, A., & Kelkar, A. (2005). Commentary Ion channels and D -amino acids. *BioEssays*, *30*(March), 147–149.

Chen, L., Tian, L., MacDonald, S. H. F., McClafferty, H., Hammond, M. S. L., Huibant, J. M., Ruth, P., Knaus, H. G., & Shipston, M. J. (2005). Functionally

diverse complement of large conductance calcium- and voltage-activated potassium channel (BK) ??-subunits generated from a single site of splicing. *Journal of Biological Chemistry*, *280*(39), 33599–33609. https://doi.org/10.1074/jbc.M505383200

Christ, G. J., Day, N., Santizo, C., Sato, Y., Zhao, W., Sclafani, T., Bakal, R., Salman, M., Davies, K., & Melman, A. (2004). Intracorporal injection of hSlo cDNA restores erectile capacity in STZ-diabetic F-344 rats in vivo. *Am J Physiol Heart Circ Physiol*, *287*(4), H1544-53. https://doi.org/10.1152/ajpheart.00792.2003

Clapham, D. E. (2007). Calcium Signaling. *Cell*, *131*(6), 1047–1058. https://doi.org/10.1016/j.cell.2007.11.028

Clare, J. J. (2010). Targeting Ion Channels for Drug Discovery. *Discovery Medicine*, *9*(46), 253–260. http://www.discoverymedicine.com/Jeffrey-J-Clare/2010/03/24/targeting-ion-channels-for-drug-discovery/

Cohen, F. S., Akabas, M. H., Zimmerberg, J., & Finkelstein, A. (1984). Parameters affecting the fusion of unilamellar phospholipid vesicles within planar bilayer membranes. *Journal of Cell Biology*, *98*(3), 1054–1062. https://doi.org/10.1083/jcb.98.3.1054

Costa, J. A., Nguyen, D. A., Leal-Pinto, E., Gordon, R. E., & Hanss, B. (2013). Wicking: A Rapid Method for Manually Inserting Ion Channels into Planar Lipid Bilayers. *PLoS ONE*, *8*(5), e60836. https://doi.org/10.1371/journal.pone.0060836

Crowley, J. J. (2003). Cholesterol Antagonizes Ethanol Potentiation of Human Brain BKCa Channels Reconstituted into Phospholipid Bilayers. *Molecular Pharmacology*, *64*(2), 365–372. https://doi.org/10.1124/mol.64.2.365

Curtis, H. J., & Cole, K. S. (1940). Membrane action potentials from the squid giant axon. *Journal of Cellular and Comparative Physiology*, *15*(2), 147–157. https://doi.org/10.1002/jcp.1030150204

Danielli, J. ~F. (1936). Some properties of lipoid films in relation to structures of the plasma membrane. *J. Cell Comp. Physiol.*, *7*(3), 393–408. https://doi.org/10.1002/jcp.1030070307

Danielli, J. F., & Davson, H. (1935). A contribution to the theory of permeability of thin films. *Journal of Cellular and Comparative Physiology*, *5*(4), 495–508. https://doi.org/10.1002/jcp.1030050409

de Wet, H., Lippiat, J., & Allen, M. (2009). Potassium Channels. In J. D. Lippiat (Ed.), *Potassium Channels* (Vol. 491). Humana Press. https://doi.org/10.1007/978-1-59745-526-8

Demarche, S., Sugihara, K., Zambelli, T., Tiefenauer, L., & Vörös, J. (2011). Techniques for recording reconstituted ion channels. *The Analyst*, *136*(6), 1077. https://doi.org/10.1039/c0an00828a

DEMPSTER, J. (2001). {CHAPTER} {FIVE} - Transducers and Sensors. In *The Laboratory Computer* (1st ed., pp. 101–135). Academic Press. https://doi.org/http://dx.doi.org/10.1016/B978-012209551-1/50038-6

Dong, Y., Phillips, K. S., & Cheng, Q. (2006). Immunosensing of Staphylococcus

enterotoxin B (SEB) in milk with PDMS microfluidic systems using reinforced supported bilayer membranes (r-SBMs). *Lab on a Chip*, *6*(5), 675. https://doi.org/10.1039/b514902a

Du, W., Bautista, J. F., Yang, H., Diez-Sampedro, A., You, S.-A., Wang, L., Kotagal, P., Lüders, H. O., Shi, J., Cui, J., Richerson, G. B., & Wang, Q. K. (2005). Calcium-sensitive potassium channelopathy in human epilepsy and paroxysmal movement disorder. *Nature Genetics*, *37*(7), 733–738. https://doi.org/10.1038/ng1585

Duclohier, H., & Wróblewski, H. (2001). Voltage-dependent pore formation and antimicrobial activity by alamethicin and analogues. *Journal of Membrane Biology*, *184*(1), 1–12. https://doi.org/10.1007/s00232-001-0077-2

Duclohier, Hervé. (2009). Structure–function studies on the voltage-gated sodium channel. *Biochimica et Biophysica Acta (BBA) - Biomembranes*, *1788*(11), 2374–2379. https://doi.org/10.1016/j.bbamem.2009.08.017

Dunlop, J., Bowlby, M., Peri, R., Vasilyev, D., & Arias, R. (2008). High-throughput electrophysiology: an emerging paradigm for ion-channel screening and physiology. *Nature Reviews Drug Discovery*, *7*(4), 358–368. https://doi.org/10.1038/nrd2552

Durick, K., & Negulescu, P. (2001). Cellular biosensors for drug discovery. *Biosensors and Bioelectronics*, *16*(7–8), 587–592. https://doi.org/10.1016/S0956-5663(01)00173-7

Eeman, M., & Deleu, M. (2010). From biological membranes to biomimetic model

membranes. *Biotechnology, Agronomy, Society and Environment*, *14*(4), 719–736. http://popups.ulg.ac.be/Base/document.php?id=6568

El-Arabi, A. M., Salazar, C. S., & Schmidt, J. J. (2012). Ion channel drug potency assay with an artificial bilayer chip. *Lab on a Chip*, *12*(13), 2409–2413. https://doi.org/10.1039/c2lc40087a

Ertel, E. a. (1990). Excised patches of plasma membrane from vertebrate rod outer segments retain a functional phototransduction enzymatic cascade. *Proceedings of the National Academy of Sciences of the United States of America*, *87*(11), 4226–4230. https://doi.org/10.1073/pnas.87.11.4226

Esumi, K., & Yamada, T. (1993). Characterisation of a Phospholipid Adsorbed Layer on Silica from Small Unilamellar Vesicles. *Langmuir*, *9*(2), 622–624. https://doi.org/10.1021/la00026a044

Faber, E. S. L., & Sah, P. (2003). Calcium-Activated Potassium Channels: Multiple Contributions to Neuronal Function. *The Neuroscientist*, *9*(3), 181–194. https://doi.org/10.1177/1073858403009003011

Fagerberg, L., Jonasson, K., Von Heijne, G., Uhlén, M., & Berglund, L. (2010). Prediction of the human membrane proteome. *Proteomics*, *10*(6), 1141–1149. https://doi.org/10.1002/pmic.200900258

Farley, J., & Rudy, B. (1988). Multiple types of voltage-dependent Ca2+-activated K+ channels of large conductance in rat brain synaptosomal membranes. *Biophysical Journal*, *53*(6), 919–934. https://doi.org/10.1016/S0006-3495(88)83173-4

Ferrer, J., Wasson, J., Salkoff, L., & Permutt, M. A. (1996). Cloning of human pancreatic islet large conductance Ca(2+)-activated K+ channel (hSlo) cDNAs: evidence for high levels of expression in pancreatic islets and identification of a flanking genetic marker. *Diabetologia*, *39*(8), 891–898. http://www.ncbi.nlm.nih.gov/pubmed/8858210

Fertig, N., Blick, R. H., & Behrends, J. C. (2002). Whole Cell Patch Clamp Recording Performed on a Planar Glass Chip. *Biophysical Journal*, *82*(6), 3056–3062. https://doi.org/10.1016/S0006-3495(02)75646-4

Finlayson, K., Witchel, H. J., McCulloch, J., & Sharkey, J. (2004). Acquired QT interval prolongation and HERG: Implications for drug discovery and development. *European Journal of Pharmacology*, *500*(1-3 SPEC. ISS.), 129–142. https://doi.org/10.1016/j.ejphar.2004.07.019

Friddin, M. S., Smithers, N. P., Beaugrand, M., Marcotte, I., Williamson, P. T. F., Morgan, H., & de Planque, M. R. R. (2013). Single-channel electrophysiology of cell-free expressed ion channels by direct incorporation in lipid bilayers. *The Analyst*, *138*(24), 7294. https://doi.org/10.1039/c3an01540h

Fujiwara, H., Fujihara, M., & Ishiwata, T. (2003). Dynamics of the spontaneous formation of a planar phospholipid bilayer: A new approach by simultaneous electrical and optical measurements. *Journal of Chemical Physics*, *119*(13), 6768–6775. https://doi.org/10.1063/1.1605372

Funakoshi, K., Suzuki, H., & Takeuchi, S. (2006). Lipid bilayer formation by contacting monolayers in a microfluidic device for membrane protein analysis. *Analytical Chemistry*, *78*(24), 8169–8174. https://doi.org/10.1021/ac0613479

Gadsby, D. C. (2004). Ion transport: Spot the difference. *Nature*, *427*(6977), 795–797. https://doi.org/10.1038/427795a

Garcia-Calvo, M., Knaus, H. G., McManus, O. B., Giangiacomo, K. M., Kaczorowski, G. J., & Garcia, M. L. (1994). Purification and reconstitution of the high-conductance, calcium- activated potassium channel from tracheal smooth muscle. *J. Biol. Chem.*, *269*(1), 676–682.

GORE, J. A. (1978). A technique for predicting in-stream flow requirements of benthic macroinvertebrates. *Freshwater Biology*, *8*(2), 141–151. https://doi.org/10.1111/j.1365-2427.1978.tb01436.x

Gouaux, E. (2005). Principles of Selective Ion Transport in Channels and Pumps. *Science*, *310*(5753), 1461–1465. https://doi.org/10.1126/science.1113666

Gross, L. C. M., Heron, A. J., Baca, S. C., & Wallace, M. I. (2011). Determining membrane capacitance by dynamic control of droplet interface bilayer area. *Langmuir*, *27*(23), 14335–14342. https://doi.org/10.1021/la203081v

Groves, J. T., & Boxer, S. G. (2002). Micropattern formation in supported lipid membranes. *Accounts of Chemical Research*, *35*(3), 149–157. https://doi.org/10.1021/ar950039m

Gu, L. Q., & Bayley, H. (2000). Interaction of the noncovalent molecular adapter, beta-cyclodextrin, with the staphylococcal alpha-hemolysin pore. *Biophysical Journal*, *79*(4), 1967–1975. https://doi.org/10.1016/S0006-3495(00)76445-9

Gu, L. Q., Braha, O., Conlan, S., Cheley, S., & Bayley, H. (1999). Stochastic sensing of organic analytes by a pore-forming protein containing a molecular adapter.

Nature, *398*(6729), 686–690. https://doi.org/10.1038/19491

Gutman, G. A., Chandy, K. G., Grissmer, S., Lazdunski, M., McKinnon, D., Pardo, L. A., Robertson, G. A., Rudy, B., Sanguinetti, M. C., Stühmer, W., & Wang, X. (2005). International Union of Pharmacology. LIII. Nomenclature and molecular relationships of voltage-gated potassium channels. *Pharmacological Reviews*, *57*(4), 473–508. https://doi.org/10.1124/pr.57.4.10.1

Hagen, B. M., Bayguinov, O., & Sanders, K. M. (2003). Beta 1-subunits are required for regulation of coupling between Ca2+ transients and Ca2+-activated K+ (BK) channels by protein kinase C. *Am.J.Physiol Cell Physiol*, *285*(5), C1270–C1280. https://doi.org/10.1152/ajpcell.00153.2003\r00153.2003 [pii]

Hamill, O. P., Marty, A., Neher, E., Sakmann, B., & Sigworth, F. J. (1981). Improved patch-clamp techniques for high-resolution current recording from cells and cell-free membrane patches. *Pfl??Gers Archiv European Journal of Physiology*, *391*(2), 85–100. https://doi.org/10.1007/BF00656997

Harmar, A. J., Hills, R. A., Rosser, E. M., Jones, M., Buneman, O. P., Dunbar, D. R., Greenhill, S. D., Hale, V. A., Sharman, J. L., Bonner, T. I., Catterall, W. A., Davenport, A. P., Delagrange, P., Dollery, C. L., Foord, S. M., Gutman, G. A., Laudet, V., Neubig, R. R., Ohlstein, E. H., … Spedding, M. (2009). IUPHAR-DB: The IUPHAR database of G protein-coupled receptors and ion channels. *Nucleic Acids Research*, *37*(SUPPL. 1), D680–D685. https://doi.org/10.1093/nar/gkn728

Heron, A. J., Thompson, J. R., Mason, A. E., & Wallace, M. I. (2007). Direct detection of membrane channels from gels using water-in-oil droplet bilayers.

Journal of the American Chemical Society, *129*(51), 16042–16047. https://doi.org/10.1021/ja075715h

Hirano-Iwata, A., Aoto, K., Oshima, A., Taira, T., Yamaguchi, R. T., Kimura, Y., & Niwano, M. (2010). Free-standing lipid bilayers in silicon chips-membrane stabilization based on microfabricated apertures with a nanometer-scale smoothness. *Langmuir*, *26*(3), 1949–1952. https://doi.org/10.1021/la902522j

Hirano-Iwata, A., Ishinari, Y., Yoshida, M., Araki, S., Tadaki, D., Miyata, R., Ishibashi, K., Yamamoto, H., Kimura, Y., & Niwano, M. (2016). Reconstitution of Human Ion Channels into Solvent-free Lipid Bilayers Enhanced by Centrifugal Forces. *Biophysical Journal*, *110*(10), 2207–2215. https://doi.org/10.1016/j.bpj.2016.04.010

Hirano-Iwata, A., Taira, T., Oshima, A., Kimura, Y., & Niwano, M. (2010). Improved stability of free-standing lipid bilayers based on nanoporous alumina films. *Applied Physics Letters*, *96*(21), 213706. https://doi.org/10.1063/1.3441298

Hladky, S. B., & Haydon, D. A. (1970). Discreteness of Conductance Change in Bimolecular Lipid Membranes in the Presence of Certain Antibiotics. *Nature*, *225*(5231), 451–453. https://doi.org/10.1038/225451a0

Hodgkin, A. L., & Huxley, A. F. (1945). Resting and action potentials in single nerve fibres. *The Journal of Physiology*, *104*(2), 176–195. https://doi.org/10.1113/jphysiol.1945.sp004114

Hodgkin, A. L., Huxley, A. F., & Katz, B. (1952). Measurement of current-voltage

relations in the membrane of the giant axon of *Loligo*. *The Journal of Physiology*, *116*(4), 424–448. https://doi.org/10.1113/jphysiol.1952.sp004716

Holden, M. A., Jung, S. Y., Yang, T., Castellana, E. T., & Cremer, P. S. (2004). Creating fluid and air-stable solid supported lipid bilayers. *Journal of the American Chemical Society*, *126*(21), 6512–6513. https://doi.org/10.1021/ja048504a

Holden, M. A., Needham, D., & Bayley, H. (2007). Functional bionetworks from nanoliter water droplets. *Journal of the American Chemical Society*, *129*(27), 8650–8655. https://doi.org/10.1021/ja072292a

Hwang, W. L., Chen, M., Cronin, B., Holden, M. A., & Bayley, H. (2008). Asymmetric droplet interface bilayers. *Journal of the American Chemical Society*, *130*(18), 5878–5879. https://doi.org/10.1021/ja802089s

Ide, T., & Ichikawa, T. (2005). A novel method for artificial lipid-bilayer formation. *Biosensors and Bioelectronics*, *21*(4), 672–677. https://doi.org/10.1016/j.bios.2004.12.018

Jeffries, O. (2010). *Palmitoylation of BK channels* (Issue August) [The University of Edinburgh]. http://www.era.lib.ed.ac.uk/handle/1842/4791

Kawano, R., Tsuji, Y., Kamiya, K., Kodama, T., Osaki, T., Miki, N., & Takeuchi, S. (2014). A portable lipid bilayer system for environmental sensing with a transmembrane protein. *PLoS ONE*, *9*(7), 1–5. https://doi.org/10.1371/journal.pone.0102427

Kawano, R., Tsuji, Y., Sato, K., Osaki, T., Kamiya, K., Hirano, M., Ide, T., Miki, N.,

& Takeuchi, S. (2013). Automated Parallel Recordings of Topologically Identified Single Ion Channels. *Scientific Reports*, *3*(1), 1995. https://doi.org/10.1038/srep01995

Kelkar, D. A., & Chattopadhyay, A. (2007). The gramicidin ion channel: A model membrane protein. *Biochimica et Biophysica Acta - Biomembranes*, *1768*(9), 2011–2025. https://doi.org/10.1016/j.bbamem.2007.05.011

Kongsuphol, P., Fang, K. B., & Ding, Z. (2013). Lipid bilayer technologies in ion channel recordings and their potential in drug screening assay. *Sensors and Actuators, B: Chemical*, *185*, 530–542. https://doi.org/10.1016/j.snb.2013.04.119

Kreir, M., Farre, C., Beckler, M., George, M., & Fertig, N. (2008). Rapid screening of membrane protein activity: electrophysiological analysis of OmpF reconstituted in proteoliposomes. *Lab on a Chip*, *8*(4), 587–595. https://doi.org/10.1039/b713982a

Kreir, M., George, M., Brueggemann, A., & Fertig, N. (2012). Ion Channel Reconstitution. In *Biophysical Journal* (Vol. 102, Issue 3). Plenum Press. https://doi.org/10.1016/j.bpj.2011.11.1354

Kresák, S., Hianik, T., & Naumann, R. L. C. (2009). Giga-seal solvent-free bilayer lipid membranes: from single nanopores to nanopore arrays. *Soft Matter*, *5*(20), 4021. https://doi.org/10.1039/b907661a

Kung, C., & Blount, P. (2004). Channels in microbes: So many holes to fill. *Molecular Microbiology*, *53*(2), 373–380. https://doi.org/10.1111/j.1365-

2958.2004.04180.x

Kutzbach, J. E. (1997). Response of the African Monsoon to Orbital Forcing and Ocean Feedbacks in the Middle Holocene. *Science*, *278*(5337), 440–443. https://doi.org/10.1126/science.278.5337.440

Latorre, R, & Alvarez, O. (1981). Voltage-dependent channels in planar lipid bilayer membranes. *Physiol Rev.*, *61*(1), 77–150.

Latorre, R, Vergara, C., & Hidalgo, C. (1982). Reconstitution in planar lipid bilayers of a Ca2+-dependent K+ channel from transverse tubule membranes isolated from rabbit skeletal muscle. *Proceedings of the National Academy of Sciences of the United States of America*, *79*(3), 805–809. https://doi.org/10.1073/pnas.79.3.805

Latorre, Ramon, Vergara, C., & Moczydlowski, E. (1983). Properties of a Ca2+-activated K+ channel in a reconstituted system. *Cell Calcium*, *4*(5–6), 343–357. https://doi.org/10.1016/0143-4160(83)90013-1

Laver, D. R. (2001). The power of single channel recording and analysis: Its application to ryanodine receptors in lipid bilayers. *Clinical and Experimental Pharmacology and Physiology*, *28*(8), 675–686. https://doi.org/10.1046/j.1440-1681.2001.03503.x

Le Pioufle, B., Suzuki, H., Tabata, K. V., Noji, H., & Takeuchi, S. (2008). Lipid bilayer microarray for parallel recording of transmembrane ion currents. *Analytical Chemistry*, *80*(1), 328–332. https://doi.org/10.1021/ac7016635

Lee, U. S., & Cui, J. (2010). BK channel activation: Structural and functional

insights. *Trends in Neurosciences*, *33*(9), 415–423. https://doi.org/10.1016/j.tins.2010.06.004

Lein, M., Huang, J., & Holden, M. A. (2013). Robust reagent addition and perfusion strategies for droplet-interface bilayers. *Lab on a Chip*, *13*(14), 2749. https://doi.org/10.1039/c3lc41323c

LeincoTechnologies. (2013). *General Western Blot Protocol*. Abcam.

Lenz, P., Ajo-Franklin, C. M., & Boxer, S. G. (2004). Patterned supported lipid bilayers and monolayers on poly(dimethylsiloxane). *Langmuir*, *20*(25), 11092–11099. https://doi.org/10.1021/la048450i

Leptihn, S., Castell, O. K., Cronin, B., Lee, E.-H., Gross, L. C. M., Marshall, D. P., Thompson, J. R., Holden, M., & Wallace, M. I. (2013). Constructing droplet interface bilayers from the contact of aqueous droplets in oil. *Nature Protocols*, *8*(6), 1048–1057. https://doi.org/10.1038/nprot.2013.061

Leptihn, S., Thompson, J. R., Ellory, J. C., Tucker, S. J., & Wallace, M. I. (2011). In vitro reconstitution of eukaryotic ion channels using droplet interface bilayers. *Journal of the American Chemical Society*, *133*(24), 9370–9375. https://doi.org/10.1021/ja200128n

Levis, R. A., & Rae, J. L. (1998). Low-noise patch-clamp techniques. *Methods in Enzymology*, *293*(1984), 218–266. https://doi.org/10.1016/S0076-6879(98)93017-8

Liu, J., Bukiya, A. N., Kuntamallappanavar, G., Singh, A. K., & Dopico, A. M. (2013). Distinct Sensitivity of Slo1 Channel Proteins to Ethanol. *Molecular*

Pharmacology, *83*(1), 235–244. https://doi.org/10.1124/mol.112.081240

Liu, Y., Mathes, C., Friis, S., & Finley, M. (2009). QPatch: The Missing Link Between HTS and Ion Channel Drug Discovery. *Combinatorial Chemistry & High Throughput Screening*, *12*(1), 78–95. https://doi.org/10.2174/138620709787047948

Low, Z. X., Chua, Y. T., Ray, B. M., Mattia, D., Metcalfe, I. S., & Patterson, D. A. (2017). Perspective on 3D printing of separation membranes and comparison to related unconventional fabrication techniques. *Journal of Membrane Science*, *523*(October 2016), 596–613. https://doi.org/10.1016/j.memsci.2016.10.006

Lu, B., Kocharyan, G., & Schmidt, J. J. (2014). Lipid bilayer arrays: Cyclically formed and measured. *Biotechnology Journal*, *9*(3), 446–451. https://doi.org/10.1002/biot.201300271

Marmont, G. (1949). Studies on the axon membrane. I. A new method. *Journal of Cellular and Comparative Physiology*, *34*(3), 351–382. https://doi.org/10.1002/jcp.1030340303

Martel, A., & Cross, B. (2012). Handling of artificial membranes using electrowetting-actuated droplets on a microfluidic device combined with integrated pA-measurements. *Biomicrofluidics*, *6*(1), 12813–128137. https://doi.org/10.1063/1.3665719

Marty, A. (1983). Ca2+-dependent K+ channels with large unitary conductance. *Trends in Neurosciences*, *6*(C), 262–265. https://doi.org/10.1016/0166-2236(83)90115-7

Masetti, M., Cavalli, A., & Recanatini, M. (2008). Modeling the hERG potassium channel in a phospholipid bilayer: Molecular dynamics and drug docking studies. *Journal of Computational Chemistry*, *29*(5), 795–808. https://doi.org/10.1002/jcc.20842

Mayer, M., Kriebel, J. K., Tosteson, M. T., & Whitesides, G. M. (2003). Microfabricated Teflon Membranes for Low-Noise Recordings of Ion Channels in Planar Lipid Bilayers. *Biophysical Journal*, *85*(4), 2684–2695. https://doi.org/10.1016/S0006-3495(03)74691-8

McCartney, C. E., McClafferty, H., Huibant, J.-M., Rowan, E. G., Shipston, M. J., & Rowe, I. C. M. (2005). A cysteine-rich motif confers hypoxia sensitivity to mammalian large conductance voltage- and Ca-activated K (BK) channel alpha-subunits. *Proceedings of the National Academy of Sciences of the United States of America*, *102*(49), 17870–17876. https://doi.org/10.1073/pnas.0505270102

McManus, O. B., Helms, L. M. H., Pallanck, L., Ganetzky, B., Swanson, R., & Leonard, R. J. (1995). Functional role of the β subunit of high conductance calcium-activated potassium channels. *Neuron*, *14*(3), 645–650. https://doi.org/10.1016/0896-6273(95)90321-6

Meredith, A. L., Thorneloe, K. S., Werner, M. E., Nelson, M. T., & Aldrich, R. W. (2004). Overactive bladder and incontinence in the absence of the BK large conductance Ca2+-activated K+ channel. *Journal of Biological Chemistry*, *279*(35), 36746–36752. https://doi.org/10.1074/jbc.M405621200

Miller, C. (1986). *Ion Channel Reconstitution* (C. Miller (ed.)). Springer US. https://doi.org/10.1007/978-1-4757-1361-9

Molleman, A. (2002). Patch Clamping. In *Wiley*. John Wiley & Sons, Ltd. https://doi.org/10.1002/0470856521

Molokanova, E., & Savchenko, A. (2008). Bright future of optical assays for ion channel drug discovery. *Drug Discovery Today*, *13*(1–2), 14–22. https://doi.org/10.1016/j.drudis.2007.11.009

Montal, M., & Mueller, P. (1972). Formation of bimolecular membranes from lipid monolayers and a study of their electrical properties. *Proceedings of the National Academy of Sciences of the United States of America*, *69*(12), 3561–3566. https://doi.org/10.1073/pnas.69.12.3561

Moran, O., & Zegarra-moran, O. (2008). On the measurement of the functional properties of the CFTR. *Journal of Cystic Fibrosis*, *7*(6), 483–494. https://doi.org/10.1016/j.jcf.2008.05.003

Mueller, P., Rudin, D. 0., Tien, H. T., & Wescott, W. C. (1962a). Methods for the Formation of Single Bimolecular Lipid Membranes in Aqceous Solution. *The Journal of Physical Chemistry*, *807*(1), 1962–1963. https://doi.org/10.1021/j100796a529

Mueller, P., Rudin, D. O., Tien, H. T., & Wescott, W. C. (1962b). Reconstitution of cell membrane structure in vitro and its transformation into an excitable system. *Nature*, *194*(4832), 979–980. https://doi.org/10.1038/194979a0

Mullis, K., Faloona, F., Scharf, S., Saiki, R., Horn, G., & Erlich, H. (1986). Specific enzymatic amplification of DNA in vitro: The polymerase chain reaction. *Cold Spring Harbor Symposia on Quantitative Biology*, *51*(1), 263–273.

https://doi.org/10.1101/SQB.1986.051.01.032

Naruse, K., Tang, Q. Y., & Sokabe, M. (2009). Stress-Axis Regulated Exon (STREX) in the C terminus of BKCa channels is responsible for the stretch sensitivity. *Biochemical and Biophysical Research Communications*, *385*(4), 634–639. https://doi.org/10.1016/j.bbrc.2009.05.105

Neumcke, B. (1990). Diversity of sodium channels in adult and cultured cells, in oocytes and in lipid bilayers. *Reviews of Physiology, Biochemistry and Pharmacology, Volume 115*, *115*, 1–49. https://doi.org/10.1007/BFb0033951

Nielsen, C. H. (2009). Biomimetic membranes for sensor and separation applications. *Analytical and Bioanalytical Chemistry*, *395*(3), 697–718. https://doi.org/10.1007/s00216-009-2960-0

O'Connell, R. J., Yuan, C., Johnston, L. J., Rinco, O., Probodh, I., & Treistman, S. N. (2006). Gating and conductance changes in BKCa channels in bilayers are reciprocal. *Journal of Membrane Biology*, *213*(3), 143–153. https://doi.org/10.1007/s00232-006-0034-1

Ogden, D. (1989). Microelectrode Techniques . In D. C. Ogden (Ed.), *Trends in Neurosciences* (2nd ed., Vol. 12, Issue 4). Company of Biologists. https://doi.org/10.1016/0166-2236(89)90053-2

Okuse, K. (2007). Pain signalling pathways: From cytokines to ion channels. *International Journal of Biochemistry and Cell Biology*, *39*(3), 490–496. https://doi.org/10.1016/j.biocel.2006.11.016

Oshima, A., Hirano-Iwata, A., Mozumi, H., Ishinari, Y., Kimura, Y., & Niwano, M.

(2013). Reconstitution of human ether-a-go-go-related gene channels in microfabricated silicon chips. *Analytical Chemistry*, *85*(9), 4363–4369. https://doi.org/10.1021/ac303484k

Pantoja, R., Sigg, D., Blunck, R., Bezanilla, F., & Heath, J. R. (2001). Bilayer Reconstitution of Voltage-Dependent Ion Channels using a Microfabricated Silicon Chip. *Biophysical Journal*, *81*(4), 2389–2394. https://doi.org/10.1016/S0006-3495(01)75885-7

Pérez, G., Lagrutta, A., Adelman, J. P., & Toro, L. (1994). Reconstitution of expressed KCa channels from Xenopus oocytes to lipid bilayers. *Biophysical Journal*, *66*(4), 1022–1027. https://doi.org/10.1016/S0006-3495(94)80883-5

Perret, D., & Luo, Z. D. (2009). Targeting Voltage-Gated Calcium Channels for Neuropathic Pain Management. *Neurotherapeutics*, *6*(4), 679–692. https://doi.org/10.1016/j.nurt.2009.07.006

Piccolino, M. (1998). Animal electricity and the birth of electrophysiology: the legacy of Luigi Galvani. *Brain Research Bulletin*, *46*(5), 381–407. https://doi.org/10.1016/S0361-9230(98)00026-4

Portonovo, S. A., Salazar, C. S., & Schmidt, J. J. (2013). HERG drug response measured in droplet bilayers. *Biomedical Microdevices*, *15*(2), 255–259. https://doi.org/10.1007/s10544-012-9725-9

Portonovo, S. A., & Schmidt, J. (2012). Masking apertures enabling automation and solution exchange in sessile droplet lipid bilayers. *Biomedical Microdevices*, *14*(1), 187–191. https://doi.org/10.1007/s10544-011-9596-5

Poulos, J L, Portonovo, S. A., Bang, H., & Schmidt, J. J. (2010). Automatable lipid bilayer formation and ion channel measurement using sessile droplets. *Journal of Physics: Condensed Matter*, *22*(45), 454105. https://doi.org/10.1088/0953-8984/22/45/454105

Poulos, Jason L., Jeon, T.-J., Damoiseaux, R., Gillespie, E. J., Bradley, K. A., & Schmidt, J. J. (2009). Ion channel and toxin measurement using a high throughput lipid membrane platform. *Biosensors and Bioelectronics*, *24*(6), 1806–1810. https://doi.org/10.1016/j.bios.2008.08.041

Poulos, Jason L., Nelson, W. C., Jeon, T.-J., Kim, C.-J. "CJ," & Schmidt, J. J. (2009). Electrowetting on dielectric-based microfluidics for integrated lipid bilayer formation and measurement. *Applied Physics Letters*, *95*(1), 013706. https://doi.org/10.1063/1.3167283

Raffaelli, G., Saviane, C., Mohajerani, M. H., Pedarzani, P., & Cherubini, E. (2004). BK potassium channels control transmitter release at CA3-CA3 synapses in the rat hippocampus. *The Journal of Physiology*, *557*(1), 147–157. https://doi.org/10.1113/jphysiol.2004.062661

Rask-Andersen, M., Almén, M. S., & Schiöth, H. B. (2011). Trends in the exploitation of novel drug targets. *Nature Reviews Drug Discovery*, *10*(8), 579–590. https://doi.org/10.1038/nrd3478

Raven, P. H., & Johnson, G. B. (2002). Membranes. In *Biology* (6th ed., pp. 103–122). McGraw-Hill.

Reimhult, E., & Kumar, K. (2008). Membrane biosensor platforms using nano- and

microporous supports. *Trends in Biotechnology*, *26*(2), 82–89. https://doi.org/10.1016/j.tibtech.2007.11.004

Robitaille, R., Garcia, M. L., Kaczorowski, G. J., & Chariton, M. P. (1993). Functional colocalization of calcium and calcium-gated potassium channels in control of transmitter release. *Neuron*, *11*(4), 645–655. https://doi.org/10.1016/0896-6273(93)90076-4

Roerdink Lander, M., Ibragimova, S., Rein, C., Vogel, J., Stibius, K., Geschke, O., Perry, M., & Hélix-Nielsen, C. (2011). Biomimetic membrane arrays on cast hydrogel supports. *Langmuir*, *27*(11), 7002–7007. https://doi.org/10.1021/la1050699

Rosemblatt, M., Hidalgo, C., Vergara, C., & Ikemoto, N. (1981). Immunological and biochemical properties of transverse tubule membranes isolated from rabbit skeletal muscle. *Journal of Biological Chemistry*, *256*(15), 8140–8148.

Ross, J. (1995). mRNA stability in mammalian cells. *Microbiological Reviews*, *59*(3), 423–450. https://doi.org/10.1002/bies.950190612

Rudnev, V. S., Ermishkin, L. N., Fonina, L. A., & Rovin, Y. G. (1981). The dependence of the conductance and lifetime of gramicidin channels on the thickness and tension of lipid bilayers. *BBA - Biomembranes*, *642*(1), 196–202. https://doi.org/10.1016/0005-2736(81)90149-8

Rüttiger, L., Sausbier, M., Zimmermann, U., Winter, H., Braig, C., Engel, J., Knirsch, M., Arntz, C., Langer, P., Hirt, B., Müller, M., Köpschall, I., Pfister, M., Münkner, S., Rohbock, K., Pfaff, I., Rüsch, A., Ruth, P., & Knipper, M.

(2004). Deletion of the Ca2+-activated potassium (BK) alpha-subunit but not the BKbeta1-subunit leads to progressive hearing loss. *Proceedings of the National Academy of Sciences of the United States of America*, *101*(35), 12922–12927. https://doi.org/10.1073/pnas.0402660101

Saito, M., Nelson, C., Salkoff, L., & Lingle, C. J. (1997). A cysteine-rich domain defined by a novel exon in a Slo variant in rat adrenal chromaffin cells and PC12 cells. *Journal of Biological Chemistry*, *272*(18), 11710–11717. https://doi.org/10.1074/jbc.272.18.11710

Salafsky, J., Groves, J. T., & Boxer, S. G. (1996). Architecture and function of membrane proteins in planar supported bilayers: A study with photosynthetic reaction centers. *Biochemistry*, *35*(47), 14773–14781. https://doi.org/10.1021/bi961432i

Saleem, F., Rowe, I. C. M., & Shipston, M. J. (2009). Characterization of BK channel splice variants using membrane potential dyes. *British Journal of Pharmacology*, *156*(1), 143–152. https://doi.org/10.1111/j.1476-5381.2008.00011.x

Salkoff, L., Butler, A., Ferreira, G., Santi, C., & Wei, A. (2006). High-conductance potassium channels of the SLO family. *Nature Reviews Neuroscience*, *7*(12), 921–931. https://doi.org/10.1038/nrn1992

Sandison, M. E., Zagnoni, M., & Morgan, H. (2007). Air-exposure technique for the formation of artificial lipid bilayers in microsystems. *Langmuir*, *23*(15), 8277–8284. https://doi.org/10.1021/la7007528

Sausbier, M, Hu, H., Arntz, C., Feil, S., Kamm, S., Adelsberger, H., Sausbier, U., Sailer, C. A., Feil, R., Hofmann, F., Korth, M., Shipston, M. J., Knaus, H.-G., Wolfer, D. P., Pedroarena, C. M., Storm, J. F., & Ruth, P. (2004). Cerebellar ataxia and Purkinje cell dysfunction caused by Ca2+-activated K+ channel deficiency. *Proceedings of the National Academy of Sciences of the United States of America*, *101*(25), 9474–9478. https://doi.org/10.1073/pnas.0401702101

Sausbier, Matthias, Arntz, C., Bucurenciu, I., Zhao, H., Zhou, X. B., Sausbier, U., Feil, S., Kamm, S., Essin, K., Sailer, C. A., Abdullah, U., Krippeit-Drews, P., Feil, R., Hoffmann, F., Knaus, H. G., Kenyon, C., Shipston, M. J., Storm, J. F., Neuhuber, W., … Ruth, P. (2005). Elevated blood pressure linked to primary hyperaldosteronism and impaired vasodilation in BK channel-deficient mice. *Circulation*, *112*(1), 60–68. https://doi.org/10.1161/01.CIR.0000156448.74296.FE

Schubert, R., & Nelson, M. T. (2001). Protein kinases: Tuners of the BKCa channel in smooth muscle. *Trends in Pharmacological Sciences*, *22*(10), 505–512. https://doi.org/10.1016/S0165-6147(00)01775-2

Sciencelab, L. (n.d.). *The Patch-Clamp Technique*. http://www.leica-microsystems.com/science-lab/the-patch-clamp-technique/

Shen, H. H., Lithgow, T., & Martin, L. L. (2013). Reconstitution of membrane proteins into model membranes: Seeking better ways to retain protein activities. *International Journal of Molecular Sciences*, *14*(1), 1589–1607. https://doi.org/10.3390/ijms14011589

Shipston, M. J., Duncan, R. R., Clark, A. G., Antoni, F. A., & Tian, L. (1999). Molecular components of large conductance calcium-activated potassium (BK) channels in mouse pituitary corticotropes. *Mol Endocrinol.*, *13*(10), 1728–1737. https://doi.org/10.1210/mend.13.10.0355

Sigworth, F. J., & Klemic, K. G. (2002). Patch Clamp on a Chip. *Biophysical Journal*, *82*(6), 2831–2832. https://doi.org/10.1016/S0006-3495(02)75625-7

Sigworth, F. J., & Klemic, K. G. (2005). Microchip technology in ion-channel research. *IEEE Transactions on Nanobioscience*, *4*(1), 121–127. https://doi.org/10.1109/TNB.2004.842471

Sondermann, M., George, M., Fertig, N., & Behrends, J. C. (2006). High-resolution electrophysiology on a chip: Transient dynamics of alamethicin channel formation. *Biochimica et Biophysica Acta - Biomembranes*, *1758*(4), 545–551. https://doi.org/10.1016/j.bbamem.2006.03.023

Song, L., Hobaugh, M. R., Shustak, C., Cheley, S., Bayley, H., & Gouaux, J. E. (1996). Structure of Staphylococcal alpha -Hemolysin, a Heptameric Transmembrane Pore. *Science*, *274*(5294), 1859–1865. https://doi.org/10.1126/science.274.5294.1859

Studer, A., Demarche, S., Langenegger, D., & Tiefenauer, L. (2011). Integration and recording of a reconstituted voltage-gated sodium channel in planar lipid bilayers. *Biosensors and Bioelectronics*, *26*(5), 1924–1928. https://doi.org/10.1016/j.bios.2010.06.008

Suzuki, H., & Takeuchi, S. (2008). Microtechnologies for membrane protein studies.

Analytical and Bioanalytical Chemistry, *391*(8), 2695–2702. https://doi.org/10.1007/s00216-008-1916-0

Tamm, L. K., & McConnell, H. M. (1985). Supported phospholipid bilayers. *Biophysical Journal*, *47*(1), 105–113. https://doi.org/10.1016/S0006-3495(85)83882-0

Tanaka, M., & Sackmann, E. (2005). Polymer-supported membranes as models of the cell surface. *Nature*, *437*(7059), 656–663. https://doi.org/10.1038/nature04164

Terlau, H., & Kirchhoff, F. (2001). Ion Channels/Excitable Membranes. In *Encyclopedic Reference of Genomics and Proteomics in Molecular Medicine* (3rd ed.). Sinauer Associates. https://doi.org/10.1007/3-540-29623-9_5640

Terrettaz, S., Mayer, M., & Vogel, H. (2003). Highly electrically insulating tethered lipid bilayers for probing the function of ion channel proteins. *Langmuir*, *19*(14), 5567–5569. https://doi.org/10.1021/la034197v

Thapliyal, T., Poulos, J. L., & Schmidt, J. J. (2011). Automated lipid bilayer and ion channel measurement platform. *Biosensors and Bioelectronics*, *26*(5), 2651–2654. https://doi.org/10.1016/j.bios.2010.01.017

Tiefenauer, L., & Demarche, S. (2012). Challenges in the development of functional assays of membrane proteins. *Materials*, *5*(11), 2205–2242. https://doi.org/10.3390/ma5112205

Tien, H. T., & Ottova, A. (2003). The Bilayer Lipid Membrane (BLM) under Electrical Fields. *IEEE Transactions on Dielectrics and Electrical Insulation*,

10(5), 717–727. https://doi.org/10.1109/TDEI.2003.1237323

Tien, H. Ti. (2003). *Planar lipid bilayers (BLMs) and their applications (Vol. Vol. 7, Membrane science and technology series).* (7th ed.). ELSEVIER SCIENCE & TECHNOLOGY.

Trapani, J. G., & Korn, S. J. (2003). Control of ion channel expression for patch clamp recordings using an inducible expression system in mammalian cell lines. *BMC Neuroscience*, *4*, 15. https://doi.org/10.1186/1471-2202-4-15

Tristram-Nagle, S., Kim, D. J., Akhunzada, N., Kuerka, N., Mathai, J. C., Katsaras, J., Zeidel, M., & Nagle, J. F. (2010). Structure and water permeability of fully hydrated diphytanoylPC. *Chemistry and Physics of Lipids*, *163*(6), 630–637. https://doi.org/10.1016/j.chemphyslip.2010.04.011

Tseng-Crank, J., Foster, C. D., Krause, J. D., Mertz, R., Godinot, N., DiChiara, T. J., & Reinhartt, P. H. (1994). Cloning, expression, and distribution of functionally distinct Ca2+-Activated K+ channel isoforms from human brain. *Neuron*, *13*(6), 1315–1330. https://doi.org/10.1016/0896-6273(94)90418-9

Tsofina, L. M., Liberman, E. a., & Babakov, a. V. (1966). Production of Bimolecular Protein-Lipid Membranes in Aqueous Solution. *Nature*, *212*(5063), 681–683. https://doi.org/10.1038/212681a0

Tsuji, Y., Kawano, R., Osaki, T., Kamiya, K., Miki, N., & Takeuchi, S. (2013). Droplet-based lipid bilayer system integrated with microfluidic channels for solution exchange. *Lab on a Chip*, *13*(8), 1476. https://doi.org/10.1039/c3lc41359d

Valincius, G., Heinrich, F., Budvytyte, R., Vanderah, D. J., McGillivray, D. J., Sokolov, Y., Hall, J. E., & Lösche, M. (2008). Soluble Amyloid β-Oligomers Affect Dielectric Membrane Properties by Bilayer Insertion and Domain Formation: Implications for Cell Toxicity. *Biophysical Journal*, *95*(10), 4845–4861. https://doi.org/10.1529/biophysj.108.130997

van Meer, G., Voelker, D. R., & Feigenson, G. W. (2008). Membrane lipids: where they are and how they behave. *Nature Reviews Molecular Cell Biology*, *9*(2), 112–124. https://doi.org/10.1038/nrm2330

Venter, J. C., Adams, M. D., Myers, E. W., Li, P. W., Mural, R. J., Sutton, G. G., Smith, H. O., Yandell, M., Evans, C. A., Holt, R. A., Gocayne, J. D., Amanatides, P., Ballew, R. M., Huson, D. H., Wortman, J. R., Zhang, Q., Kodira, C. D., Zheng, X. H., Chen, L., … Zhu, X. (2001). The sequence of the human genome. *Science (New York, N.Y.)*, *291*(5507), 1304–1351. https://doi.org/10.1126/science.1058040

Villar, G., Graham, A. D., & Bayley, H. (2013). A Tissue-Like Printed Material. *Science*, *340*(6128), 48–52. https://doi.org/10.1126/science.1229495

Wang, L., & Tonggu, L. (2015). Membrane protein reconstitution for functional and structural studies. *Science China Life Sciences*, *58*(1), 66–74. https://doi.org/10.1007/s11427-014-4769-0

Weaver, A. K., Liu, X., & Sontheimer, H. (2004). Role for calcium-activated potassium channels (BK) in growth control of human malignant glioma cells. *Journal of Neuroscience Research*, *78*(2), 224–234. https://doi.org/10.1002/jnr.20240

Werner, M. E., Zvara, P., Meredith, A. L., Aldrich, R. W., & Nelson, M. T. (2005). Erectile dysfunction in mice lacking the large-conductance calcium-activated potassium (BK) channel. *The Journal of Physiology*, *567*(Pt 2), 545–556. https://doi.org/10.1113/jphysiol.2005.093823

White, S. H., Petersen, D. C., Simon, S., & Yafuso, M. (1976). Formation of planar bilayer membranes from lipid monolayers. A critique. *Biophysical Journal*, *16*(5), 481–489. https://doi.org/10.1016/S0006-3495(76)85703-7

Wible, B. A., Hawryluk, P., Ficker, E., Kuryshev, Y. A., Kirsch, G., & Brown, A. M. (2005). HERG-Lite??: A novel comprehensive high-throughput screen for drug-induced hERG risk. *Journal of Pharmacological and Toxicological Methods*, *52*(1), 136–145. https://doi.org/10.1016/j.vascn.2005.03.008

Wiegand, G., Arribas-Layton, N., Hillebrandt, H., Sackmann, E., & Wagner, P. (2002). Electrical properties of supported lipid bilayer membranes. *Journal of Physical Chemistry B*, *106*(16), 4245–4254. https://doi.org/10.1021/jp014337e

Williams, A. J. (1985). The measurement of cardiac membrane channels following their incorporation into phospholipid bilayers. *Advances in Myocardiology*, *5*, 77–84. http://www.ncbi.nlm.nih.gov/pubmed/2578684

Womack, M. D. (2004). Dendritic Control of Spontaneous Bursting in Cerebellar Purkinje Cells. *Journal of Neuroscience*, *24*(14), 3511–3521. https://doi.org/10.1523/JNEUROSCI.0290-04.2004

Wonderlin, W. F., Finkel, A., & French, R. J. (1990). Optimizing planar lipid bilayer single-channel recordings for high resolution with rapid voltage steps.

Biophysical Journal, *58*(2), 289–297. https://doi.org/10.1016/S0006-3495(90)82376-6

Woodbury, D. J., & Miller, C. (1990). Nystatin-induced liposome fusion. A versatile approach to ion channel reconstitution into planar bilayers. *Biophysical Journal*, *58*(4), 833–839. https://doi.org/10.1016/S0006-3495(90)82429-2

Wulff, H., Castle, N. A., & Pardo, L. A. (2009). Voltage-gated potassium channels as therapeutic targets. *Nature Reviews Drug Discovery*, *8*(12), 982–1001. https://doi.org/10.1038/nrd2983

Xie, J. (1998). Control of Alternative Splicing of Potassium Channels by Stress Hormones. *Science*, *280*(5362), 443–446. https://doi.org/10.1126/science.280.5362.443

Xu, J., Wang, X., Ensign, B., Li, M., Wu, L., Guia, A., & Xu, J. (2001). Ion-channel assay technologies: Quo vadis? *Drug Discovery Today*, *6*(24), 1278–1287. https://doi.org/10.1016/S1359-6446(01)02095-5

Yuan, C., O'Connell, R. J., Feinberg-Zadek, P. L., Johnston, L. J., & Treistman, S. N. (2004). Bilayer thickness modulates the conductance of the BK channel in model membranes. *Biophysical Journal*, *86*(6), 3620–3633. https://doi.org/10.1529/biophysj.103.029678

Zagnoni, M. (2012). Miniaturised technologies for the development of artificial lipid bilayer systems. *Lab on a Chip*, *12*(6), 1026. https://doi.org/10.1039/c2lc20991h

Zagnoni, M., Sandison, M. E., Marius, P., & Morgan, H. (2009). Bilayer lipid membranes from falling droplets. *Analytical and Bioanalytical Chemistry*,

393(6–7), 1601–1605. https://doi.org/10.1007/s00216-008-2588-5

Zasadzinski, J., Viswanathan, R., Madsen, L., Garnaes, J., & Schwartz, D. (1994). Langmuir-Blodgett films. *Science*, *263*(5154), 1726–1733. https://doi.org/10.1126/science.8134836

Zhang, Y. L., Dunlop, J., & Dalziel, J. E. (2007). Recombinant human voltage-gated skeletal muscle sodium channels are pharmacologically functional in planar lipid bilayers. *Biosensors and Bioelectronics*, *22*(6), 1006–1012. https://doi.org/10.1016/j.bios.2006.04.009

Zhao, Y., Inayat, S., Dikin, D. A., Singer, J. H., Ruoff, R. S., & Troy, J. B. (2008). Patch clamp technique: Review of the current state of the art and potential contributions from nanoengineering. *Proceedings of the Institution of Mechanical Engineers, Part N: Journal of Nanoengineering and Nanosystems*, *222*(1), 1–11. https://doi.org/10.1243/17403499JNN149

Zhu, N., Eghbali, M., Helguera, G., Song, M., Stefani, E., & Toro, L. (2005). Alternative splicing of Slo channel gene programmed by estrogen, progesterone and pregnancy. *FEBS Letters*, *579*(21), 4856–4860. https://doi.org/10.1016/j.febslet.2005.07.069

Zou, B., Yu, H., Babcock, J. J., Chanda, P., Bader, J. S., McManus, O. B., & Li, M. (2010). Profiling Diverse Compounds by Flux- and Electrophysiology-Based Primary Screens for Inhibition of Human *Ether-à-go-go* Related Gene Potassium Channels. *ASSAY and Drug Development Technologies*, *8*(6), 743–754. https://doi.org/10.1089/adt.2010.0339